arXiv:1108.0662v1 [astro-ph.SR] 2 Aug 2011

# THE PHYSICS OF MERGERS

# THE PHYSICS OF MERGERS: THEORETICAL AND STATISTICAL TECHNIQUES APPLIED TO STELLAR MERGERS IN DENSE STAR CLUSTERS

By
NATHAN LEIGH, B.Sc., M.Sc.

A Thesis
Submitted to the School of Graduate Studies
in Partial Fulfillment of the Requirements
for the Degree of

Doctor of Philosophy

McMaster University

© Nathan W. C. Leigh, June 2011

DOCTOR OF PHILOSOPHY (2010) McMaster University
(Physics and Astronomy) Hamilton, Ontario

TITLE: The Physics of Mergers: Theoretical and Statistical Techniques Applied to Stellar Mergers in Dense Star Clusters

AUTHOR: Nathan W. C. Leigh, B.Sc. (University of Toronto), M.Sc. (McMaster University)

SUPERVISOR: Professor Alison Sills

NUMBER OF PAGES: xvi, 184

# Abstract

In this thesis, we present theoretical and statistical techniques broadly related to systems of dynamically-interacting particles. We apply these techniques to observations of dense star clusters in order to study gravitational interactions between stars. These include both long- and short-range interactions, as well as encounters leading to direct collisions and mergers. The latter have long been suspected to be an important formation channel for several curious types of stars whose origins are unknown. The former drive the structural evolution of star clusters and, by leading to their eventual dissolution and the subsequent dispersal of their stars throughout the Milky Way Galaxy, have played an important role in shaping its history. Within the last few decades, theoretical work has painted a comprehensive picture for the evolution of star clusters. And yet, we are still lacking direct observational confirmation that many of the processes thought to be driving this evolution are actually occuring. The results presented in this thesis have connected several of these processes to real observations of star clusters, in many cases for the first time. This has allowed us to directly link the observed properties of several stellar populations to the physical processes responsible for their origins.

We present a new method of quantifying the frequency of encounters involving single, binary and triple stars using an adaptation of the classical mean free path approximation. With this technique, we have shown that dynamical encounters involving triple stars occur commonly in star clusters, and that they are likely to be an important dynamical channel for stellar mergers to occur. This is a new result that has important implications for the origins of several peculiar types of stars (and binary stars), in particular blue stragglers. We further present several new statistical techniques that are broadly applicable to systems of dynamically-interacting particles composed of several different types of populations. These are applied to observations of star clusters in order to obtain quantitative constraints for the degree to which dynamical interactions affect the relative sizes and spatial distributions of their

different stellar populations. To this end, we perform an extensive analysis of a large sample of colour-magnitude diagrams taken from the ACS Survey for Globular Clusters. The results of this analysis can be summarized as follows: (1) We have compiled a homogeneous catalogue of stellar populations, including main-sequence, main-sequence turn-off, red giant branch, horizontal branch and blue straggler stars. (2) With this catalogue, we have quantified the effects of the cluster dynamics in determining the relative sizes and spatial distributions of these stellar populations. (3) These results are particularly interesting for blue stragglers since they provide compelling evidence that they are descended from binary stars. (4) Our analysis of the main-sequence populations is consistent with a remarkably universal initial stellar mass function in old massive star clusters in the Milky Way. This is a new result with important implications for our understanding of star formation in the early Universe and, more generally, the history of our Galaxy. Finally, we describe how the techniques presented in this thesis are ideally suited for application to a number of other outstanding puzzles of modern astrophysics, including chemical reactions in the interstellar medium and mergers between galaxies in galaxy clusters and groups.

*To my parents*

# Co-Authorship

Chapters 2, 3, 4, and 5 of this thesis all represent original papers written by myself, Nathan W. C. Leigh and published in the *Monthly Notices of the Royal Astronomical Society* (*MNRAS*). The reference for Chapter 2 is Leigh N., Sills A. 2010, *MNRAS*, 410, 2370, and Dr. Alison Sills is the only co-author. The reference for Chapter 3 is Leigh N., Sills A., Knigge C. 2009, *MNRAS*, 399L, 179, and Dr. Alison Sills and Dr. Christian Knigge are co-authors. Chapters 4 and 5 have both been accepted for publication in the *MNRAS*, however they had not yet been assigned journal codes at the time of publication of this thesis. Dr. Alison Sills and Dr. Christian Knigge are co-authors on both of these two publications. Dr. Knigge provided a great deal of guidance in choosing the appropriate statistical techniques throughout all of our analyses, and offered considerable advice in analyzing and interpreting our results. He also had a number of noteworthy creative contributions to the analytic model presented in Chapter 5. All previously published material has been reformatted to conform to the required thesis style. I grant an irrevocable, non-exclusive license to McMaster University and the National Library of Canada to reproduce this material as part of this thesis.

# Acknowledgements

The work presented in this thesis represents the culmination of over 6 years of research. I did not embark upon this endeavor alone, and here I wish to thank the people who supported me the most along the way.

First and foremost, I owe a profound thank you to my thesis supervisor Dr. Alison Sills. Her patient guidance, support, and friendship made my journey through graduate school not only successful, but also a hell of a lot of fun. I am grateful for all of her creative input and meticulous advice, and this thesis has been made immeasurably stronger because of it. Her dedicated support of my education and her relentless encouragement of my pursuits were unwavering. The woman is a hero. A heart-felt thank you must also be extended to Dr. Christian Knigge and Dr. Robert Mathieu whose guidance, advice and tutelage have played a significant role in shaping my abilities and identity as a researcher and scientist.

I also wish to thank my parents. I am incredibly fortunate to be able to look upon my parents as my greatest and most trusted friends. There is nobody in this world who knows me better, and your acceptance and support have meant everything to me. This thesis is for you. A sincere thank you to my brother Peter as well, for setting the bar high when it came to a great many things. Despite being the big brother, I have looked up to you often.

I also wish to thank my thesis advisors and committtee members Dr. Bill Harris, Dr. Alan Chen, Dr. Michael Shara, Dr. Christine Wilson and Dr. Ethan Vishniac. Your insight and guidance have helped me greatly, and this thesis would not be what it is without you.

Finally, I wish to thank my friends and collaborators. You have influenced me in countless ways, and have helped shape my perception of the world. Not only have your words given me inspiration, they have made me laugh, smile and cry time and time again. For this I will always be grateful. There are too many of you to list here by name, however Dr. Aaron Geller,

Dr. Evert Glebbeek, Dr. Charles-Philippe Lajoie and Dr. David Chernoff must be mentioned explicitly for their contributions to the work presented in this thesis, and for their exhaustive efforts in dumbing-down concepts to a sufficiently basic level that I can understand them.

"Imagination is more important than knowlege."

---

Albert Einstein (1879-1955)

"The surest way to corrupt a youth is to instruct him to hold in higher esteem those who think alike than those who think differently."

---

Friedrich Nietzsche (1844-1900)

"When the going gets weird, the weird turn pro."

---

Hunter S. Thompson (1937-2005)

"Instead of building newer and larger weapons of mass destruction, I think mankind should try to get more use out of the ones we have."

---

Jack Handey (1949-present)

# Table of Contents

**Abstract** iii

**Co-Authorship** vii

**Acknowledgments** viii

**List of Figures** xv

**List of Tables** xvii

**Chapter 1**
**Introduction** 1
1.1 Stellar Populations in Star Clusters . . . . . 5
1.1.1 Single Star Evolution . . . . . 5
1.1.2 Additional Features of Colour-Magnitude Diagrams . . 11
1.1.2.1 Horizontal Branch Morphology . . . . . 12
1.1.2.2 Blue Stragglers . . . . . 14
1.1.2.3 Binary Stars . . . . . 18
1.2 Stellar Dynamics in Star Clusters . . . . . 19
1.2.1 Two-Body Relaxation . . . . . 20
1.2.2 Small-N Dynamics . . . . . 24
1.3 Where To Go From Here . . . . . 26

**Chapter 2**
**An Analytic Technique for Constraining the Dynamical Origins of Multiple Star Systems Containing Merger Products** 38
2.1 Introduction . . . . . 38
2.2 Method . . . . . 41

2.2.1 Conservation of Energy . . . 43
2.2.2 Generalized Approach . . . 50
2.3 Results . . . 58
2.3.1 The Case of S1082 . . . 59
2.3.2 The Period-Eccentricity Distribution of the Blue Straggler Binary Population in NGC 188 . . . 66
2.4 Summary & Discussion . . . 79

**Chapter 3**
**Stellar Populations in Globular Cluster Cores: Evidence for a Peculiar Trend Among Red Giant Branch Stars 97**
3.1 Introduction . . . 97
3.2 The Data . . . 99
3.3 Results . . . 100
3.4 Discussion . . . 106
3.4.1 Stellar evolution . . . 107
3.4.2 Single star dynamics . . . 107
3.4.3 Binary effects . . . 109
3.4.4 Core helium-burning stars . . . 110
3.4.5 An evolutionary link with blue stragglers? . . . 111
3.5 Summary . . . 112

**Chapter 4**
**Dissecting the Colour-Magnitude Diagram: A Homogeneous Catalogue of Stellar Populations in Globular Clusters 116**
4.1 Introduction . . . 116
4.2 Method . . . 121
4.2.1 The Data . . . 121
4.2.2 Stellar Population Selection Criteria . . . 122
4.2.3 Spatial Coverage . . . 124
4.2.4 King Models . . . 125
4.3 Results . . . 126
4.3.1 Catalogue . . . 126
4.3.2 Population Statistics . . . 128
4.3.3 Blue Stragglers and Single-Single Collisions . . . 136
4.4 Summary & Discussion . . . 137
4.4.1 Blue Stragglers . . . 138
4.4.2 Red Giant Branch Stars . . . 141
4.4.3 Horizontal Branch Stars . . . 144
4.4.4 Additional Considerations . . . 144

**Chapter 5**
**An Analytic Model for Blue Straggler Formation in Globular Clusters** **157**
5.1 Introduction . . . 157
5.2 The Data . . . 160
5.3 Method . . . 161
5.3.1 Model . . . 162
5.3.1.1 Stellar Collisions . . . 163
5.3.1.2 Binary Star Evolution . . . 166
5.3.1.3 Migration Into and Out of the Core . . . 167
5.3.2 Statistical Comparison with Observations . . . 170
5.4 Results . . . 171
5.4.1 Initial Assumptions . . . 172
5.4.2 Binary Fraction . . . 172
5.4.3 Average BS Lifetime . . . 177
5.4.4 Migration . . . 178
5.4.5 Average Binary Semi-Major Axis . . . 180
5.5 Summary & Discussion . . . 181

**Chapter 6**
**A New Quantitative Method for Comparing the Stellar Mass Functions in a Large Sample of Star Clusters: Evidence for a Universal Initial Mass Function in Massive Star Clusters in the Early Universe** **194**
6.1 Introduction . . . 194
6.2 Method . . . 199
6.2.1 The Data . . . 199
6.2.2 Mass Bin Selection Criteria . . . 200
6.2.3 Weighted Lines of Best-Fit . . . 201
6.3 Results . . . 204
6.4 Summary & Discussion . . . 209

**Chapter 7**
**Summary & Future Work** **221**

**Chapter A**
**Appendix A** **228**

**Chapter B**
**Appendix B** **231**

# List of Figures


1.1 An image taken with the *Hubble Space Telescope* of the globular cluster NGC 7078 . . . . . 2
1.2 CMD for the Milky Way globular cluster NGC 6205 . . . . . 7
1.3 CMD sections for the Milky Way globular clusters NGC 6205, NGC 104, NGC 1261 and NGC 6934 . . . . . 13

2.1 Plot showing the parameter space in the $f_b$-$f_t$ plane for which each of the various encounter types dominate . . . . . 52
2.2 Plot showing the typical periods of BS binaries expected to form during 1+3 encounters in which the hard inner binary of the triple merges . . . . . 76
2.3 Histogram of the period distribution expected for BS binaries formed during 1+3 encounters . . . . . 78

3.1 Colour-magnitude diagram for NGC 362 in the (F439W-F555W)-F555W plane. Boundaries enclosing the selected RGB, HB and MSTO populations are shown. . . . . 101
3.2 $N_{core}$ versus $N_{MS,RGB,HB}$ . . . . . 104

4.1 Plot showing the parameter space in the (F606W-F814W)-F814W plane defining each of the different stellar populations for the GC NGC 6205 . . . . . 124
4.2 Plot showing the RA and Dec coordinates for all stars in NGC 6205 . . . . . 125
4.3 Plot showing for each circle the logarithm of the number of stars belonging to each stellar population as a function of the logarithm of the total stellar mass . . . . . 130
4.4 Plot showing for each annulus the logarithm of the number of stars belonging to each stellar population as a function of the logarithm of the total stellar mass . . . . . 131

4.5 Plot showing the logarithm of the number of BSs predicted to have formed in the core from single-single collisions versus the logarithm of the observed number of BSs in the core. . . . . 137

5.1 The predicted number of BSs plotted versus the total stellar mass in the core for the best-fitting model parameters found for our initial choice of assumptions . . . . . 173
5.2 The predicted number of BSs plotted versus the total stellar mass in the core for the best-fitting model parameters found using the binary fractions of Sollima et al. (2007) with $f_b^{min} = 0.01$ 175
5.3 The predicted number of BSs plotted versus the total stellar mass in the core for the best-fitting model parameters found using the binary fractions of Sollima et al. (2007) with $f_b^{min} = 0.1$ 176
5.4 The predicted number of BSs plotted versus the total stellar mass in the core for the best-fitting model parameters found using an average BS lifetime of 5 Gyrs and the relation for the cluster binary fraction provided in Equation 5.14 with $f_b^{min} = 0.1$ 179

6.1 Logarithm of the number of stars belonging to each mass bin as a function of the logarithm of the total number of stars spanning all five mass bins in the core . . . . . 205
6.2 Logarithm of the number of stars belonging to each mass bin as a function of the logarithm of the total number of stars spanning all five mass bins within two core radii from the cluster centre 207
6.3 Logarithm of the number of stars belonging to each mass bin as a function of the logarithm of the total number of stars spanning all five mass bins within three core radii from the cluster centre 208
6.4 Mass Functions in Pie Chart Form . . . . . 210

# List of Tables


4.1 Stellar Population Catalogue . . . . . 127
4.2 Lines of Best Fit for $\log(M_{circle}/10^3)$ Versus $\log(N_{pop})$ . . . . . 132
4.3 Lines of Best Fit for $\log(M_{annulus}/10^3)$ Versus $\log(N_{pop})$ . . . . 133

6.1 Lines of Best Fit for $\log N_{MS} = (a \pm \Delta a)\log (N_{tot}/10^3) + (b \pm \Delta b)$ . . . . . 206

A.1 Pericenters Assumed for Each Encounter Type . . . . . 229

Chapter 1

# Introduction

The vast majority of the stars in our Universe are found in galaxies, each of which is typically populated by billions of members. The hierarchy of stellar communities within galaxies can be understood if an analogy is made between stars and people. In this context, parallels can be drawn between galaxies and countries, star clusters and cities, as well as multiple star systems and families. It is now known that at least half of the stars in galaxies were born in star clusters (e.g. Kroupa, 2002; Kroupa & Boily, 2002), spherical conglomerates composed of anywhere from a few hundred to a few million members all orbiting their common center of mass (see Figure 1.1). Within these stellar nurseries, around 50% of all stars are thought to spend the majority of their lives in close proximity to one or more of their siblings by forming multiple star systems (e.g. Durisen & Sterzik, 1994; Bate & Bonnell, 1997; Bate, 1997; Kroupa, 2001; Sollima et al., 2010). Most of these are binary star systems, which consist of two stars orbiting their common centre of mass under the influence of their mutual gravitation attraction. Although less common, stable configurations of triple, quadruple and quintuple star systems also exist, along

with even higher order multiples (e.g. Latham, 2005; Eggleton & Tokovinin, 2008; Tokovinin, 2008). Despite the fact that stars typically spend at most a small fraction of their considerably long lives in even relative isolation, our understanding of the mechanisms via which the presence of their siblings can affect their evolution is far from complete.



Figure 1.1 An image taken with the *Hubble Space Telescope* of NGC 7078 (M15), a globular cluster in the Milky Way galaxy. Image credit: NASA, ESA, and The Hubble Heritage Team.

Gravity mediates a wide variety of interactions between stars. Within the dense cores of star clusters, for instance, strong gravitational encounters often occur in which the distance of closest approach is comparable to the radii of the stars (e.g. Spitzer & Thuan, 1972; Spitzer & Shull, 1975; Heggie, 1975; Hut & Bahcall, 1983). These encounters often lead to complex dances that can result in stars being ejected from their host clusters (e.g. Henon, 1969;

Hut & Djorgovski, 1992; Kroupa & Boily, 2002; De Marchi, Paresce & Portegies Zwart, 2010), or even stellar collisions (e.g. Leonard, 1989; Sills et al., 2001). Binary stars are also at the mercy of gravity and, if their orbital separation becomes sufficiently small, this can lead to the transfer of mass from the surface of one component to the other (McCrea, 1964), or even their complete coalescence (e.g. Andronov, Pinsonneault & Terndrup, 2006). Not only are gravitational interactions important for stellar mergers, they also drive the evolution of star clusters. Gravity slowly acts to dissolve clusters, continuously ejecting stars so that they may join the rest of the Galactic population (e.g. Portegies Zwart et al., 2001). It follows that a complete understanding of the dominant physical processes operating in clusters, including how their stars are formed and the dynamical interactions that cause their stars to escape, is a key ingredient in piecing together the history of our Galaxy.

Mergers are a particularly interesting and important outcome of stellar interactions. Observations have revealed numerous examples of curious stars and mysterious astrophysical processes that are thought to be related to stellar mergers (e.g. Sandage, 1953; Webbink, 1984; Paczynski, 1986; Troja, Rosswog & Gehrels, 2010; Miroshnichenko et al., 2007; Farrell et al., 2009). Many of these objects are commonly found in dense star clusters, hinting at the complexity of their dynamical evolution and the potential importance of dynamics for stellar mergers. Although their origins remain unknown, some of these objects have served as important tools for furthering our understanding of the Universe. For instance, Type Ia supernovae have provided the most robust constraints to date for the rate of Universal expansion (e.g. Perlmutter et al., 1999). Despite their considerable astrophysical significance, we are far from completely understanding the physical mechanisms that cause mergers to occur.

Stellar mergers are but one example of this ubiquitous physical process, which occurs between objects on many scales. From colliding galaxies to fusing atoms, mergers occur on spatial and temporal scales ranging by many orders of magnitude. Familiar principles such as conservation of energy and momentum often apply, however, regardless of scale. This is certainly the case for the various forms of dynamical interactions that lead to mergers. Examples include chemical reactions in the interstellar medium, strong gravitational interactions involving massive black holes and even encounters between galaxies in galaxy clusters. It follows that the development of tools designed to further our understanding of stellar dynamics and mergers also have applications for a number of other physical sub-disciplines.

In this thesis, we present statistical and theoretical techniques related to the physics of mergers. These are applied to observations of dense star clusters in order to study the mergers of stars. In this chapter, we will outline our motivation for conducting this research. In Section 1.1, we briefly review our current understanding of stellar evolution theory, and discuss the observed properties of star clusters and their stellar populations, including the various types of stellar exotica. In Section 1.2, we provide a brief description of the dominant physical processes that drive the dynamical evolution of star clusters. All of these issues are connected in Section 1.3, where we describe how they have motivated the development of the techniques that will be presented in this thesis, along with their application to observations of star clusters.

## 1.1 Stellar Populations in Star Clusters

### 1.1.1 Single Star Evolution

By serving as sites for star formation, star clusters have played a crucial role in shaping the present-day features of our Galaxy. And yet, this is but one example of their astrophysical significance. Star clusters are also ideal laboratories for learning about stellar evolution. Historically, their importance in this regard has stemmed from the often-adopted assumption that all of the stars in a given cluster were born from the same gas cloud at more or less the same time. If true, star clusters offer a large sample of stars with a wide range of masses, but a very narrow range in both age and chemical composition. Therefore, observations of star clusters offer robust constraints for stellar evolution theories by providing direct tests for their predictions for a diverse spectrum of stellar masses of known age and composition.

Colour-magnitude diagrams (CMDs) are one of the most important tools available to astronomers for studying stellar evolution (Hertzsprung, 1909). In these diagrams, the observed surface temperature is plotted against luminosity (or brightness) for every star in the cluster. The latter quantity is plotted backwards, and provides a proxy for colour – hot stars are blue and cool stars are red. This creates a characteristic appearance that is observed in all cluster CMDs. An example is shown in Figure 1.2 for the GC NGC 6205. This characteristic shape can be understood by considering two principles of stellar evolution. The first is called the Vogt-Russell Theorem and states that the mass, composition and age of a star uniquely determine its radius, luminosity and internal structure, in addition to its subsequent evolution (Vogt, 1925; Russell, 1925). The second is simply that the rate at which a star evolves, and

in so doing changes its brightness and colour, is inversely proportional to some power of its mass (e.g. Iben, 1991). It follows that, for a cluster composed of a large number of stars with a distribution of masses but similar compositions (at birth) and ages, the most massive stars are also the most evolved. Therefore, every evolutionary phase in the life of a star is typically represented in at least moderately old clusters, and this causes the distribution of stars in the CMD to adhere to the characteristic shape shown in Figure 1.2. Our understanding of single star evolution is sufficiently complete that it is now known how this shape changes as a function of composition and age. In general, the majority of the features characteristic of CMDs are well understood, although exceptions do exist. Before getting to these in Section 1.1.2, we will review the life cycle of a typical star in our Galaxy and connect each evolutionary phase to its corresponding location in the CMD.

Most of the star clusters in our Galaxy were born from gas clouds composed primarily of hydrogen and, to a lesser extent, helium (as well as heavier elements in trace amounts) (e.g. Lada, 1985; Pringle, 1989). Gravity contracted the gas into clumps, which grew increasingly hot and dense as they accreted material from the surrounding medium. When the central temperature of a clump becomes sufficiently high (on the order of $10^7$ K), hydrogen is ignited at its centre. A star is born. This marks the beginning of the main-sequence (MS) phase, during which time hydrogen is fused into helium in the stellar core.

Let us consider the life of a typical low-mass star in the Milky Way, from beginning to end. Most of the stars in our Galaxy have low masses roughly spanning the range $0.08 \lesssim m \lesssim 2.0$ $M_\odot$ (e.g. Kroupa, 2002). There are two reasons for this. First, the least massive stars are also the longest

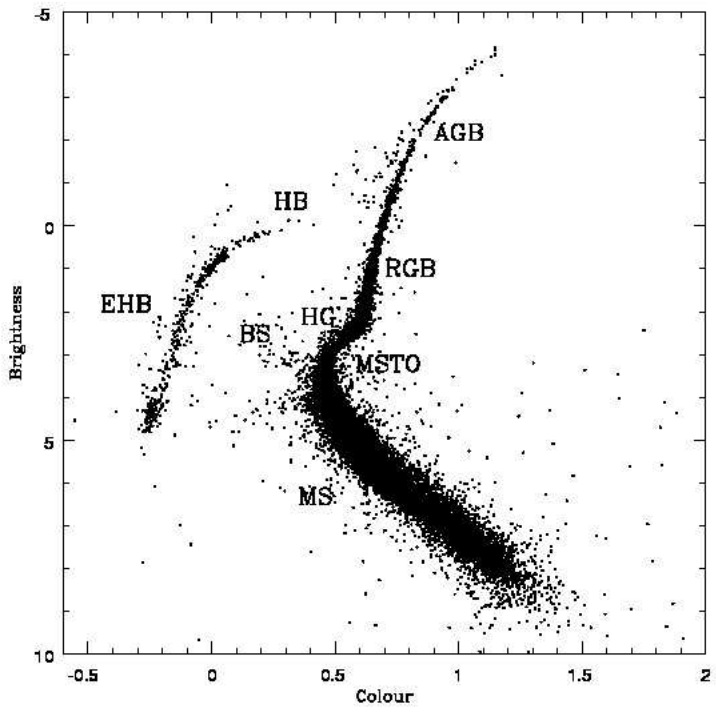



Figure 1.2 Colour-magnitude diagram for the Milky Way globular cluster NGC 6205. The data used to create this plot were taken from Sarajedini et al. (2007). As described in the text, the x-axis can be read as temperature (or, equivalently, colour), which increases from right to left (red to blue). On the y-axis, brightness increases from bottom to top. Labels for blue straggler (BS), red giant branch (RGB), horizontal branch (HB), extended horizontal branch (EHB), asymptotic giant branch (AGB), Hertzsprung gap (HG), main-sequence turn-off (MSTO) and main-sequence (MS) stars are shown. Stars with large photometric errors have been omitted from this plot.

lived. Second, Salpeter (1955) showed that the initial distribution of stellar masses for stars in the solar-neighbourhood with masses in the range $0.4 - 10$ $M_\odot$ can be described by a power-law form with an index $\alpha \sim 2.35$. Today, we know that the distribution flattens below $\sim 0.5$ $M_\odot$, however the primary conclusion is the same: most of the stars in our Galaxy have masses lower than that of our Sun. What's more, most of these are MS stars since, for stars

of very low-mass, the time-scale for this evolutionary phase exceeds the age of the Universe.

Nuclear reactions in the stellar core release heat, and are the primary source of energy generation within stars, driving their high luminosities (e.g. Clayton, 1968). The transport of energy outward within stars in turn causes their compositional and structural profiles to evolve. This occurs on a typically slow time-scale on the order of millions of years or longer (e.g. Kippenhahn & Weigert, 1990; Maeder, 2009). Both the rate and outcome of the complex interplay of physical processes occurring within stars to drive their evolution depend somewhat sensitively on their mass. As a result, stellar evolution varies considerably between low- and high-mass stars. Below, we focus our description of this evolution to stars with masses $\lesssim 2.0$ $M_{\odot}$.

The MS crosses the CMD from bottom right to top left, as shown in Figure 1.2. During the MS phase, the radius (and hence surface temperature) and luminosity of a star are primarily determined by its mass, however its age and initial composition also contribute (e.g. Iben, 1991; Tout et al., 1996). As a result, the lowest mass stars in a cluster occupy the bottom right end of the MS, with stellar mass increasing upward and blue-ward. Most stars spend the majority of their lives on the MS slowly converting hydrogen into helium in their cores. After slowly increasing their radius and luminosity by a factor of about 2.5-3, stars reach the end of the MS phase of their evolution (Eggleton, 2006). This can roughly be defined as the point at which the hydrogen fuel within a central core containing about 10% of the star's mass has run out. Found at the left-most tip of the MS in the CMD, called the main-sequence turn-off (MSTO), the most massive MS stars are in the process of depleting their hydrogen fuel in and near their centres. At this point, loosely referred

to as the terminal-age main-sequence (TAMS), stars leave the MS and start moving to the right across the CMD, becoming increasingly red.

The stellar evolution time-scales shorten considerably at this point, and the helium core begins to contract while the envelope expands. This causes a drop in the surface temperature of the star, causing it to move horizontally across the CMD, crossing what is called the Hertzsprung gap (Figure 1.2) (e.g. Popper, 1980). The reason for this rapid reddening can be understood as follows. Once the surface temperature drops well below about $10^4$ K, the primary mechanism of energy transport in the envelope changes (Eggleton, 2006). This is because the drop in temperature allows free electrons to recombine with free protons to form hydrogen atoms, which can then act to absorb out-going radiation. This presents a challenge for the star since energy still needs to be transported outward from its nuclear-burning centre, yet radiation can no longer leak out freely. To compensate, convection takes over as the dominant form of energy transport (e.g. Bohm-Vitense, 1958). As the convective base of the envelope deepens, stars of a given luminosity and mass converge to an approximately unique radius. The change in stellar radius that occurs during this short-lived phase of evolution can range from a factor of less than two for very low-mass stars to a factor of $\gtrsim 100$ for very massive stars (Iben, 1991). This marks the beginning of the red giant branch (RGB) phase of evolution, and the base of its corresponding sequence in the CMD (Figure 1.2).

Due to the unique envelope structure created by the deepening of the convective envelope, stars of a given mass but different luminosities must lie on a roughly vertical locus in the CMD (Hayashi, Nishida & Sugimoto, 1962). This structure also causes the stellar luminosity to increase steeply as a function of the mass of the helium core (e.g. Iben, 1968). As hydrogen burning

progresses in a shell immediately outside the core, the helium that is produced rains down onto it, slowly increasing its mass. This in turn causes the star to brighten by up to several orders of magnitude and, in so doing, ascend the RGB in the CMD.

Eventually, the mass and temperature of the helium core reach $\sim 0.47$ $M_\odot$ and $\sim 10^8$ K, respectively, although the precise values depend on both the total stellar mass and chemical composition (Eggleton, 2006). It is at this point that helium ignites, producing mainly carbon at first, although later the production of oxygen takes over. The horizontal branch (HB) in CMDs (Figure 1.2) corresponds to the core-helium burning phase. It is not clear why HBs show such a large spread in their colours since, in principle, both the luminosity and surface temperature should be roughly constant for core helium-burning stars. This mysterious and ubiquitous feature of CMDs marks a significant gap in our understanding of stellar evolution theory. We will return to the curious HB morphologies observed in the CMDs of old star clusters in Section 1.1.2.1.

Within about $10^8$ years of the onset of core helium-burning, low-mass stars will typically possess a core composed of carbon and oxygen with a mass of $\sim 0.55$ $M_\odot$ (Iben, 1974). The core is surrounded by a much less massive shell composed primarily of helium and next to no hydrogen. This, in turn, is surrounded by an envelope of unprocessed material extending out to 30-50 $R_\odot$ from the core (Maeder, 2009). Two burning shells now power the star as it continues its rise in luminosity above the RGB. The sequence in the CMD corresponding to this phase of evolution is called the asymptotic giant branch (AGB). As this phase progresses, the radius and luminosity of the star continue to grow and severe mass-loss typically occurs due to powerful stellar winds.

The life of a typical low-mass star ends when the last of its envelope is burnt, leaving its luminosity to plummet by several orders of magnitude and its surface temperature to increase dramatically. The product is an incredibly dense remnant composed of carbon and oxygen called a C/O white dwarf (WD) (Iben, 1974). This the case for stars with masses up to $\sim 2$ $M_{\odot}$ when mass-loss on the AGB is factored in (Eggleton, 2006). For stars more massive than this, stellar death can be considerably more dramatic, ending in the ignition of carbon and a subsequent thermonuclear explosion. As previously explained, these stars are short-lived and do not occur commonly in old star clusters, which will be the focus of this thesis. Therefore, we refer the interested reader to Clayton (1968) and Maeder (2009) for descriptions of the evolution of massive stars.

### 1.1.2 Additional Features of Colour-Magnitude Diagrams

There remain several features characteristic of CMDs that cannot be explained by standard single star evolution. In order to account for their existence, it is necessary to invoke the aid of other physical processes known to be operating in star clusters, such as binary star evolution and stellar dynamics. As described in the subsequent sections, these processes are thought to be responsible for producing various types of exotic stellar populations and multiple star systems. These curious objects typically appear as outliers in CMDs, and do not fall on any single star evolution tracks. We will discuss the various mysterious features of CMDs and types of stellar exotica known to populate star clusters, and review the currently favoured hypotheses for their origins.

#### 1.1.2.1 Horizontal Branch Morphology

The horizontal branches of star clusters in the Milky Way have been observed to display a range of morphologies. That is, most CMDs have a horizontal sequence that extends blue-ward from the top of the red giant branch, and this is referred to as the horizontal branch. However, the length and appearance of this sequence varies considerably from cluster-to-cluster and, in some cases, it makes a sharp vertical transition to dimmer luminosities at its blue-most tip. CMDs are shown in Figure 1.3 for four different clusters, each of which has a distinct HB morphology. The source of this variance is unknown, however our current best guess is mass-loss due to stellar winds, most likely on the RGB (e.g. Iben, 1974; Dotter et al., 2010). The more mass-loss that occurs, the smaller the mass of the remaining envelope. The surface temperature increases with decreasing envelope mass since this leaves more of the hot core exposed. Consequently, the amount of mass-loss is thought to determine the colours of HB stars, with stars that experience the greatest loss in mass ending up the bluest. In order to reproduce the observed surface temperatures of the hottest HB stars, the envelope must lose a mass of 0.2-0.3 $M_{\odot}$ (Eggleton, 2006). This seems reasonable and agrees rather well with empirical estimates (e.g. Judge & Stencel, 1991). It is not yet clear, however, why stars of comparable mass in the same cluster would experience such different degrees of mass-loss. It is also unknown how or why this mass-loss distribution should change from cluster-to-cluster, although the rate of mass-loss is thought to depend on metallicity (e.g. Reimers, 1975).

Previous studies have confirmed that the observed differences in the HBs of Milky Way clusters are related to metallicity (Sandage & Wallerstein,

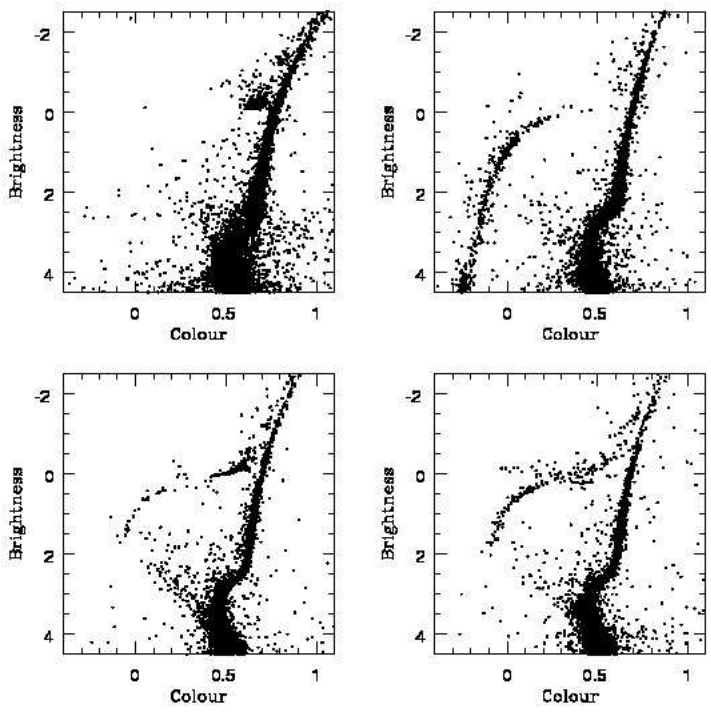



Figure 1.3 Colour-magnitude diagram sections for the Milky Way globular clusters NGC 104 (top left inset), NGC 6205 (top right inset), NGC 1261 (lower left inset) and NGC 6934 (lower right inset). Note the distinct HB morphology characteristic of each cluster. Blue stragglers are also clearly visible just brighter and bluer than the MSTO. The data used to create this plot were taken from Sarajedini et al. (2007).

1960). This does not tell the whole story, however, since at least one additional parameter is required to explain the spread in their colours (see Figure 1.3). Many cluster properties have been suggested as possible Second and Third Parameters. These include age, the cluster luminosity and central density. Unfortunately, no definitive candidates have as of yet been identified (e.g. Rood, 1973; Fusi Pecci et al., 1993). Notwithstanding, observations have revealed several peculiar trends for this curious stellar population in individual clusters. For instance, Saviane et al. (1998) presented evidence that blue HB

stars could be more centrally concentrated than red HB stars in the cluster NGC 1851. Conversely, Cohen et al. (1997) showed that blue HB stars could be centrally depleted relative to other stellar types in the cluster NGC 6205. To date, no clear evidence has been found linking the spatial distributions of HB stars to any global cluster properties.

The bluest HB stars are often called extreme horizontal branch (EHB) stars. It has been suggested that RGB stars can shed their entire envelopes and still ignite helium as EHB stars (d'Cruz et al., 1996). Moreover, it is thought that EHB stars could skip the AGB phase and evolve into WDs directly (e.g. Maeder, 2009). EHB stars also go by the name of sub-dwarf B (sdB) stars. Both are core-helium burning stars with very small outer envelopes. Interestingly, EHB stars in the field tend to have binary companions (Maxted et al., 2001). This could be interpreted as evidence that the presence of a binary companion is responsible for causing the dramatic loss of envelope mass. On the other hand, most EHB stars in clusters have been shown to lack a binary companion (e.g. Moni Bidin et al., 2006, 2009, 2011). Consequently, the mechanism responsible for (at least) *their* extreme mass-loss is still less clear.

#### 1.1.2.2 Blue Stragglers

First discovered by Sandage (1953), blue straggler stars occupy the region of the CMD that is just brighter and bluer than the MSTO (see Figure 1.3). That is, they appear as an extension of the main-sequence. And yet, if all of the stars in a cluster were born at more or less the same time, then standard single star evolution predicts that this region of the CMD should be bare. Normal MS stars that are of sufficiently high mass to occupy this region should have long ago evolved onto the RGB and beyond. The presence of BSs in star

clusters therefore defies the predictions of single star evolution theory, and signifies another one of its mysteries.

This puzzle can perhaps be solved if blue stragglers are produced via the addition of fresh hydrogen to the cores of normal main-sequence stars (e.g. Sills et al., 2001). This is the currently favoured origin for BSs. It can occur via multiple channels, most of which involve the mergers of low-mass MS stars. Stars in binaries can be driven to merge if enough orbital angular momentum is lost. This can be mediated by dynamical interactions with other stars (e.g. Leonard, 1989; Leonard & Linnell, 1992), magnetized stellar winds (e.g. Ivanova & Taam, 2003), tidal dissipation (e.g. Cleary & Monaghan, 1990; Chen & Han, 2008b) or even an outer triple companion (e.g. Fabrycky & Tremaine, 2007; Perets & Fabrycky, 2009). Alternatively, stars can collide directly, although this is also thought to usually be mediated by multiple star systems (Leonard, 1989). Stars in close binaries can transfer mass if their orbital separations become sufficiently small for one of the components to over-fill its Roche lobe. This can also deliver fresh hydrogen to normal MS stars and in so doing produce BSs.

Whatever the dominant BS formation mechanism(s) operating in dense star clusters, dynamical interactions are sufficiently common that they should play at least some role. For example, even if blue stragglers are formed as a result of binary evolution processes such as mass-transfer, the progenitor binaries themselves are expected to have experienced at least one dynamical interaction over the course of their lifetime (e.g. Hut & Bahcall, 1983; Leonard, 1989; Davies, Piotto & De Angeli, 2004). It follows that the study of BSs in star clusters offers an indirect means of probing the interplay between stellar evolution and stellar dynamics.

In order to explain recent observations of BS populations in star clusters, it has been suggested that several BS formation mechanisms operate simultaneously. For example, several studies have reported a bi-modal radial distribution for blue stragglers (e.g. Ferraro et al., 1997, 1999, 2004; Lanzoni et al., 2007; Geller et al., 2008). That is, the number of BSs is the highest in the central cluster regions, then falls off as the distance from the cluster centre increases but eventually rises again in the cluster outskirts. This has primarily been observed in globular clusters (GCs), which are particularly massive, dense and old star clusters usually found in the outer reaches of our Galaxy. One theory proposed to explain this result is that the blue stragglers found in the cluster core were formed from collisions, whereas those in the cluster outskirts were formed from binary mass-transfer (Ferraro et al., 2004). This hypothesis is motivated by the fact that the time-scale for collisions to occur between stars is very short in the core, but drops off considerably in the cluster outskirts where the stellar densities are much lower (Leonard, 1989). Alternatively, it has been suggested that the blue stragglers in the cluster outskirts could have been formed in the core but were later kicked out as a result of dynamical encounters involving binary stars (e.g. Sigurdsson & Phinney, 1993; Mapelli et al., 2006).

A spectroscopic survey of the cluster NGC 188 performed by Mathieu & Geller (2009) revealed that most, if not all, of its BSs have binary companions. Mathieu & Geller (2009) proposed that their results are consistent with the general picture that both mass-transfer and mergers are simultaneously producing BSs in NGC 188, which is also consistent with the results of Chen & Han (2008a). The latter authors fit theoretical stellar evolution tracks to the observed colour-magnitude diagram for NGC 188. Based on their results, they

argue that most BSs in this cluster are too massive to have formed from mass-transfer alone. If true, this suggests that many BSs in NGC 188 must be the products of stellar mergers. In support of this, Perets & Fabrycky (2009) argued that the results of Mathieu & Geller (2009) can be explained if triple stars play an important role in BS formation by acting as catalysts for mergers (Perets & Fabrycky, 2009). Triple stars can evolve internally by transferring angular momentum between their inner and outer orbits. This can cause the eccentricity of the inner binary to increase dramatically (Kozai, 1962). Tidal friction can then act to reduce the orbital separation by removing orbital energy from the inner binary at each periastron passage (Fabrycky & Tremaine, 2007) (the term periastron refers to the point of closest approach for an eccentric binary orbit).

Blue stragglers have also been found in the field of our Galaxy. Observations of these BSs suggest that both mass-transfer and binary coalescence are occurring. For example, Di Stefano et al. (2010) recently reported the discovery of two BSs with white dwarf companions in the field of our Galaxy. The authors suggest that these BSs were formed from mass-transfer when the white dwarf progenitors evolved to ascend the RGB and in so doing over-filled their Roche lobes. Moreover, Brown et al. (2010) discovered a $\sim 9.1$ $M_{\odot}$ hypervelocity MS star in the field. The authors argue that it must be a blue straggler since its flight time from the Milky Way (MW) exceeds its MS lifetime. They conclude that this BS must be the product of a close binary that coalesced sometime after being ejected from the Galactic centre. This could explain its hypervelocity provided its ejection was caused by a dynamical interaction involving the central massive black hole.

Several spectroscopic studies have also been performed to study indi-

vidual BSs in clusters. For example, at least two BSs in the globular cluster 47 Tuc have been found with masses exceeding twice that of the main-sequence turn-off (MSTO) (Shara, Saffer & Livio, 1997; Knigge et al., 2008). The large masses of these BSs suggest that they are the products of the mergers of two or more low-mass MS stars. Another similarly massive BS was reported by van den Berg et al. (2001) in the old open cluster M67. This BS is thought to be a member of a triple star system that contains not one, but two BSs (Sandquist et al., 2003). BSs have been identified in both binaries and triples in several other clusters as well, including the open cluster NGC 6819 (Talamantes et al., 2010).

#### 1.1.2.3 Binary Stars

Unresolved binary stars pollute the CMDs of star clusters, which become peppered with peculiar outliers that do not fall on any single star evolution tracks. This is because clusters are located at sufficiently great distances from us that the components of a given binary pair are indistinguishable and they appear as a single object. The combined light of the binary components blends together, producing a combination of colour and brightness that ordinary single stars are never expected to display over the course of their evolution. This typically creates a secondary sequence in cluster CMDs located above the MS (e.g. Milone et al., 2008). The reason for this is that most cluster binaries are composed of normal MS stars (e.g. Geller et al., 2008), and the combined light of their components makes these binaries appear slightly brighter than ordinary single MS stars.

There are many examples of objects that are almost certainly bonafide cluster members but appear in curious locations in the CMD. Examples in-

clude red stragglers (e.g. Kaluzny, 2003), yellow stragglers (e.g. Latham, 2005), and the sub-subgiant branch stars found in M67 (Mathieu et al., 2003). Red stragglers appear to the right (red-ward) of the RGB, yellow stragglers appear to the left (blue-ward) of the RGB and above the Hertzsprung gap, and sub-subgiant branch stars appear below the Hertzsprung gap. Most of these are thought to be unresolved binaries or triples and, in some cases, their curious CMD locations are speculated to be due to a recent episode of mass-transfer.

## 1.2 Stellar Dynamics in Star Clusters

Star clusters are in many ways analogous to stars themselves. They are both, in effect, self-gravitating spheres of interacting particles. In both cases, gravity plays a key role in driving the structural and compositional changes that characterize their evolution. Virial equilibrium is a central physical principle that deepens this analogy. This condition must be satisfied in order for any self-gravitating system to achieve a state of dynamic equilibrium, at which point the inward pull of gravity is balanced by the outward push of the pressure endowed to the system by the relative motions of its particles. The condition for virial equilibrium in a star cluster can be expressed in the following form:

$$2T + W = 0, \tag{1.1}$$

where $T$ is the total kinetic energy of the system and $W$ is its total gravitational energy. Although additional physics must be factored in, such as the energy generated from nuclear-burning, a similar criterion for virial equilibrium exists for stars (e.g. Chandrasekhar, 1939). It follows that star clusters are virialized

systems composed of objects which are themselves virialized.

Both short- and long-range gravitational interactions between stars act to evolve the structures and compositions of star clusters on time-scales ranging from millions to billions of years. In the following sections, we describe the primary dynamical processes responsible for this evolution.

### 1.2.1 Two-Body Relaxation

Although many of the details are still unclear, star clusters are thought to be born from massive gas clouds that fragment on several length scales to form a large number of stars (e.g. Lada & Lada, 1995; McKee & Ostriker, 2007). It ends up that the presently observed structures of star clusters are largely independent of the details of this collapse. This is because gravity will quickly act to mix the stars into a gravitationally-bound spherical distribution for almost any initial configuration (Heggie & Hut, 2003). Once settled, most of the stars in a cluster will traverse stable orbits, often with rosette-shapes, throughout it (Heggie & Hut, 2003). Their paths will typically remain more or less undisturbed during a single orbit. Over longer time-scales, however, the motions of the stars are affected by the cumulative effects of distant gravitational encounters as well as the odd close encounter.

Like stars, star clusters evolve via the slow diffusion of heat from their centres to their outer edges. Gravitational encounters between pairs of stars act as the mechanism for heat transport in much the same way collisions between pairs of molecules govern the flow of heat throughout an ideal gas. In the case of star clusters, however, it is the cumulative effect of many weak, and therefore distant, encounters that dominates, as opposed to the odd strong or

close encounter (Heggie & Hut, 2003). This process is called two-body relaxation. The time-scale for it to occur, called the relaxation time, is considerably longer than the time required for a given star to cross the length of the cluster, called the crossing time. A useful measure of the relaxation time for the entire cluster comes from the half-mass relaxation time $t_{rh}$, which is calculated from average quantities inside the half-mass radius $r_h$ (defined as the distance from the cluster centre containing half its total mass). This is given by:

$$t_{rh} \sim \frac{0.138 N^{1/2} r_h^{3/2}}{(Gm)^{1/2} ln\Lambda}, \tag{1.2}$$

where $m$ and $N$ are the average stellar mass and the total number of stars inside $r_h$, respectively. The Coulomb logarithm $\ln\Lambda$ is the factor by which small-angle encounters (i.e. encounters for which the angle between the initial and final velocity vectors of the deflected star is small) are more effective than large-angle encounters in a star cluster with given density and velocity distributions.

For a typical Milky Way GC, $t_{rh}$ is on the order of a billion years. GCs are among the oldest objects in the Universe, with ages usually ranging from $\sim$ 9-12 Gyrs (e.g. De Angeli et al., 2005). Consequently, we expect that most will have had sufficient time for two-body relaxation to have played a significant role in shaping their present-day features. Indeed, two-body relaxation has been shown to dominate cluster evolution for a significant fraction of the lives of old MW GCs (e.g. Gieles, Heggie & Zhao, 2011). Other effects also play their part. For example, mass-loss due to stellar evolution has also been shown to affect the dynamical evolution of star clusters, although its primary role is played during their early evolutionary phases when mas-

sive stars with powerful stellar winds are still present (e.g. Applegate, 1986; Chernoff & Weinberg, 1990; Fukushige & Heggie, 1995). The gas expelled by these winds can be significant. It escapes from the cluster, which expands in response to the loss in mass. This serves to delay the evolutionary progression induced by two-body relaxation.

Equation 1.2 provides only a rough guide since the cumulative effects of two-body encounters depend on the stellar mass. This brings us to another central concept of stellar dynamics: equipartition of kinetic energies (e.g. Henon, 1969; Giersz & Heggie, 1996). This is the tendency for all stars in a cluster to end up with comparable kinetic energies. This results from the fact that, during an individual gravitational encounter, the more massive star will impart a net positive acceleration to the less massive star, increasing its speed. This comes at the expense of the kinetic energy of the more massive star, which receives a corresponding net deceleration and slows down. In systems where stars of widely differing mass occur, which is the case for real star clusters, the cumulative effects of these gravitational encounters cause stars with masses greater than the average stellar mass to lose kinetic energy. As a result, massive stars tend to slow down and sink to lower orbits within the cluster potential. At the same time, stars with masses less than the average stellar mass tend to gain kinetic energy and speed up, causing them to rise within the potential well of the cluster. In conjunction with close encounters occurring primarily within the dense cluster core, this process contributes to a steady stream of stars escaping from the system. The important point is that the stars that comprise clusters are all born with comparable *velocities*, but over time they tend toward a state in which they all have comparable *kinetic energies*.

The tendency for the most massive stars in a cluster to accumulate in the central regions and low-mass stars to be dispersed to wider orbits is called mass segregation. The time-scale for it to occur is typically short compared to the half-mass relaxation time. This can be understood as follows. The time-scale on which two-body encounters operate on an average star of mass $m$ has been shown to be well-approximated by Equation 1.2 (Spitzer, 1987). In general, however, the time-scale on which this process operates on a star of mass $M >> m$ is given by (Vishniac, 1978; Spitzer, 1987):

$$t_r \sim \frac{m}{M} t_{rh}. \tag{1.3}$$

This implies that the most massive stars in a cluster will segregate into the core on a time-scale much shorter than $t_{rh}$. It follows that most GCs will become fully mass segregated very early on in their lifetimes (e.g. Gaburov & Gieles, 2008; McMillan, Vesperini & Portegies Zwart, 2007). This means that the spatial distributions of their stars become stratified according to their mass. In other words, the probability of finding a star in the cluster outskirts is inversely proportional to its mass. It is important to note, however, that we still see a range of masses at all cluster radii.

Two-body relaxation is one of the primary mechanisms responsible for the transfer of heat outward within a cluster. This causes the inner cluster regions to contract, and the outer regions to expand. To see why this is the case, consider what occurs if energy is transferred from the inner part of an isolated system of gravitationally-interacting particles to the outer part. The inner part should cool. However, gravity then causes these stars to drop to lower orbits within the cluster potential and, in so doing, speed up. The net

effect of this is that the average velocity of stars in the inner part increases, causing its temperature to increase. The energy transferred to the outer part causes it to heat up as well, but it expands in response to the addition of heat. In general, the increase in the temperature of the outer part is larger when it is smaller in size. This creates a temperature gradient between the inner and outer parts. As a result, more heat flows outward and the temperature gradient is enhanced. This leads to a runaway effect that has been dubbed the gravothermal catastrophe. For typical MW GCs, a phenomenon known as core collapse occurs within about 10-20 half-mass relaxation times (Henon, 1969; Spitzer & Shull, 1975; Hut & Djorgovski, 1992). This marks an enhancement in the central density by several orders of magnitude.

Theoretical models suggest that the time-scale for core collapse to occur is often longer than the age of the Universe. Therefore, most MW GCs should currently be in a phase of core contraction. This evolutionary phase will only come to an end once the central density becomes sufficiently high for encounters involving binaries to halt the process (e.g. Hut, 1983; Goodman & Hut, 1993; Fregeau, Ivanova & Rasio, 2009). The net effect of these interactions is for single stars to steal energy from the orbits of the binaries. This imparts additional kinetic energy to the single stars at the expense of reducing the orbital separations of the binaries. In turn, this provides a heat source for the cluster, and ultimately halts the collapse of the core.

### 1.2.2 Small-N Dynamics

Our discussion of cluster evolution has naturally brought us to the issue of small-N gravitational dynamics. These are short-range interactions involving

only a few stars for which the distance of closest approach can be comparable to the stellar radii. During single-binary and binary-binary encounters, resonant interactions often occur in which the stars remain bound for many crossing times. Two objects (where an object can refer to a single, binary or even triple star) approach one another and a series of close, or strong, gravitational interactions ensue. A number of outcomes are possible. These include exchanges between the components of binaries or even their complete dissociation, the formation of triples, as well as stellar collisions and mergers.

Numerous scattering experiments have been performed to explore the outcomes of binary-binary and, in particular, single-binary encounters (e.g. McMillan, 1986; Sigurdsson & Phinney, 1993; Fregeau et al., 2004). Most of the earliest of these studies were performed in the point-particle limit. Consequently, they ignored the the stars' finite sizes, and so neglected the importance of taking into account the dissipative effects of tidal interactions and direct contact between stars (e.g. Hut & Verbunt, 1983; Mikkola, 1983). This was later remedied by, for instance, McMillan et al. (1987) and Cleary & Monaghan (1990). Encounters involving four or more stars require longer integration times to run the simulations to completion, and involve a large number of free parameters. As a result, few studies have been conducted to explore the outcomes of binary-binary encounters or interactions involving triple systems. To date, none of these have considered the finite sizes of the stars in a completely realistic way.

It has been known for some time that encounters between stars, and even direct collisions, can occur frequently in dense stellar systems (Hills & Day, 1976; Hut & Verbunt, 1983; Leonard, 1989, e.g.). In the cores of globular clusters (GCs), the time between collisions involving two single stars can be much

shorter than the cluster lifetime (Leonard, 1989). The time between encounters involving binary stars can be considerably shorter still given their much larger cross-sections for collision. In globular and, especially, open clusters with high binary fractions, mergers are thought to occur frequently during resonant interactions involving binaries (e.g. Leonard & Linnell, 1992). What's more, collision products have a significant probability of undergoing a second or even third collision collision during a given single-binary or binary-binary interaction. This is because the impact causes the collision product to expand, increasing the cross-section for a subsequent collision to occur (e.g. Fregeau et al., 2004).

Small-N dynamical interactions play a number of important roles in star cluster evolution. By acting as an important heat source for clusters, binaries become modified by dynamical interactions. Although the details are not yet clear, this can change the distribution of orbital parameters of binary populations in clusters (e.g. Hut & Bahcall, 1983; Sigurdsson & Phinney, 1993). In turn, this could have important implications for binary star evolution by, for example, stimulating mass-transfer. Observational evidence has been found in support of this. Previous studies have reported evidence that the sizes of some binary populations thought to be undergoing mass-transfer are correlated with the rate of stellar collisions (e.g. Pooley & Hut, 2006).

## 1.3 Where To Go From Here

We have a good working knowledge of both stellar evolution and stellar dynamics in star clusters. But our understanding is far from complete. This brings us to the question: Where do we go from here? The interaction be-

tween stellar evolution and stellar dynamics in star clusters remains a largely unexplored frontier. What observational effects might we expect to find? How will these affect star cluster evolution, and what implications could they have for the history of our Galaxy? The search for answers to these questions will be the primary focus of this thesis.

The techniques presented in this thesis are motivated by our current understanding of both stellar evolution and stellar dynamics, in addition to evidence that suggests that their interaction could account for the origins of several mysterious stellar populations. Gravitational dynamics is the common theme unifying all of these methods. They will be applied to observations of dense star clusters in order to study, among other things, stellar mergers. An emphasis will be placed on the development of statistical and theoretical tools that can be applied to a number of other astrophysical sub-disciplines with analogous dynamical processes and population statistics. These tools will be used in this thesis to further our understanding of the various channels via which stellar evolution and stellar dynamics interact in star clusters, as well as to quantify the implications of these effects for observations of stellar populations.

In Chapter 2, we introduce a new adaptation of the classical mean free path approximation. With it, we compare the rates of gravitational encounters occurring between single, binary and triple stars using observations of real star clusters. This has allowed us to outline a systematic methodology that can be used to constrain the dynamical origins of observed multiple star systems containing merger products. In Chapter 3, we introduce a statistical technique that can be used to compare the relative sizes of the different stellar populations in a large sample of star clusters spanning a diverse range of prop-

erties. In order to study the effects had by the cluster dynamics on each of the different stellar populations, we apply our method to a large sample of 56 Milky Way GCs. In Chapter 4, we refine this technique and apply it to a new sample of 35 GCs compiled using much more sophisticated observations taken from the ACS Survey for Globular Clusters. Using this new data, we present a homogeneous catalogue for the different stellar populations, along with a simple prescription to select stars out of the CMD belonging to each population. In Chapter 5, we present an analytic model for blue straggler formation in globular clusters. We compare its predictions to observed BS numbers taken from our stellar population catalogue using a new statistical technique. With this method, we constrain the dominant blue straggler formation mechanism operating in GCs. In Chapter 6, we present a new method of quantifying cluster-to-cluster differences in the stellar mass functions of a large sample of clusters. We apply our technique to the ACS data, and use it to constrain the degree of universality of the initial mass function for our sample. Given the very old ages of Milky Way globular clusters, this has important implications for our understanding of star formation in the early Universe. Finally, in Chapter 7, we summarize our results and discuss directions for future research.

# Bibliography


Applegate J. H. 1986, ApJ, 301, 132

Andronov N., Pinsonneault M. H., Terndrup D. M. 2006, ApJ, 646, 1160

Bate M. R., Bonnell I. A. 1997, MNRAS, 285, 33

Bate M. R. 1997, MNRAS, 285, 16

Binney J., Tremaine S. 1987, Galactic Dynamics (Princeton: Princeton University Press)

Bohm-Vitense E., 1958, ZsAp, 46, 108

Brown, W. R., Anderson, J., Gnedin, O. Y., Bond, H.E., Geller, M. J., Kenyon, S. J. & Livio, M. 2010, ApJL, 719, L23

Chandrasekhar S. 1939, An Introduction to the Study of Stellar Structure, Chicago: University of Chicago Press

Chen X., Han Z. 2008, MNRAS, 387, 1416

Chen X., Han Z. 2008, MNRAS, 384, 1263

Chernoff D. F., Weinberg M. D. 1990, ApJ, 351, 121

Clayton D. D. 1968, Principles of Stellar Evolution and Nucleosynthesis, New York: McGraw-Hill

Cleary P. W., Monaghan J. J., 1990, ApJ, 349, 150

Cohen R. L., Guhathakurta P., Yanny B., Schneider D. P., Bahcall J. N. 1997, AJ, 113, 669

Davies M. B., Piotto G., De Angeli F. 2004, MNRAS, 348, 129

d'Cruz N. L., Dorman B., Rood R. T., O'Connell R. W. 1996, ApJ, 466, 359

De Angeli F., Piotto G., Cassisi S., Busso G., Recio-Blanco A., Salaris M., Aparicio A., Rosenberg A. 2005, AJ, 130, 116

De Marchi G., Paresce F., Portegies Zwart S. 2010, ApJ, 718, 105

Di Stefano, R. 2010, arXiv:1002.3009v1

Dotter A., Sarajedini A., Anderson J., Aparicio A., Bedin L. R., Chaboyer B., Majewski S., Marin-Franch A., Milone A., Paust N., Piotto G., Reid I. N., Rosenberg A., Siegel M. 2010, ApJ, 708, 698

Durisen R. H., Sterzik M. F. 1994, A&A, 286, 84

Eggleton P. P. 2006, Evolutionary Processes in Binary and Multiple Stars. Cambridge Univ. Press, Cambridge, MA

Eggleton P. P., Tokovinin A. A. 2008, MNRAS, 389, 869

Fabrycky D. & Tremaine S. 2007, ApJ, 669, 1298

Farrell S. A., Webb N. A., Barrett D., Godet O., Rodrigues J. M. 2009, Nature, 460, 73

Ferraro F. R., Paltrinieri B., Fusi Pecci F., Cacciari C., Dorman B., Rood R. T., Buonanno R., Corsi C. E., Burgarella D., Laget M. 1997, A&A, 324, 915

Ferraro F. R., Paltrinieri B., Rood R. T., Dorman B. 1999, ApJ, 522, 983

Ferraro F. R., Beccari G., Rood, R. T., Bellazzini M., Sills A., Sabbi E. 2004, ApJ, 603, 127

Fregeau J. M., Cheung P., Portegies Zwart S. F., Rasio F. A. 2004, MNRAS, 352, 1

Fregeau J. M., Ivanova N., Rasio F. A. 2009, ApJ, 707, 1533

Fukushige T., Heggie D. C. 1995, MNRAS, 276, 206

Fusi Pecci F., Ferraro F. R., Corsi C. E., Cacciari C., Buonanno R. 1992, AJ, 104, 1831

Fusi Pecci F., Ferraro F. R., Bellazzini M., et al. 1993, AJ, 105, 1145

Gaburov E., Gieles M. 2008, MNRAS, 391, 190

Geller A. M., Mathieu R. D., Harris H. C., McClure R. D., 2008, AJ, 135, 2264

Gieles M., Heggie D., Zhao H. 2011, MNRAS, accepted

Giersz M., Heggie D. C. 1996, MNRAS, 279, 1037

Goodman J., Hut P. 1993, ApJ, 403, 271

Hayashi C., Nishida M., Sugimoto D. 1962, PThPh, 27, 1233

Heggie D. C. 1975, MNRAS, 173, 729

Heggie D. C., Hut P. 2003, The Gravitational Million-Body Problem: A Multidisciplinary Approach to Sar Cluster Dynamics (Cambridge: Cambridge University Press)

Henon M. 1969, A&A, 2, 151

Hertzsprung A. 1909, AN 4296, 179, 373

Hills J. G., Day C. A. 1976, ApJL, 17, 87

Hurley, J. R., Pols, O. R., Aarseth, S. J. & Tout, C. A. 2005, MNRAS, 363, 293

Hut P., Verbunt F., 1983, Nature, 301, 587

Hut P., Bahcall J. N. 1983, ApJ, 268, 319

Hut P. 1983, ApJ, 272, 29

Hut P., Djorgovski S. 1992, Nature, 359, 806

Iben I. Jr. 1968, ApJ, 154, 581

Iben I. Jr. 1974, A. Rev. A & A, 12, 215

Iben I. Jr. 1991, ApJS, 76, 55

Ivanova N., Taam R. E. 2003, ApJ, 599, 516

Judge P. G., Stencel R. E. 1991, ApJ, 371, 357

Kaluzny J. 2003, Acta Astronomica, 53, 51

Kippenhahn R., Weigert A. 1990, Stellar Structure and Evolution. Springer-Verlag, Berlin

Knigge C., Dieball, A., Maiz Apellaniz, J., Long, K. S., Zurek, D. R. & Shara, M. M. 2008, ApJ, 683, 1006

Knigge C., Leigh N., Sills A. 2009, Nature, 457, 288

Kozai, Y. 1962, AJ, 67, 591

Kroupa P., Burkert A. 2001, ApJ, 555, 945

Kroupa P. 2002, Science, 295, 82

Kroupa P., Boily C. M. 2002, MNRAS, 336, 1188

Lada C. J. 1985, ARA&A, 23, 267

Lada E. A., Lada C. J. 1995, AJ, 109, 1682

Lanzoni B., Dalessandro E., Perina S., Ferraro F. R., Rood R. T., Sollima A. 2007, ApJ, 670, 1065

Latham D. W., 2005, Highlights of Astronomy, 14, 444

Leigh N., Sills A., Knigge C. 2009, MNRAS, 399, L179

Leonard P. J. T. 1989, AJ, 98, 217

Leonard P. J. T., Linnell A. P. 1992, AJ, 103, 1928

Lombardi, J. C. Jr., Warren, J. S., Rasio, F. A., Sills, A. & Warren, A. R. 2002, ApJ, 568, 939

Maeder A. 2009, Physics, Formation and Evolution of Rotating Stars. Springer, Berlin

Mapelli M., Sigurdsson S., Ferraro F. R., Colpi M., Possenti A., Lanzoni B. 2006, MNRAS, 373, 361

Mathieu R. D., van den Berg M., Torres G., Latham D., Verbunt F., Stassun K. 2003, AJ, 125, 246

Mathieu R. D., Geller A. M. 2009, Nature, 462, 1032

Maxted P. F. L., Heber U., Marsh T. R., North R. C. 2001, MNRAS, 326, 1391

McCrea W. H. 1964, MNRAS, 128, 147

McKee C. F., Ostriker E. C. 2007, ARA&A, 45, 565

McMillan S. L. W. 1986, ApJ, 306, 552

McMillan S. L. W., McDermott P. N., Taam R. E., 1987, ApJ, 318, 261

McMillan S. L. W., Vesperini E., Portegies Zwart S. 2007, ApJ, 655, 45

Mikkola S. 1983, MNRAS, 203, 1107

Milone A. P., Piotto G., Bedin L. R., Sarajedini A. 2008, MmSAI, 79, 623

Miroshnichenko A. S., Manset N., Kusakin A. V., Chentsov E. L., Klochkova V. G., Zharikov S. V., Gray R. O., Grankin K. N., Gandet T. L., Bjorkman K. S., Rudy R. J., Lynch D. K., Venturini C. C., Mazuk S., Puetter R. C., Perry R. B., Levato H., Grosso M., Bernabei S., Polcaro V. F., Viotti R. F., Norci L., Kuratov K. S. 2007, ApJ, 671, 828

Moni Bidin C., Moehler S., Piotto G., Recio-Blanco A., Momany Y., Mendez R. A. 2006, A&A, 451, 499

Moni Bidin C., Moehler S., Piotto G., Momany Y., Recio-Blanco A. 2009, A&A, 498, 737

Moni Bidin C., Villanova S., Piotto G., Momany Y. 2011, A&A, 528, 127

Paczynski B. 1986, ApJ, 308, L43

Perets H. B., Fabrycky D. C. 2009, ApJ, 697, 1048

Perlmutter S., Aldering G., Goldhaber G., Knop R. A., Nugent P., Castro P. G., Deustua S., Fabbro S., Goobar A., Groom D. E., Hook I. M., Kim A. G., Kim M. Y., Lee J. C., Nunes N. J., Pain R., Pennypacker C. R., Quimby R., Lidman C., Ellis R. S., Irwin M., McMahon R. G., Ruiz-Lapuente P., Walton N., Schaefer B., Boyle B. J., Filippenko A. V., Matheson T., Fruchter A. S., Panagia N., Newberg H. J. M., Couch W. J., The Supernova Cosmology Project. 1999, ApJ, 517, 565

Pooley D., Hut P. 2006, ApJL, 646, 143

Popper D. M. 1980, A. Rev. A & A, 18, 115

Portegies Zwart S. F., McMillan S. L. W., Hut P., Makino J. 2001, MNRAS, 321, 199

Pringle J. E. 1989, MNRAS, 239, 361

Reimers D. 1975, Mem. Roy. Soc. Liege 6e Ser., 8, 369

Rood R. T. 1973, ApJ, 184, 815

Russell H. N. 1925, MNRAS, 85, 935

Salpeter E. E. 1955, ApJ, 121, 161

Sandage, A. R. 1953, AJ, 58, 61

Sandage A., Wallerstein G. 1960, ApJ, 131, 598

Sandquist E. L., Latham D. W., Shetrone M. D., Milone A. A. E., 2003, AJ, 125, 810

Sarajedini A., Bedin L. R., Chaboyer B., Dotter A., Siegel M., Anderson J., Aparicio A., King I., Majewski S., Marin-Franch A., Piotto G., Reid I. N., Rosenberg A., Steven M. 2007, AJ, 133, 1658

Saviane I., Piotto G., Fagotto F., Zaggia S., Capaccioli M., Aparicio A. 1998, A&A, 333, 479

Shara M. M., Drissen L., Bergeron L. E., Paresce F. 1995, ApJ, 441, 617

Shara M. M., Saffer R. A., Livio M. 1997, ApJ, 489, L59

Sigurdsson S., Phinney E. S., 1993, ApJ, 415, 631

Sills A., Bailyn C. D. 1999, ApJ, 513, 428

Sills A., Faber J. A., Lombardi J. C. Jr., Rasio F. A., Warren A. R. 2001, ApJ, 548, 323

Sills A., Adams T., Davies M. B., Bate M. R. 2002, MNRAS, 332, 49

Sills A., Adams T., Davies M. B. 2005, MNRAS, 358, 716

Sollima A., Carballo-Bello J. A., Beccari G., Ferraro F. R., Pecci F. Fusi, Lanzoni B. 2010, MNRAS, 401, 577

Spitzer L. Jr., Thuan T. X. 1972, ApJ, 175, 31

Spitzer L. Jr., Shull J. M. 1975, ApJ, 201, 773

Spitzer, L. 1987, Dynamical Evolution of Globular Clusters (Princeton: Princeton University Press)

Talamantes A., Sandquist E. L., Clem J. L., Robb R. M., Balam D. D., Shetrone M. 2010, AJ, 140, 1268

Tokovinin A. 2008, MNRAS, 389, 925

Tout C. A., Pols O. R., Han Z., Eggleton P. P. 1996, MNRAS, 281, 257

Troja E., Rosswog S., Gehrels N. 2010, ApJ, 723, 1711

van den Berg M., Orosz J., Verbunt F., Stassun K. 2001, A&A, 375, 375

Vishniac E. T. 1978, ApJ, 223, 986

Vogt H. 1925, Astron. Nachr. 223, 229

Webbink R. F. 1984, ApJ, 277, 355

Chapter 2

# An Analytic Technique for Constraining the Dynamical Origins of Multiple Star Systems Containing Merger Products

## 2.1 Introduction

It has been known for some time that encounters, and even direct collisions, can occur frequently between stars in dense stellar systems (Hills & Day, 1976; Hut & Verbunt, 1983; Leonard, 1989, e.g.). In the cores of globular clusters (GCs), the time between collisions involving two single stars can be much shorter than the cluster lifetime (Leonard, 1989). The time between encounters involving binary stars can be considerably shorter still given their much larger cross sections for collision. In globular and, especially, open clusters (OCs) with high binary fractions, mergers are thought to occur frequently

during resonant interactions involving binaries (e.g. Leonard & Linnell, 1992). What's more, collision products have a significant probability of undergoing more than one collision during a given single-binary or binary-binary interaction since the initial impact is expected to result in shock heating followed by adiabatic expansion, increasing the cross section for a second collision to occur (e.g. Fregeau et al., 2004).

Several types of stars whose origins remain a mystery are speculated to be the products of stellar mergers. Blue stragglers (BSs) in particular are thought to be produced via the addition of fresh hydrogen to the cores of low-mass main-sequence (MS) stars. Recent evidence has shown that, whatever the dominant BS formation mechanism(s) operating in both globular and open clusters, it is likely to in some way depend on binary stars (Knigge, Leigh & Sills, 2009; Mathieu & Geller, 2009). The currently favored mechanisms include collisions during single-binary and binary-binary encounters (e.g. Leonard, 1989), mass transfer between the components of a binary system (e.g. Chen & Han, 2008a,b) and the coalescence of two stars in a close binary due to perturbations from an orbiting triple companion (e.g. Eggleton, 2006; Perets & Fabrycky, 2009).

A handful of spectroscopic studies have revealed that in some GCs there exist BSs with masses exceeding twice that of the MS turn-off (e.g. Shara, Saffer & Livio, 1997; Knigge et al., 2008). Such massive BSs must have been formed from the mergers of two or more low-mass MS stars since they are too massive to have been formed from mass transfer. In a few cases, this can also be argued for entire BS populations using photometry. For instance, Chen & Han (2008b) performed detailed binary evolution calculations to study dynamical stability during mass transfer from an evolving giant star onto a MS

companion. Based on their results, it can arguably be inferred that most BSs in NGC 188 are sufficiently bright that they probably could not have formed from mass transfer alone. If true, this suggests that most of these BSs must be the products of stellar mergers. Regardless of the dominant BS formation mechanism(s) operating in dense star clusters, dynamical interactions should play at least some role. For example, even if blue stragglers are formed as a result of binary evolution processes such as mass transfer, the progenitor binaries themselves should have been affected by at least one dynamical interaction over the course of their lifetime.

Numerous scattering experiments have been performed to explore the outcomes of binary-binary and, in particular, single-binary encounters (e.g. McMillan, 1986; Sigurdsson & Phinney, 1993; Fregeau et al., 2004). Most of the earliest of these studies were performed in the point-particle limit, ignoring altogether the often non-negligible implications of the stars' finite sizes (e.g. Hut & Bahcall, 1983; Mikkola, 1983). Later, more realistic simulations clearly demonstrated the importance of taking into account the dissipative effects of tidal interactions and direct contact between stars (e.g. McMillan et al., 1987; Cleary & Monaghan, 1990). As a result of the increased number of free parameters for the encounters and the longer integration times required to run the simulations to completion, few studies have been conducted to explore the outcomes of binary-binary encounters or interactions involving triple systems.

In this chapter, we introduce an analytic technique to constrain the most probable dynamical origin of an observed binary or triple system containing one or more merger products. Provided the observed system is found within a moderately dense cluster environment with binary and/or triple fractions of at least a few percent, the probability is often high that it formed from

a merger during an encounter involving one or more binary or triple stars. In Section 2.2, we present an equation for energy conservation during individual stellar encounters and outline the process for applying our technique. Specifically, we present a step-by-step methodology to evaluate whether or not an assumed dynamical history could have realistically produced an observed system and describe how to determine the most probable dynamical formation scenario. In Section 2.3, we apply our technique to a few observed binary and triple systems thought to contain merger products, in particular a triple system that is thought to contain two BSs and the peculiar period-eccentricity distribution of the BS binary population in NGC 188. We discuss the implications of our results in Section 2.4.

## 2.2 Method

In this section, we present a general prescription for conservation of energy during stellar encounters. We will limit the discussion to typical interactions thought to occur in globular and old open clusters, although our technique can be generalized to any choice of parameter space. The types of encounters of interest in this chapter will predominantly involve low-mass MS stars with relative velocities at infinity ranging from $\lesssim 1$ km/s to $\sim 10$ km/s (e.g. Leonard, 1989; Sigurdsson & Phinney, 1993). Our technique describes how to isolate the most probable dynamical formation history for an observed binary or triple containing one or more merger products by providing an estimate for the time required for a given interaction to occur in a realistic cluster environment.

We begin by assuming that an observed system was formed directly

from a dynamical interaction (or sequence of interactions). In this case, the observed parameters of the system provide the final distribution of energies for the system resulting from the interaction(s). After choosing an appropriate dynamical scenario (i.e. whether the objects involved in the interaction(s) are single, binary or triple stars), we can work backwards using energy conservation to constrain the initial energies going into the encounter. This provides an estimate for the initial orbital energies and therefore semi-major axes of any binaries or triples going into the interaction. This in turn gives the cross section for collision and hence the time required for the hypothesized interaction(s) to occur.

Since the formation event must have happened in the last $\tau_{BS}$ years, where $\tau_{BS}$ is the lifetime of the merger product, a formation scenario is likely only if the derived encounter time-scale is shorter than the lifetime of the merger product(s). Conversely, if the derived encounter time-scale is longer than the lifetime of the merger product(s), then that dynamical formation scenario is unlikely to have occurred in the last $\tau_{BS}$ years. In general, the shorter the derived encounter time-scale, the more likely it is that one or more such encounters actually took place within the lifetime of the merger product(s). Finally, if the derived encounter time-scale is longer than $\tau_{BS}$ for every possible dynamical formation scenario, then a dynamical origin is altogether unlikely for an observed multiple star system containing one or more BSs. Either that, or the encounter time-scales must have been shorter in the recent past (or, equivalently, the central cluster density must have been higher).

### 2.2.1 Conservation of Energy

Consider an encounter in which at least one of the two bodies involved is a binary or triple star. Though a complex exchange of energies occurs, energy must ultimately be conserved in any dynamical interaction. The total energy that goes into the encounter must therefore be equal to the total energy contained in the remaining configuration:

$$\begin{aligned}
\sum_{i}^{N_i} \Omega_i(I_i,\omega_i) + \sum_{i}^{N_i} W_i(m_i,X_i,Z_i,\tau_i) \\
\sum_{i}^{N_i} U_i(m_i,X_i,Z_i,\tau_i) + \sum_{j}^{S_i} T_j(M_{cl},M_j) + \\
\sum_{k}^{M_i} \epsilon_k(\mu_k,M_k,a_k) = \sum_{ii}^{N_f} \Omega_{ii}(I_{ii},\omega_{ii}) + \\
\sum_{ii}^{N_f} W_{ii}(m_{ii},X_{ii},Z_{ii},\tau_{ii}) + \sum_{ii}^{N_f} U_{ii}(m_{ii},X_{ii},Z_{ii},\tau_{ii}) \\
+ \sum_{jj}^{S_f} T_{jj}(M_{jj}) + \sum_{kk}^{M_f} \epsilon_{kk}(\mu_{kk},M_{kk},a_{kk}) + \Delta,
\end{aligned} \tag{2.1}$$

where $N_i$, $S_i$ and $M_i$ are the total number of stars, objects (single, binary, triple or even quadruple stars) and orbits, respectively, that went into the encounter. Similarly, $N_f$, $S_f$ and $M_f$ are the total number of stars, objects and orbits remaining after the encounter.

We let $\Omega_i = \Omega_i(I_i,\omega_i)$ represent the bulk rotational kinetic energy in star $i$, which is a function of the star's moment of inertia $I_i$ and angular rotation rate $\omega_i$:

$$\Omega_i(I_i,\omega_i) = \frac{1}{2} I_i \omega_i^2 \tag{2.2}$$

The moment of inertia is in turn a function of the density profile within a star,

which changes along with its internal structure and composition as the star evolves. The moment of inertia is given by (Claret & Gimenez, 1989):

$$\begin{aligned} I &= \frac{8\pi}{3}\int_0^R \rho(r) r^4 dr \\ &= \beta^2 m R^2, \end{aligned} \tag{2.3}$$

where $\beta$ is the radius of gyration. For example, a typical 1 $M_\odot$ star in an old open cluster having an age of $\sim$ 6 Gyrs has $\beta = 0.241$. For comparison, a 1 $M_\odot$ star in a typical Milky Way GC having an age of $\sim$ 11 Gyrs has $\beta = 0.357$ (Claret & Gimenez, 1989). A large spread of rotation speeds have been observed for MS stars in open and globular clusters, with measured values ranging from $\sim$ 1 - 20 km $s^{-1}$ (Mathieu & Geller, 2009). A 1 $M_\odot$ star having a radius of 1 $R_\odot$ and a rotation speed of 2 km $s^{-1}$ with $\beta = 0.241$ has $\Omega \sim 10^{36}$ Joules.

We let $W_i = W_i(m_i, X_i, Z_i, \tau_i)$ represent the gravitational binding energy of star $i$, where $m_i$ is the star's mass, $X_i$ is its initial hydrogen mass fraction, $Z_i$ is its initial metallicity and $\tau_i$ is its age. For a spherical mass with a density distribution $\rho_i(r)$, the gravitational binding energy is given by:

$$\begin{aligned} W_i(m_i, X_i, Z_i, \tau_i) &= \frac{16\pi^2 G}{3}\int_0^{R_i} \rho_i(r) r^4 dr \\ &= -\delta(m_i, X_i, Z_i, \tau_i) G \frac{m_i^2}{R_i}, \end{aligned} \tag{2.4}$$

where the parameter $\delta$ is chosen to reflect the structure of the star and is therefore a function of its mass, age and chemical composition. For instance, a typical 1 $M_\odot$ star with $(X, Z) = (0.70, 0.02)$ in an old open cluster with an age of $\sim$ 6 Gyrs has $\delta = 1.892$. For comparison, an older but otherwise identical

star in a typical Milky Way GC with an age of $\sim$ 11 Gyrs has $\delta = 6.337$ (Claret & Gimenez, 1989). Roughly regardless of age, this gives $|W| \sim 10^{42}$ Joules for a 1 $M_\odot$ star with a radius of 1 $R_\odot$.

We let $U_i = U_i(m_i, X_i, Z_i, \tau_i)$ represent the total internal energy contained in star $i$ (i.e. the star's thermal energy arising from the random motions of its particles). By solving the equations of stellar structure, the total internal energy of a purely isolated single star is uniquely determined by its mass, initial composition and age. Stars are made up of a more or less virialized fluid so that, ignoring magnetic fields, the gravitational binding energy of a star in hydrostatic equilibrium is about twice its internal thermal energy (Chandrasekhar, 1939). Using this version of the virial theorem, a 1 $M_\odot$ star having a radius of 1 $R_\odot$ has $U \sim 5 \times 10^{41}$ Joules.

The total translational kinetic energy of object $j$ (single, binary, triple, etc. star) is represented by $T_j$:

$$T_j(M_{cl}, M_j) = \frac{1}{2} M_j v_j^2, \tag{2.5}$$

where $M_j$ is the total mass of the object, and $v_j$ is its bulk translational speed. The translational velocities of stars in clusters for which energy equipartition has been achieved as a result of two-body relaxation obey a Maxwell-Boltzmann distribution, with the heaviest stars typically having the lowest velocities and vice versa (Spitzer, 1987). According to the virial theorem, the root-mean-square velocity $v_{rms}$ of the distribution depends on the total mass of the cluster $M_{cl}$. It follows that the velocities of stars in a fully relaxed cluster are approximately determined by their mass and the total mass of the cluster. Assuming that the typical velocity of a $< m >$ star is roughly equal to

$v_{rms}$, where $< m >$ is the average stellar mass in the cluster, energy equipartition can be invoked in some clusters to approximate the translational kinetic energy, and hence velocity, of a star or binary of mass $M_j$:

$$v_j = \left(\frac{< m >}{M_j}\right)^{1/2} v_{rms}. \tag{2.6}$$

We note that Equation 2.6 can only be applied in clusters for which the half-mass relaxation time is much shorter than the cluster lifetime. At the same time, the tidal truncation of the velocity distribution must not be significant. We will return to this in Section 2.2.2.

For a 1 $M_\odot$ star with a translational speed of 1 km $s^{-1}$ (typical of stars in old open clusters), we find $T \sim 10^{36}$ Joules. For comparison, the same star traveling at a speed of 10 km $s^{-1}$ (typical of stars in globular clusters) has $T \sim 10^{38}$ Joules. We can put this into perspective by equating Equation 2.5 with Equation 2.4, which shows that a direct collision between two 1 $M_\odot$ stars would require an impact velocity of $\sim$ 1000 km $s^{-1}$ in order to completely unbind the merger remnant.

The total orbital energy of orbit $k$ is denoted $\epsilon_k$, and is given by:

$$\epsilon_k(\mu_k, M_k, a_k) = -\frac{G\mu_k M_k}{2a_k}, \tag{2.7}$$

where $\mu_k = m_1 m_2/(m_1+m_2)$ is the reduced mass of the orbit, $M_k = m_1+m_2$ is the total mass and $a_k$ is the orbital semi-major axis. A binary composed of two 1 $M_\odot$ stars with a period of 1000 days has $|\epsilon| = 10^{38}$ Joules. For comparison, an otherwise identical binary with a period of 1 day has $|\epsilon| = 10^{40}$ Joules. Since most stable triples are observed to have outer periods of $\sim$ 1000 days

with close inner binaries (Tokovinin, 1997; Perets & Fabrycky, 2009), it follows that the total orbital energies of stable triples will be dominated by the orbital energies of their inner binaries.

After the encounter occurs, the energies that collectively define the state of the newly formed system include the rotational kinetic ($\Omega_{ii}(I_{ii}, \omega_{ii})$), thermal ($U_{ii}(m_{ii}, X_{ii}, Z_{ii}, \tau_{ii})$) and gravitational binding ($W_{ii}(m_{ii}, X_{ii}, Z_{ii}, \tau_{ii})$) energies of the stars that are left-over, as well as the total translational kinetic ($T_{jj}(m_{jj})$) and orbital ($\epsilon_{kk}(\mu_{kk}, M_{kk}, a_{kk})$) energies of any left-over stars, binaries or triples. The internal and gravitational binding energies of the left-over stars once again depend on their mass, composition and age. The mass, composition and evolutionary status of a star will decide how it responds to tidal interactions (and therefore how much tidal energy is deposited) since these are the principal factors that determine its internal structure, in particular whether or not its envelope is radiative or convective (Podsiadlowski, 1996). Finally, we let $\Delta$ represent the energy lost from the system due to radiation and mass loss. We do not expect this term to be significant for the majority of the encounters we will consider since the rate of mass-loss from low-mass MS stars is small and the time-scales under consideration are relatively short compared to the lifetimes of the stars. Moreover, the velocity dispersions characteristic of the clusters we will consider are sufficiently small that we expect most collisions to have a relatively low impact velocity. Though significant mass loss can occur for high impact collisions as often occur in the Galactic centre, mass loss is only $\lesssim 5\%$ for the low impact velocity collisions expected to occur in open and globular clusters (Sills et al., 2001). Therefore, we will henceforth assume $\Delta \sim 0$.

Depending on the initial parameters of the encounter, one or more terms

in Equation 2.1 can often be neglected. For example, given that the rotational energies of typical MS stars in both open and globular clusters are several orders of magnitude smaller than the other terms in Equation 2.1, we can neglect these terms for the types of encounters of interest. Even a 1 $M_{\odot}$ star rotating at a rate of 100 km $s^{-1}$ has a rotational energy of only $\sim 10^{39}$ Joules. This is considerably higher than even the highest rotation rates observed for both BSs and normal MS stars (e.g. Mathieu & Geller, 2009). From this, we expect typical rotational energies to be significantly smaller than the orbital energies of even moderately hard binaries. Furthermore, Equation 2.5 can be combined with Equation 2.6 and equated to Equation 2.7 in order to define the hard-soft boundary for a given cluster. If a binary is hard, its initial orbital energy will outweigh its initial translational kinetic energy during typical stellar encounters (Heggie, 1975). We do not expect soft binaries to survive for very long in dynamically-active clusters (Heggie, 1975) (i.e. most binaries are hard), so that the translational kinetic energies of the stars, binaries and triples typically found in OCs can usually be neglected when applying Equation 2.1. This suggests $T_j = 0$. However, the final translational kinetic energies of the stars, binaries and triples left-over should not be neglected for encounter outcomes in which one or more stars are ejected with very high velocities. This can leave the remaining stars in a much more tightly bound configuration since stars ejected with high velocities carry off significant amounts of energy. Finally, provided there are no very high impact collisions and tides dissipate a negligible amount of energy from the system, we also expect that:

$$\sum_{i}^{N_i} U_i + \sum_{i}^{N_i} W_i \sim \sum_{ii}^{N_f} U_{ii} + \sum_{ii}^{N_f} W_{ii}. \tag{2.8}$$

We can simplify our energy conservation prescription considerably for the majority of encounters occurring in old OCs. Neglecting the rotational kinetic energies of the stars, Equation 2.1 becomes:

$$\sum_{k}^{M_i} \epsilon_k(\mu_k, M_k, a_k) = \sum_{kk}^{M_f} \epsilon_{kk}(\mu_{kk}, M_{kk}, a_{kk}) + \sum_{jj}^{S_f} T_{jj}(M_{jj}) - \Delta_m, \tag{2.9}$$

where we have assumed $T_j = 0$ and $\Delta_m$ is the amount of energy deposited in any merger products formed during the encounter. In other words, the term $\Delta_m$ provides the required correction to Equation 2.8 resulting from internal energy being deposited in the merger product(s) as a result of collisions and tides. If no mergers occur or all of the orbital energy of the merging binary is imparted to the other interacting stars, $\Delta_m = 0$.

Both the total linear and angular momenta must also be conserved during any dynamical interaction. This provides two additional constraints that must also be satisfied, however the total linear and angular momenta are vector quantities that depend on the angle of approach as well as the relative orientations of the objects. As a result, there are more free parameters to fit when trying to constrain the initial parameters of an encounter using conservation of linear and angular momentum. Therefore, it is considerably more difficult to extract information pertaining to the initial orbital parameters of an encounter using conservation of momentum than it is with conservation of energy.

We have assumed that exchange interactions do not occur in applying our technique. Clearly, this assumption could be invalid for some systems.

If this is the case, then our method is also invalid. This suggests that our technique is ideally suited to clusters for which the encounter time-scales are comparable to the lifetime of a typical merger product. This maximizes the probability that BSs do not experience any subsequent dynamical interactions after they are formed. Of course, most clusters of interest are unlikely to satisfy this criterion. We can assess the probability that an exchange encounter has occurred for a particular system by calculating the different encounter time-scales and comparing to the lifetime of the merger product. If the time-scales are sufficiently short, then the possibility of an exchange interaction having occurred after the system's formation must be properly addressed. We will discuss this further in Section 2.4.

### 2.2.2 Generalized Approach

In this section, we outline a step-by-step methodology to constrain realistic dynamical formation scenarios that could have resulted in the production of an observed stellar system containing one or more merger products. These steps are:

1. We must first find *qualitative* constraints for the system's dynamical history and, in so doing, converge on the most probable formation scenario. The choice of formation history should be guided by the observed properties of the binary or triple system containing the merger product(s). The following guidelines can be applied to find the most probable scenario.

   First, the analytic rates for single-single (1+1), single-binary (1+2), single-triple (1+3), binary-binary (2+2), binary-triple (2+3) and triple-triple (3+3) encounters can be compared to obtain a rough guide as to

which of these encounter types will dominate in a given cluster. The total rate of encounters of a given type in a cluster core is well approximated by (Leonard, 1989) (see Appendix A for a more generalized form for this equation):

$$\Gamma = N_0 n_0 \sigma_{gf}(v_{rel,rms}) v_{rel,rms}, \tag{2.10}$$

where $N_0$ is the number of single, binary or triple stars in the core and $n_0$ is the mean stellar, binary or triple number density in the core. The gravitationally-focused cross section for collision $\sigma_{gf}$ is given by Equation 6 of Leonard (1989). Gravitationally-focused cross sections for the various encounter types are provided in Appendix A along with the values assumed for their pericenters.

In general, the number of single, binary and triple stars are given by, respectively, $(1 - f_b - f_t)N_c$, $f_b N_c$ and $f_t N_c$, where $N_c = 2/3\pi n_0 r_c^3$ is the total number of objects in the core (Leonard, 1989), $f_b$ is the fraction of objects that are binaries and $f_t$ is the fraction of objects that are triples. Assuming for simplicity that $v_{rel}$ is roughly equal for all types of encounters, the rates for two types of encounters can be compared to find the parameter space for which one type of encounter will dominate over another. These relations can be plotted in the $f_b - f_t$ plane in order to partition the parameter space for which each of the various encounter types will occur with the greatest frequency, as illustrated in Figure 2.1. Given a cluster's binary and triple fractions, this provides a simple means of finding the type of encounter that will occur with the greatest frequency. Our results are in rough agreement with those of

Sigurdsson & Phinney (1993) who found that single-binary interactions dominate over binary-binary interactions in clusters having core binary fractions $f_b \lesssim 0.1$, and may dominate for $f_b$ up to 0.25-0.5 in some cases.

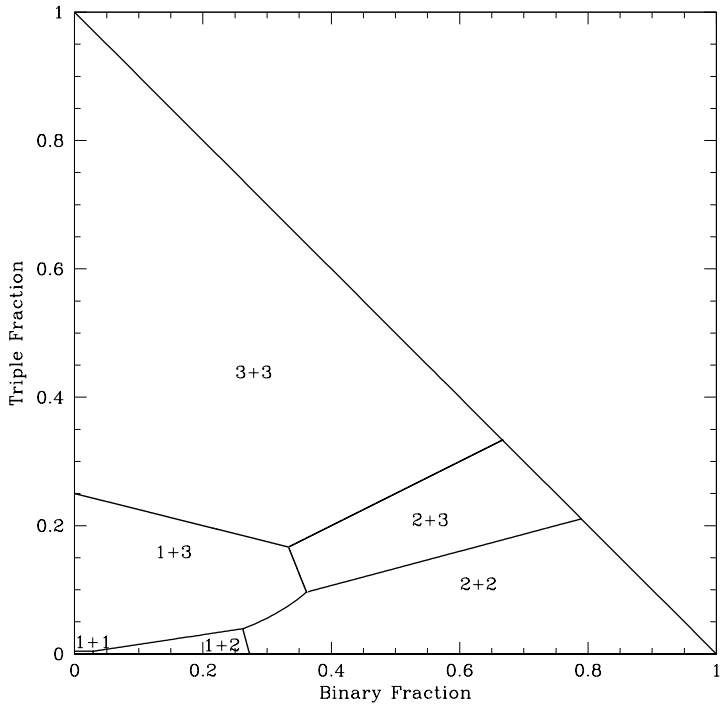



Figure 2.1 Plot showing the parameter space in the $f_b - f_t$ plane for which each of the various encounter types dominate. Boundaries between regions are indicated by solid lines, each segment of which is obtained by equating two particular encounter rates using Equation 2.10 and the relevant cross sections derived using Equation 6 of Leonard (1989). We assume $a_t = 5a_b$ and $a_b = 90R$ in obtaining the relations between encounter rates. This is a reasonable choice for the ratio between the average binary and triple geometric cross sections given that the ratio between the outer and inner orbital semi-major axes of triples must be relatively large (by a factor of $\gtrsim 10$) in order for them to be stable (Mardling, 2001).

Second, the masses of the components of an observed binary or triple system provide a lower limit for the number of stars that could have gone into its formation. The minimum number of stars that must have

merged to form a given collision product, labelled $N_{min,i}$, is equal to the integer nearest to and larger than the quantity $m_{rem}/m_{TO}$, where $m_{rem}$ is the mass of the merger remnant and $m_{TO}$ corresponds to the mass of the main-sequence turn-off (MSTO). This assumes that $m_{TO}$ has not changed significantly since the dynamical formation of the system, which should be valid provided the merger products are significantly more massive than the turn-off so that their lifetimes are relatively short. The number of stars that went into an encounter $N_i$ must therefore satisfy:

$$N_i \geq \sum_{i}^{M} N_{min,i} + M_0, \tag{2.11}$$

where $M_0$ is the number of normal stars (i.e. not formed from mergers) and $M$ denotes the number of merger products.

Third, an estimate for the average stellar mass, and therefore the masses of typical stars expected to undergo encounters, should be guided by a realistic stellar mass function for the host cluster. First of all, observations have shown that a significant depletion of low-mass stars occurs in dynamically evolved clusters (i.e. those for which $t_{rh} \ll t_{age}$, where $t_{rh}$ is the half-mass relaxation time and $t_{age}$ is the cluster age) since they are preferentially ejected from the cluster during close encounters (e.g. von Hippel & Sarajedini, 1998; Bonatto, Bica & Santos, 2005; De Marchi, Paresce & Portegies Zwart, 2010). This suggests that OCs and the least massive Milky Way GCs should have stellar mass functions that, at least in their central cluster regions, appear eroded at the low-mass end. From this, we expect $< m > \lesssim m_{TO}$. Finally, most of the stars involved in dynamical encounters should have masses close

to or even slightly greater than the average stellar mass $< m >$. This is because gravitational focusing is strongest for the most massive objects, contributing to a shorter encounter time-scale.

Finally, the most likely formation scenario will, strictly speaking, minimize the total or cumulative encounter time-scale. However, the total time-scale required for a dynamical formation scenario that involves more than one encounter will typically be dominated by the second encounter. This is because, after an initial encounter has occurred between any two suitable objects to form a new stellar configuration, the time-scale for a second encounter to occur is given by the time required for the product of the initial encounter to experience a subsequent encounter. *This increases the encounter time-scale by a factor* $N_0$. In other words, Equation 2.10 provides the time required for *any* two of the specified objects to experience an encounter (two binaries, a binary and a triple, etc.). It can be multiplied by $N_0$ to obtain an estimate for the time required for a *specific* object to experience an encounter. For example, to find the time required for a specific binary to experience an encounter with another single, binary or triple star, we must multiply by a factor $f_b N_c$. It follows that the time-scale for multiple encounters to occur is considerably longer than any of the single encounter time-scales. Therefore, unless the number of either binary or triple stars is very low, scenarios involving the fewest number of encounters are generally preferred since this tends to minimize the total time required for the encounter(s) to occur in a realistic cluster environment.

The times *between* the various types of encounters can be derived using

Equation 2.10 and have been provided in Appendix A. These time-scales can be multiplied by $(1-f_b-f_t)N_c$, $f_bN_c$ or $f_tN_c$ to find the time required for a *particular* single, binary or triple star, respectively, to encounter another object. This yields time-scales that are in rough agreement with Equation 8-125 of Binney & Tremaine (1987). As an example, we can multiply Equation A.8 by $f_bN_c$ to find the time for a particular binary to experience an encounter with another binary. This gives:

$$\tau^b_{2+2} = 2.7 \times 10^{10} f_b^{-1} \Big(\frac{10^3 pc^{-3}}{n_0}\Big) \Big(\frac{v_{rms}}{5km/s}\Big)\Big(\frac{0.5M_\odot}{<m>}\Big)\Big(\frac{1AU}{a_b}\Big)\text{years}, \tag{2.12}$$

Provided the derived encounter time-scale is shorter than the lifetime of the merger product(s), this suggests that the encounter scenario in question could be realistic and is therefore a candidate formation history. Conversely, if the derived encounter time-scale is longer than the lifetime of the merger product(s), then the dynamical formation history is unlikely to have actually occurred. In general, the shorter the derived encounter time-scale, the more likely it is that one or more such encounters actually took place within the lifetime of the merger product(s).

The preceding guidelines specify a narrow range of allowed formation scenarios. In particular, they constrain the number of stars involved in the encounter(s), the types of objects (i.e. single, binary or triple stars) involved, and the number of encounters that took place. In most cases, these guidelines will converge on a single qualitative formation history that is unique up to the possible initial distribution of energies that describe suitable interactions.

2. Next, we must assign an approximate value based on the observations to every parameter possible in Equation 2.1. Nearly all of the required information pertaining to the final distribution of energies in Equation 2.1 can be found from spectroscopy alone, though repeated measurements spread out over a sufficiently long time-line will typically be required to obtain orbital solutions and to detect outer triple companions whenever they are present. This gives the final orbital energies $\epsilon_{kk}$ as well as the gravitational binding energies $W_{ii}$ of the stars according to Equation 2.7 and Equation 2.4, respectively. Since merger products have been shown to typically be in hydrodynamic equilibrium (e.g. Sills et al., 2001), the stars' internal energies $U_{ii}$ can then be approximated using the virial theorem. Alternatively, stellar models can be used together with photometry.

   The measured broadening of spectral lines gives an estimate for the stars' rotation speeds (although there is a strong dependence on the angle of inclination of the stars' axis of rotation relative to the line of sight), which in turn provides their rotational kinetic energies $\Omega_{ii}$ according to Equation 2.2. In conjunction with proper motions, radial velocity measurements also provide an estimate for the systemic velocity of the final stellar configuration relative to the cluster mean, which in turn gives its translational kinetic energy $T_{jj}$ according to Equation 2.5. Finally, the cluster velocity dispersion provides an estimate of the relative velocity at infinity for a typical encounter, which in turn decides the initial translational kinetic energies $T_j$ of stars or binaries involved in the encounter. Under the assumption of energy equipartition for both single

and binary stars, the initial velocities of the impactors can be approximated by Equation 2.6. The assumption of energy equipartition should be valid in clusters for which the half-mass relaxation time is considerably shorter than the cluster lifetime, and this is the case for most GCs (Harris, 1996, 2010 update; De Angeli et al., 2005). On the other hand, this assumption is likely invalid for most open clusters. This is because the tidal truncation of the velocity distributions are significant in OCs since they are much less centrally concentrated. In this case, the initial velocities of the impactors can be approximated from the velocity dispersion, which is nearly independent of mass.

3. We can now obtain *quantitative* constraints for the initial encounter(s). Once we have decided on a qualitative encounter scenario that could have produced the observed merger product(s), we can estimate the orbital energies of the initial binaries or triples going into the encounter using Equation 2.9. This gives us an equation that relates the initial orbital semi-major axes of all orbits going into the encounter (to each other). If only one orbit goes into the encounter, then we can solve for it explicitly. From this, we can constrain the initial collisional cross sections for realistic encounters. If the derived cross section is significantly smaller than the average semi-major axes of all binaries and/or triples in the cluster, then we can infer that the time required for the encounter to occur is significantly longer than the corresponding time-scale given in Appendix A. If we use our derived cross section found from Equation 2.9 instead of this average semi-major axis, this should give us an idea of the time required for that particular type of encounter to occur. Strictly speak-

ing, however, this is only a rough approximation since these are typical time-scales found using the average period (or, equivalently, semi-major axis and hence cross section).

If we find that the derived encounter time-scale is longer than the life-time of a typical merger product, then the chosen formation history is unlikely to have actually occurred. In this case, it becomes necessary to re-evaluate the possible dynamical formation histories of the observed binary or triple system, choosing the next most likely qualitative scenario for further quantitative analysis. These steps can be repeated until either a suitable formation history is found or the list of possibilities is exhausted so that the only remaining conclusion is that the observed binary or triple system is unlikely to have a dynamical origin.

## 2.3 Results

In this section, we apply our technique to two particular cases of observed binaries and triples containing merger products. The first is an observed triple system in the old open cluster M67 that is thought to contain two BSs (van den Berg et al., 2001; Sandquist et al., 2003). The second is the period-eccentricity distribution of the BS binary population of the OC NGC 188, which bears a remarkable resemblance to M67 (Mathieu & Geller, 2009). After determining the most probable qualitative formation scenarios, we obtain quantitative constraints for suitable initial conditions that could have produced the observed orbital parameters.

### 2.3.1 The Case of S1082

S1082 is believed to be a triple system in the old OC M67 (van den Berg et al., 2001; Sandquist et al., 2003). The observations suggest that a distant triple companion orbits a close binary containing a BS and another peculiar star. The companion to the BS has a photometric appearance that puts it close to the MSTO in the CMD and yet, curiously, its derived mass is significantly greater than that of the turn-off. The outer companion is a BS in its own right, so that S1082 is thought to be composed of two BSs. Although both the inner and outer components of this suspected triple have systemic velocities that suggest they are both cluster members, it is important to note that there is no direct evidence proving a dynamical link between the two (Sandquist et al., 2003). Assuming for the time being that a dynamical link does exist, we can apply the procedure outlined in Section 2.2.2 to the case of S1082:

1. Before applying our technique, it is important to convince ourselves that a dynamical origin is possible for the observed system. This is certainly the case for S1082 since no known BS formation mechanism could have produced the observed stellar configuration without at least some help from dynamical interactions. The first step of our procedure is to find qualitative constraints and, in so doing, isolate the most probable encounter scenario.

   First, we need to know the cluster binary and triple fractions in order to use Figure 2.1 to find the encounter type occurring with the greatest frequency. From this, we find that 2+2 encounters presently dominate in M67. Fan et al. (1996) showed that observations of M67 are consistent with a cluster multiple star fraction $\sim 50\%$. More recent studies

report a lower limit for $f_b + f_t$ that is consistent with their results (e.g. Latham, 2005; Davenport & Sandquist, 2010). Radial velocity surveys and simulations of dynamical interactions suggest that old OCs like M67 are likely to host a number of triples with outer periods $\lesssim 4000$ days (e.g. Latham, 2005; Ivanova et al., 2008). We assume $f_t/f_b \sim 0.1$ and, using the result of Fan et al. (1996), this gives $f_b \sim 0.45$ and $f_t \sim 0.05$. Our assumed ratio $f_t/f_b$ is slightly lower than found for the field, or $f_t/f_b \sim 0.2$ (Eggleton & Tokovinin, 2008).

Second, we need to constrain the number of stars that went into the encounter. The mass of the MSTO in M67 is estimated to be $\sim 1.3$ $M_\odot$ (Mathieu & Geller, 2009). The total mass of S1082 is $\sim 5.8$ $M_\odot$ (Sandquist et al., 2003). From Equation 2.11, its formation must therefore have involved at least 5 stars.

At this point, we can conclude that a single 2+2 encounter could not have produced S1082 since this scenario involves only 4 stars and we know that at least 5 stars are needed. We must therefore consider either a single 2+3 or 3+3 encounter, or a multiple encounter scenario. In order to isolate the most probable of these possibilities, we must calculate and compare their encounter time-scales. To do this, we require estimates from the observations for a few additional cluster parameters. For M67, the core radius is $r_c \sim 1.23$ pc (Bonatto, Bica & Santos, 2005; Giersz, Heggie & Hurley, 2008). From this and the central velocity dispersion, we can calculate the central mass density using Equation 4-124b of Binney & Tremaine (1987), which gives $\rho_0 \sim 10^{1.9}$ $M_\odot$ $pc^{-3}$. The cen-

tral stellar number density can then be approximated according to:

$$n_0 = \frac{\rho_0}{< m >} \frac{M}{L}, \tag{2.13}$$

where M/L is the cluster mass-to-light ratio and should be around 1.5 for an OC as old as M67 (e.g. De Grijs et al., 2008). We take $f_t \sim 0.05$ and assume most stable triples have outer periods of $P \sim 1000$ days so that $a_t \sim 3$ AU (assuming all three stars have a mass of 1 $M_\odot$). We also take $f_b \sim 0.45$ and assume an average binary period of $P \sim 100$ days so that $a_b \sim 0.6$ AU (assuming both components have a mass of 1 $M_\odot$). We assume an average stellar mass of $< m > \sim 1.0$ $M_\odot$, which is in reasonable agreement with the observations (Girard et al., 1989). Assuming that the average mass of merger remnants is equal to $2 < m >$ and extrapolating the results of Sills et al. (2001) for solar metallicity and more massive parent stars, we will assume that the typical lifetime of a merger product is $\tau_{BS} \sim 1.5$ Gyrs.

A comparison of the relevant encounter time-scales suggests that the most probable dynamical formation scenario for S1082 is a single 2+3 encounter, although a single 3+3 encounter is almost equally as probable. Given our assumptions, we find $8.9 \times 10^8$ years and $3.3 \times 10^9$ years for the times between 2+3 and 3+3 encounters, respectively, in the core of M67. From this, we expect approximately two and zero 2+3 and 3+3 encounters, respectively, to have occurred within the last $\tau_{BS}$ years.

From Equation 2.12, we find that the time for a particular binary to encounter another binary is $7.3 \times 10^{10}$ years. Similarly, the time for a particular quadruple to encounter another binary is $8.9 \times 10^9$ years (using

Equation 2.12 and assuming the quadruple has a mass of $4 < m >$ and its geometric cross section is twice as large as the average outer semi-major axis of triples). Since these time-scales are considerably longer than the cluster lifetime, this suggests that a formation scenario for S1082 involving back-to-back 2+2 encounters is unlikely, even if the second encounter occurred sufficiently soon after the first that all four stars comprising the initial pair of interacting binaries are still gravitationally bound. If we replace one of the 3 binaries involved in this scenario with a triple system, the total encounter time remains longer than the cluster lifetime.

2. Before more quantitative constraints can be found, we must refer to the literature in order to obtain estimates for every term in Equation 2.9. The observations suggest that a binary system composed of a 2.52 $M_{\odot}$ blue straggler (component Aa) and a 1.58 $M_{\odot}$ MS star (component Ab) has a period of $P \sim 1.068$ days (van den Berg et al., 2001). There is also evidence for a 1.7 $M_{\odot}$ blue straggler companion (component B) that acts as a stable outer triple with a period of $P \sim 1188.5$ days (Sandquist et al., 2003). From this, we can calculate the final orbital energies ($\epsilon_A$ and $\epsilon_B$) of the triple:

$$|\epsilon_A| + |\epsilon_B| \sim |\epsilon_A| \sim 10^{41} J, \tag{2.14}$$

where we have used the fact that $|\epsilon_A| \gg |\epsilon_B|$ since $|\epsilon_B| \sim 10^{39}$ J. It is important to note that these peculiar stars are often under-luminous, so the inferred mass of the tertiary companion should be taken with caution (van den Berg et al., 2001).

The systemic radial velocity of the system is 33.76±0.12 km/s (Sandquist et al., 2003). Although this only provides us with an estimate for the systemic velocity of S1082 in one dimension, it is consistent with the cluster mean velocity of 33.5 km/s. Therefore, the available knowledge for the systemic velocity of S1082 is consistent with its final translational kinetic energy being negligible. From this, we take $T_{A,B} \sim 0$. The central velocity dispersion in M67 is only 0.5 km $s^{-1}$ (Mathieu & Latham, 1986; Mathieu et al., 1990). This suggests that the relative velocity at infinity, and therefore the typical impact velocities of collisions, should be small compared to the significant orbital energy of component A in S1082 (and any very hard binaries that went into the encounter). From this, we take $\Delta_m \sim 0$.

3. We are now ready to obtain quantitative constraints for the formation of S1082. We can use Equation 2.9 since M67 is an old OC with a small central velocity dispersion so that the assumptions used to derive this equation are valid. At this point, we must consider the details of our chosen formation scenario more carefully in order to choose a set of initial conditions that will satisfy Equation 2.9 as well as reproduce the observed parameters of S1082. In doing so, we find that it is not possible to form S1082 with a single 2+3 encounter. This is because 5 stars with masses $m < m_{TO}$ are insufficient to form both an inner binary with a total mass $\sim 4.1$ $M_\odot$ and an outer tertiary companion with a mass 1.7 $M_\odot$. That is, the total mass of the inner binary is larger than three times the mass of the MSTO so that its formation must have involved four or more stars.

A single 3+3 encounter is therefore the most probable formation scenario for S1082. Although there are a number of ways we can reproduce the observed parameters of S1082 with a 3+3 encounter, including the component masses, we must use Equation 2.9 to identify the most probable of these scenarios. To do this, we can solve for the initial orbital energies of all binaries and/or triples going into the encounter, which will in turn constrain their initial semi-major axes and therefore cross sections for collision. In applying Equation 2.9, we are only concerned with the initial and final orbital energies of the inner binaries of the triples. This is because the orbital energies of any outer triple companions will be significantly outweighed by the orbital energies of their inner binaries. It follows that the contribution from the outer orbital energies of triples to the total energy of the encounter will be negligible.

From Equation 2.9, we find that the formation of S1082 should have involved at least one hard binary with $|\epsilon_i| \sim 10^{41} J$ whose components did not merge (with each other) during the encounter in order to account for the significant orbital energy of component A. This need not be the case, however, if one or more stars were ejected from the system with an escape velocity of $\gtrsim 100$ km/s. Of course, this would require an increase in the total number of stars involved in the interaction and therefore a single encounter scenario involving 7 or more stars, and hence one or more quadruple systems. Although very few observational constraints for the fraction of quadruple systems in clusters exist, this seems unlikely.

The orbital energies of the inner binaries of the two triples initially going into the encounter should both be on the order of $10^{41}$ J. Although we

have found that only one hard binary with $|\epsilon_i| \sim 10^{41}$ J is required, triples are only dynamically stable if the ratio of their inner to outer orbital periods is large (roughly a factor of ten or more) (e.g. Mardling, 2001). We do not expect very wide binaries to survive for very long in dense cluster environments, which suggests that the inner binary of every triple is very hard. We expect from this that these inner binaries should, to within an order of magnitude, all have roughly the same orbital energy.

The presence of outer triple companions is required in order for most very hard binaries to actually experience encounters within the lifetime of a typical merger product. Assuming masses of 1 $M_\odot$ for both components, an orbital energy of $10^{41}$ J corresponds to a period $\sim$ 0.4 days, or a semi-major axis $\sim$ 0.02 AU. Therefore, the cross section for collision for a 2+2 encounter in which both binaries are very hard is smaller than the average cross section for a 2+2 encounter (found from the observed binary period distribution) by a factor of $\sim$ 30. This suggests that the time required for an encounter to occur between two very hard binaries is considerably longer than the cluster lifetime. This is not the case if the hard binaries have triple companions, however, since the outer orbit significantly increases the collisional cross section and hence decreases the encounter time-scale.

Energy conservation also suggests that if S1082 did form from a single 3+3 encounter, it is likely that the close inner binaries of the two triples collided directly. If two separate mergers then subsequently occurred during this interaction, this could have reproduced the observed orbital parameters of the close inner binary of S1082 (component A). The for-

mation of the outer triple companion is more difficult to explain via a single 3+3 encounter since it also appears to be the product of a stellar merger. Nonetheless, if the outer companions of both triples undergoing the encounter end up orbiting the interacting (or merged) pair of close inner binaries at comparable distances, it is possible that their orbits would overlap as a result of gravitational focussing. Although this seems unlikely, it could produce a blue straggler of the right mass and orbital period to account for component B. We will return to this possibility in Section 2.4.

Even though the analytic estimates presented here are only approximate, they serve to highlight the low probability of a system such as S1082 having formed dynamically in M67. Based on our results, the most likely formation scenario for S1082 is a single 3+3 encounter, although we expect very few, if any, to have occurred in the lifetime of a typical merger product. This need not be the case, however, provided M67 had a higher central density in the recent past since this would increase the total encounter frequency. This will be discussed further in Section 2.4.

### 2.3.2 The Period-Eccentricity Distribution of the Blue Straggler Binary Population in NGC 188

Mathieu & Geller (2009) found 21 blue stragglers in the old open cluster NGC 188. Of these, 16 are known to have a binary companion. Orbital solutions have been found for 15 of these known BS binaries. From this, Mathieu & Geller (2009) showed that the BS binary population in NGC 188 has a curious period-eccentricity distribution, with all but 3 having periods of

$\sim$ 1000 days. Of these three, two have periods of $\lesssim$ 10 days (binaries 5078 and 7782). Interestingly, one of these short-period BS binaries has a non-zero eccentricity. The normal MS binary population, on the other hand, shows no sign of a period gap for $10 \lesssim P \lesssim 1000$ days (Mathieu & Geller, 2009). We can apply the procedure outlined in Section 2.2.2 to better understand how we expect mergers formed during dynamical encounters to contribute to the BS binary population in NGC 188. Although the method described in Section 2.2.2 treats one system at a time, we will apply our technique to the BS binary population of NGC 188 as a whole.

1. Before applying our technique, we must satisfy ourselves that a dynamical origin is possible for a large fraction of the observed BS population. Several examples of evidence in favour of a dynamical origin exist. For one thing, most BSs in NGC 188 have been found to have binary companions (Mathieu & Geller, 2009). This should not be the case if most BSs are the products of the coalescence of isolated binary systems. On the other hand, a binary companion should be expected if the BSs were formed from mass transfer. However, the results of Chen & Han (2008b) could suggest that most of the BSs in NGC 188 were not formed from mass transfer alone, providing indirect evidence that many BSs were formed from mergers. A binary companion should also be expected if the coalesced binary had a tertiary companion to begin with. Although the Kozai mechanism can act to decrease the orbital separation of the inner binary of a triple, an additional perturbation is often required in order to fully induce the binary to merge (Perets & Fabrycky, 2009). All of this suggests that dynamical interactions likely played at least some

role in the formation of a significant fraction of the BS binary population in NGC 188.

The first step of our technique is to find the most commonly occurring type(s) of encounter(s). Geller et al. (2008) found a completeness-corrected multiple star fraction $f_b + f_t \sim 0.27$ out to a period of $\sim 4000$ days. This represents a lower limit since it does not include binaries with $P \gtrsim 4000$ days. Using the same lower limit for the ratio $f_t/f_b \sim 0.1$ found by Latham (2005), Figure 2.1 suggests that 1+2 encounters should currently dominate in NGC 188.

Second, we must constrain the minimum number of stars required to form the observed systems. From this, we can show that a merger occurring during all but a 1+1 encounter could produce a BS in a binary since this is the only type of encounter that involves less than 3 stars. By dividing the total mass of an observed system by $m_{TO}$, we can find an estimate for the minimum number of stars required to have been involved in its formation. Since all but one BS binary contain only a single merger product with a mass $\geq m_{TO}$, realistic dynamical formation scenarios for these systems require 3 or more stars. Binary 7782, on the other hand, is thought to contain two BSs so that if its formation involved two separate mergers it must have required 4 or more stars.

A more quantitative comparison of the different encounter types is required since we do not yet know if *enough* encounters occurred in the last $\tau_{BS}$ years to account for all 16 observed BS binaries. To do this, we require estimates from the observations for a few additional cluster parameters in order to calculate and compare the relative encounter

time-scales. NGC 188 has been found to have a central density of $\rho_0 = 10^{2.2}$ $L_\odot$ $pc^{-3}$ (Sandquist et al., 2003) and a core radius of $r_c \sim 1.3$ pc (Bonatto, Bica & Santos, 2005). We found an average stellar mass for the cluster of $< m > \sim 0.9$ $M_\odot$. This was done by determining the cluster luminosity function using only those stars known to be cluster members from the proper-motion study of Platais et al. (2003). With this, a theoretical isochrone taken from Pols et al. (1998) was used to determine the cluster mass function and the average stellar mass was calculated.

A sufficient number of suitable dynamical interactions should have occurred in the last $\tau_{BS}$ years for the formation of every BS binary in NGC 188 to have been directly mediated by the cluster dynamics. Assuming once again that $\tau_{BS} \sim 1.5$ Gyrs, the encounter time-scales derived in Appendix A suggest that a minimum of nine, eight, eight, three and one 1+2, 2+2, 1+3, 2+3 and 3+3 encounters, respectively, occurred within the lifetime of a typical merger product. It follows that at least $\sim 29$ dynamical encounters should have occurred in NGC 188 in the last $\tau_{BS}$ years. Of these 29 encounters, 12 should have involved triples. In deriving these time-scales, we have taken $f_b + f_t \sim 0.27$ from Geller at al. (2009) and have adopted the same ratio $f_t/f_b \sim 0.1$ as found for M67. Consequently, these represent lower limits for $f_b$ and $f_t$, so that our derived encounter rates are also lower limits. We have also assumed an average outer semi-major axis for triples of $a_t \sim 3$ AU (corresponding to a period of $\sim 1000$ days for a binary composed of two 1 $M_\odot$ stars).

2. The next step is to apply our energy conservation prescription to the

observed BS population. This will allow us to constrain the orbital energies of typical binaries or triples expected to form BS binaries via dynamical interactions. First, we must refer to the literature in order to obtain estimates for every term in Equation 2.9. From the observed BS period-eccentricity distribution in NGC 188, we know that most BS binaries have periods of $\sim$ 1000 days (we will call these long-period binaries), although there are a couple with very short periods of $\sim$ 10 days (which we will call short-period binaries). This provides an estimate for the final orbital energies $\epsilon_{kk}$ of BS binaries formed during dynamical interactions. Specifically, we find $|\epsilon_{kk}| \sim 10^{39}$ J and $|\epsilon_{kk}| \sim 10^{40}$ J for the final absolute orbital energies of the long- and short-period BS binaries, respectively.

Every BS in NGC 188 with a high cluster membership probability has both radial and proper motion velocities that, to within their respective uncertainties, are consistent with the observed central velocity dispersion of $\sigma_0 = 0.41$ km s$^{-1}$ (Platais et al., 2003; Geller et al., 2008; Geller at al., 2009). From this, we assume that the final translational kinetic energies of any binaries or triples formed from dynamical interactions will be negligible, or $T_{jj} \sim 0$. As for M67, we assume $\Delta_m \sim 0$ since we expect low impact velocities for collisions as a result of the low velocity dispersion in NGC 188.

3. We are now equipped with estimates from the literature that will allow us to obtain quantitative constraints for specific encounter scenarios. In particular, we can use Equation 2.9 to constrain the initial orbital energies of all binaries and/or triples going into an encounter. We can

also constrain the specific details of interactions for which the encounter outcome reproduces the observed parameters of the BS binary. We will consider energy conservation separately for two different classes of BS binaries, namely short- and long-period.

The short-period BS binaries have large (absolute) orbital energies. Equation 2.9 suggests that this energy requires that at least one hard binary was involved in the encounter. Alternatively, an encounter which involved only softer binaries must have resulted in at least one star escaping with a significant velocity ($\gtrsim$ 100 km/s). However, in order to produce a merger product in a short-period binary, encounters involving triples are the most favoured. Binary-binary (and especially 1+2) encounters which involve at least one hard binary will have smaller cross sections for collision than those encounters involving wide binaries. But energy conservation suggests that 2+2 encounters involving wide binaries are unlikely to produce a merger product in a close binary. Stable triples, on the other hand, contain a hard inner binary (Mardling, 2001) which will naturally account for the large orbital energy of the resulting BS binary. Stable triples also have a large cross section for collision because of the wide orbit of the tertiary companion. The times between 1+2, 2+2 and 1+3 encounters are all comparable, suggesting that most encounters involving hard binaries are 1+3 encounters.

The short-period BS binaries could have formed from a direct stellar collision that occurred within a dynamical encounter of a hard binary and another single or (hard) binary star (we call this Mechanism I). If at least one of the objects going into the encounter was a triple, then four or

more stars were involved in the interaction. Therefore, if binaries 5078 and 7782 were formed from this mechanism, they could possess triple companions with sufficiently long periods that they would have thus far evaded detection. This is consistent with the requirements for both conservation of energy and angular momentum. Interestingly, the presence of an outer triple companion could also contribute to hardening these BS binaries via Kozai cycles operating in conjunction with tidal friction (Fabrycky & Tremaine, 2007). In this case, Equation 2.1 shows that tides can contribute to making a binary's orbital energy more negative by depositing internal energy into the component stars.

Although 2+2 encounters should also contribute to the observed BS population, most of these should occur between a short-period binary and a long-period binary. This is because most encounters resulting in mergers involve very hard binaries and binaries with long periods have large cross sections for collision and therefore short encounter times. Equation 2.9 indicates that the minimum period of a BS binary formed during a 2+2 encounter is usually determined by the orbital energy of the softest binary going into the encounter. This is because the most likely merger scenario is one for which the hard binary is driven to coalesce by imparting energy and angular momentum to other stars involved in the interaction (Fregeau et al., 2004). Assuming most of this energy is imparted to only one of the stars causing it to escape the system, we can take $\Delta_m$ in Equation 2.9 to be very small and the orbital energy of the left-over BS binary will be comparable to the orbital energy of the initial wide binary going into the encounter. As more energy is imparted to the

star left bound to the merger product over the course of the interaction, its final orbital separation effectively increases. This in turn contributes to an increase in the final orbital energy of the left-over BS binary. Finally, from Equation A.8, the period of the initial wide binary should be relatively long (roughly $\gtrsim 1000$ days) since the contribution from the very hard binary to the total cross section for collision is negligible. Otherwise, the time required for such a 2+2 encounter to occur could exceed $\tau_{BS}$.

Now let us consider the long-period BS binaries in NGC 188. Based on Equation 2.9, we expect encounters involving 3 or more stars and only one very hard binary to typically produce long-period BS binaries if the hard binary is driven to merge during the encounter. This is because the hard binary merges so that its significant (negative) orbital energy can only be re-distributed to the other stars by giving them positive energy. Since the only other orbits involved in the interaction are wide, the left-over BS binary should also have a wide orbit. Alternatively, BSs formed during interactions involving more than one very hard binary should be left in a wide binary provided enough energy is extracted from the orbit of the binary that merges. In this case, a significant fraction of this energy must be imparted to the other stars in order to counter-balance the significant orbital energy of the other very hard binary. If not, the other short-period binaries are required to either merge or be ejected from the system. Otherwise Equation 2.9 suggests that the left-over BS binary should be very hard. However, it is important to recall that we are neglecting other non-dynamical mechanisms for energy extraction.

We will return to this last point in Section 2.4.

In order to help us obtain more quantitative estimates for the long-period BS binaries, consider two additional mechanisms for mergers during dynamical interactions that involve both short- and long-period orbits. First, a merger can occur if a sufficient amount of orbital energy is extracted from a hard binary by other interacting stars (called Mechanism IIa). Alternatively, a merger can occur if the encounter progresses in such a way that the eccentricity of a hard binary becomes sufficiently increased that the stellar radii overlap, causing the stars to collide and merge (called Mechanism IIb). In the case of Mechanism IIb, most of the orbital energy of the close binary must end up in the form of internal and gravitational binding energy in the merger remnant after the majority of its orbital angular momentum has been redistributed to the other stars (and tides have extracted orbital energy). In the case of Mechanism IIa, however, most of the orbital energy of the close binary must be imparted to one or more of the other interacting stars in the form of bulk kinetic motion. Consequently, one or more stars are likely to obtain a positive total energy and escape the system. This need not necessarily be the case for 2+3 and 3+3 encounters provided the second hardest binary orbit involved in the interaction has a sufficiently negative energy.

Regardless of the type of encounter, Equation 2.9 shows that the extraction of orbital energy from a hard binary in stimulating it to merge should increase the final orbital period of a BS binary. To illustrate this, we will consider 1+3 encounters since the predictions of energy conservation are nearly identical for the other encounter types of interest. Moreover, we

have shown that encounters with triples are the most likely to involve very hard binaries. Equation 2.9 can be re-written for 1+3 encounters:

$$\epsilon_{12,4} = \epsilon_{12,3} - f_{12} \times \epsilon_{12}, \tag{2.15}$$

where we have assumed that stars 1 and 2 comprise the initial hard inner binary of the triple, star 3 is the initial outer triple companion and star 4 is the interloping single star. Stars 1 and 2 are assumed to merge during the encounter by exchanging energy and angular momentum with stars 3 and 4. We further assume that enough energy is imparted to star 3 that it escapes the system. We let $f_{12}$ represent the fraction of energy extracted from the orbital energy of the hard inner binary of the triple in the form of bulk kinetic motion by star 4. Since the remaining orbital energy of the close inner binary will end up in the form of internal and gravitational binding energy in the merger remnant, we have assumed $(1 + f_{12}) \times \epsilon_{12} \sim T_3 - \Delta_m$ in obtaining Equation 2.15 from Equation 2.9.

This formation mechanism could leave the BS as a single star if $f_{12}$ exceeds a few percent. As shown in Figure 2.2, the period of a BS binary formed during a 1+3 encounter via Mechanism IIa ($P_{12,4}$) is only slightly smaller than the period of the outer orbit of the triple initially going into the encounter ($P_{12,3}$). This assumes, however, that no energy is exchanged between the hard inner binary and star 4 (i.e. $f_{12} = 0$). The predictions from energy conservation for this case are therefore identical for Mechanism IIb. In general, as the amount of energy extracted from the hard inner binary of the triple by star 4 increases, so too does the rate at which $P_{12,4}$ increases with increasing $P_{12,3}$. If the amount of energy

extracted is $\gtrsim 5\%$ of the orbital energy of the initial inner binary of the triple, $P_{12,4}$ becomes a very steeply increasing function of $P_{12,3}$.

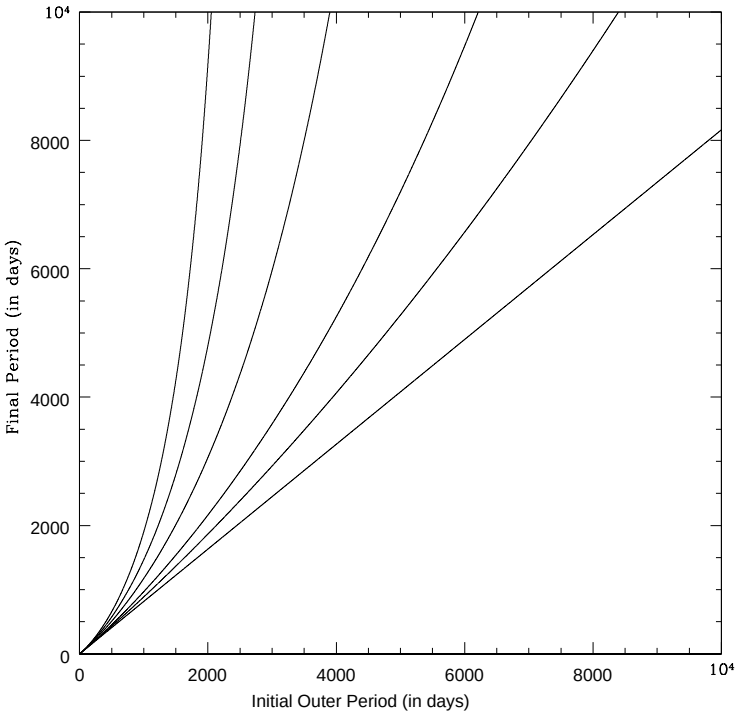



Figure 2.2 Plot showing the typical periods of BS binaries formed from 1+3 encounters in which the hard inner binary of the triple merges. As described in the text, the period of the BS binary formed during the interaction is denoted $P_{12,4}$ and corresponds to the y-axis, whereas the period of the outer orbit of the triple initially going into the encounter is denoted $P_{12,3}$ and corresponds to the x-axis. The lower straight line corresponds to the case where no energy was extracted from the inner binary of the triple by star 4 (i.e. $f_{12} = 0$). As the amount of energy extracted increases, however, so too will the rate at which $P_{12,4}$ increases with increasing $P_{12,3}$. Cases where $f_{12} = 0.005$, $f_{12} = 0.01$, $f_{12} = 0.02$, $f_{12} = 0.03$ and $f_{12} = 0.04$ are shown as lines of increasing slope.

Interestingly, the two general qualitative merger scenarios described above (Mechanisms I and II) naturally create a bi-modal period distribution similar to the period gap observed for the BS binaries if we assume that 1+3 encounters produced these objects. To illustrate this, Figure 2.3

shows a histogram of periods for 15 BS binaries formed during 1+3 encounters via these two generic merger scenarios. In order to obtain this plot, we have used the observed period-eccentricity distribution for the regular MS-MS binary population in NGC 188 from Geller at al. (2009) to obtain estimates for the orbital energies of any binaries and/or triples going into encounters. Specifically, in order to obtain periods for the outer orbits of triples undergoing encounters, we randomly sampled the regular period distribution, including only those binaries with periods satisfying 400 days $< P <$ 4000 days. We have shown that the initial outer orbits of triples going into 1+3 encounters provide a rough lower limit for the periods of BS binaries formed via Mechanism II. Therefore, any BS binaries formed in this way could only have been identified as binaries by radial velocity surveys if the triple going into the encounter had a period $<$ 4000 days (since this corresponds to the current cut-off for detection). All triples are taken to have a ratio of 30 between their inner and outer orbital semi-major axes. This ratio has been chosen to be arbitrarily large enough that the triples should be dynamically stable, however we will return to this assumption in Section 2.4.

We will adopt a ratio based on the observations of Mathieu & Geller (2009) for the fraction of outcomes that result in each of these two possible merger scenarios. In particular, if we assume that the three BS binaries with $P <$ 150 days were formed via Mechanism I whereas the other 12 were formed via Mechanism II (either IIa or IIb since energy conservation predicts similar periods for the left-over BS binaries), this would suggest that Mechanism II is $\sim 4$ times more likely to occur than

Mechanism I during any given 1+3 encounter. We will return to this assumption in Section 2.4.

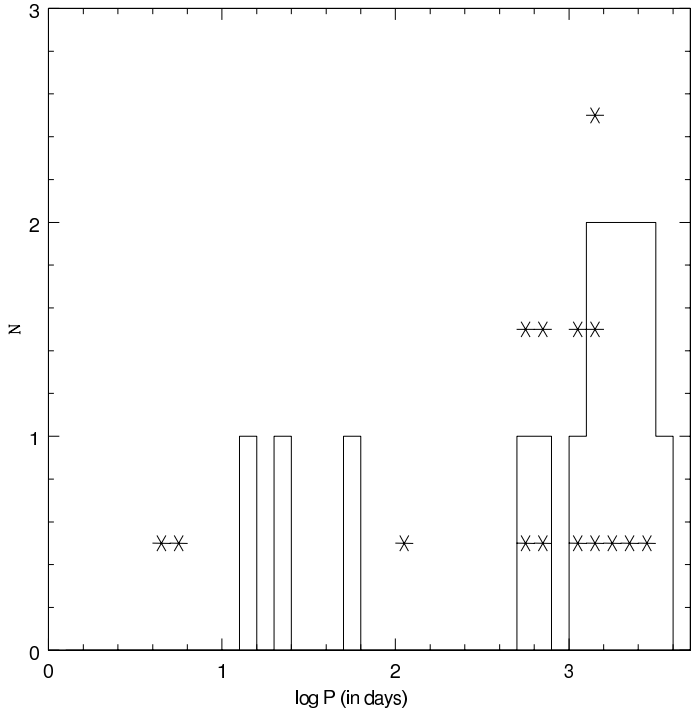



Figure 2.3 Histogram of the period distribution (in days) expected for BS binaries formed during 15 1+3 encounters. The parameter space assumed for the encounters is described in the text. The stars show the observed BS binary period distribution in NGC 188 taken from Mathieu & Geller (2009), where each star represents a single BS binary.

As a result of the requirement for conservation of angular momentum, we would expect to see a large spread in the distribution of eccentricities for BSs in long-period binaries formed from encounters involving triples. This is because conservation of momentum requires that the total momentum going into the encounter must be equal to the total momentum left over after the interaction. However, the total initial momentum depends not only on the initial orbital eccentricities of any binaries or triples going into the encounter, but also the relative orientations and

trajectories of the colliding objects. Since the relative orientations and trajectories are random, the final eccentricities of the BS binaries can take on a range of values. In other words, we cannot predict the final distribution of momenta for BS binaries formed from dynamical encounters. However, the observed BS binaries in NGC 188 are observed to have a range of eccentricities and this is not inconsistent with a dynamical origin involving triples.

BSs in short-period binaries formed via Mechanism I can also end up with just about any eccentricity immediately after the encounter for the same reasons outlined above. However, tidal effects become increasingly significant with decreasing orbital separation so that the hardest binaries should typically circularize the fastest. Although theoretical estimates for the rate of tidal circularization are uncertain (Meibom et al., 2005), the circularization cut-off period is estimated to be $\sim$ 15 days in NGC 188 (Mathieu et al., 2004). From this, it is entirely possible that recently formed BS binaries with P $\sim$ 10 days have not yet become fully circularized.

## 2.4 Summary & Discussion

In this chapter, we have presented a generalized analytic prescription for energy conservation during stellar encounters. Our method can be used to identify the most probable dynamical formation scenario for an observed binary or triple system containing one or more merger products. We have shown that, using the observed orbital parameters of the system, the allowed initial orbital semi-major axes of any binary or triple systems involved in its formation can

be constrained. The initial semi-major axes of the orbits in turn provide an estimate for the collisional cross section and therefore the time-scale for the encounter to occur in its host cluster. In order to apply our technique, repeated spectroscopic measurements of the binary or triple system containing the merger product(s) are needed in order to obtain its orbital solution and systemic velocity. However, the time-scales provided in Appendix A can still be applied if only the fraction of binary and triple stars are known, which can be determined either spectroscopically (e.g. Mathieu et al., 1990; Latham, 2005) or photometrically (e.g. Fan et al., 1996).

As we have shown, consideration of the requirement for energy conservation is ideal for identifying trends during stellar encounters, whereas numerical scattering experiments can require hundreds or even thousands of simulation runs before patterns will emerge. Some of these trends include:

- At least one short-period binary is usually required in a dynamical interaction to produce another binary having a similarly short-period (provided no stars are ejected with escape velocities $\gtrsim$ 100 km/s). This is because the orbital energy of a short-period binary is sufficiently negative that it tends to considerably outweigh the other energy terms in Equation 2.1 for most of the encounters that typically occur in the cores of globular and especially open clusters. This has been confirmed by Hurley et al. (2005).

- Previous studies have found that in order for triples to remain stable for many dynamical times, the ratio of their inner to outer orbital periods must be relatively large (roughly a factor of ten or more) (e.g. Mardling, 2001). Based on our results, this has two important corollaries for stellar

mergers in dense cluster environments hosting a significant population of triples:

1. The longest-lived triples will contain very hard inner binaries with a large $|\epsilon|$. This is important since stellar radii are in general more likely to overlap and hence mergers to occur during resonant interactions involving very hard binaries (e.g. Fregeau et al., 2004; Hurley et al., 2005). We therefore expect stellar mergers to be common during encounters involving stable triple systems.

2. The longest-lived triples will contain wide outer orbits, creating a large cross section for collision. This suggests that the time-scale required for a stable triple system to encounter another object is typically short relative to the cluster age in dense environments. A significant fraction of encounters involving very hard binaries, and hence resulting in stellar mergers, will therefore involve triples in old open clusters such as M67 and NGC 188.

van den Berg et al. (2001) and Sandquist et al. (2003) suggest that back-to-back binary-binary encounters, or even a single 3+3 encounter, could have formed S1082. We have improved upon these previous studies by estimating time-scales required for possible dynamical formation scenarios to occur. Since we have argued in Section 2.3 that the formation of S1082 must have involved at least 6 stars, it follows that only a 3+3 interaction could have reproduced the observed configuration via a single encounter. However, the derived 3+3 encounter time-scale is sufficiently long that we expect very few, if any, 3+3 encounters occurred within the lifetime of a typical merger product. Moreover, we have argued that the times for multiple encounters to occur are longer than

the cluster age. Although we cannot rule out a dynamical origin for S1082, our results suggest that it is unlikely (provided the derived encounter time-scales were not significantly higher in the recent past, which we will return to below). From this, it follows that a dynamical link between the close binary and third star is unlikely to exist.

On the other hand, we have so far ignored the cluster evolution, and assumed that the currently observed cluster parameters have not changed in the last few Gyrs. N-body models suggest that the central density in M67 could have been significantly higher in the recent past. Specifically, Figure 5 of Hurley et al. (2005) indicates that the presently observed central density in M67 could have been higher within the past Gyr by a factor of $\gtrsim 2$. If this was indeed the case, our previous estimates for each of the different encounter frequencies should increase by a factor of $\sim 4$, so that a significant number of dynamical encounters involving single, binary and triple stars should have occurred in M67 within the last $\tau_{BS}$ years. It follows that a dynamical origin for S1082 is not unlikely if the central density in M67 was recently larger than its presently observed value by a factor of $\gtrsim 2$. This also increases the probability that a scenario involving multiple encounters created S1082, although we have shown that such a scenario is still likely to have involved one or more triples.

Based on the preceding arguments, S1082 offers an excellent example of how observations of individual multiple star systems containing BSs can be used to directly constrain the dynamical history of their host cluster. If a definitive dynamical link between components A and B is established, this would suggest that the central density in M67 was higher in the last 1-2 Gyrs. This is also required in order for the cluster dynamics to have played a role in the formation of a significant fraction of the observed BS population in M67.

Based on the current density, the encounter time-scales are sufficiently long that too few encounters should have occurred in the last $\tau_{BS}$ years for mergers during dynamical interactions to be a significant contributor to BS formation.

We have obtained quantitative constraints for two generic channels for mergers during encounters involving triples – one in which a direct stellar collision occurs within a dynamical interaction of the hard inner binary of a triple and another single or (hard) binary star (Mechanism I) and one in which the hard inner binary of a triple is driven to coalesce by imparting energy and/or angular momentum to other stars involved in the interaction (Mechanism II). Our results suggest that these two general merger mechanisms could contribute to a bi-modal period distribution for BS binaries similar to that observed in NGC 188. These dual mechanisms predict a gap in period, with those BS binaries formed via Mechanism I having periods of a few to $\sim 100$ days and those formed via Mechanism II having periods closer to $\sim 1000$ days. Some 2+2, 2+3 and even 1+3 encounters could involve orbits with periods in this range, and Equation 2.9 confirms that the final period of a BS binary formed via Mechanism II will typically be determined by that of the second hardest binary orbit. Therefore, we might still expect some BS binaries to have periods that fall in the gap (100 days $\lesssim$ P $\lesssim$ 1000 days). Our results do indeed predict one such BS binary, as shown in Figure 2.3.

A number of assumptions went into obtaining Figure 2.3, many of which were chosen specifically to reproduce the observed BS binary period distribution. Regardless, our assumptions were chosen to reflect encounter scenarios that are the most likely to result in mergers. These should involve triples with very hard inner binaries since these are the most likely to merge during encounters. The triples should also have outer companions on very wide orbits

since these have the largest cross sections for collision. From this, we have assumed a ratio of 30 between the inner and outer semi-major axes of all triples. This ensures that all triples are dynamically stable. This also leads us to assume a minimum period of 400 days for the outer orbits of triples so that the corresponding minimum period of their inner orbits is not too small. These assumptions serve to show that encounters involving triples could produce both long-period and short-period BS binaries as well as a period gap.

Our results predict that the short-period peak in Figure 2.3 is at a slightly longer period than the observations suggest. If we decrease the assumed ratio between the inner and outer orbital separations of triples, the short-period peak will move to even longer periods. However, if one or more stars were ejected with a high escape velocity or the dissipative effects of tides are considered (which are expected to be the most significant for encounters involving hard binaries) this would move the short-period peak to even shorter periods. In order to obtain the desired agreement with the observations at the short-period end of the BS period distribution, energy must have somehow been dissipated or removed from the hard inner binaries of the triples during (or even after) the encounter, or the inner binaries must have initially been even harder than we have assumed in obtaining Figure 2.3.

Our results could suggest that the hard BS binaries in NGC 188 (binaries 5078 and 7782) may have outer triple companions, perhaps with sufficiently long periods that they would have thus far evaded detection. This is consistent with the requirement for energy conservation since the orbital energy of the outer orbit of the triple is negligible compared to that of its inner binary. If binaries 5078 and 7782 do have outer triple companions, it is also possible that Kozai oscillations combined with tidal friction contributed to decreasing

their orbital periods (Eggleton, 2006). Finally, the BS binaries in NGC 188 are observed to have a wide range of eccentricities, which we have argued is not inconsistent with a dynamical origin involving triples.

We have assumed that Mechanism II is more likely to occur than Mechanism I during any given 1+3 encounter. This is a reasonable assumption since numerical scattering experiments of 1+2 and 2+2 encounters have shown that the coalescence of a hard binary is much more likely to occur during an encounter than a direct collision between a hard binary and an interacting single or binary star (e.g. Fregeau et al., 2004). The ratio we have assumed for the frequencies with which Mechanisms I and II occur was specifically chosen in order to reproduce the observed numbers of short- and long-period BS binaries. The important point to take away is that the observed BS binary period-eccentricity distribution offers a potential constraint on the fraction of encounters that result in different merger scenarios.

Based on our results, Mechanism II must occur $\sim 4$ times more often than Mechanism I in order to reproduce the observed BS period distribution from 1+3 encounters (or, equivalently, 2+3 encounters involving a very wide binary and 2+2 encounters between a short-period binary and a long-period binary). This can be tested by performing numerical scattering experiments of encounters involving triples. Therefore, our results highlight the need for simulations of 1+3, 2+3 and 3+3 encounters to be performed in order to better understand their expected contributions to BS populations in open and globular clusters. Once a preferred encounter scenario has been identified for an observed binary or triple containing one or more BSs, numerical scattering experiments can be used to further constrain the conditions under which that scenario will occur (or to show that it cannot occur). We have demonstrated

that a combination of observational and analytic constraints can be used to isolate the parameter space relevant to the dynamical formation of an observed multiple star system (or population of star systems) containing one or more merger products. This will drastically narrow the relevant parameter space for numerical scattering experiments.

We have improved upon the results of Perets & Fabrycky (2009) and Mathieu & Geller (2009) since we have shown that dynamical encounters involving triples could not only be contributing to the long-period BS binaries in NGC 188, but they could also be an important formation mechanism for short-period BS binaries and triples containing BSs. We have not ruled out mass transfer or Kozai-induced mergers in triples (primordial or otherwise) (Mathieu & Geller, 2009; Perets & Fabrycky, 2009), or even various combinations of different mechanisms, as contributing formation channels to the BS binary population in NGC 188. For instance, a 1+3 exchange interaction could stimulate a merger indirectly if the resulting angle of inclination between the inner and outer orbits of the triple exceeds $\sim 39^{\circ}$, ultimately allowing the triple to evolve via the Kozai mechanism so that the eccentricity of the inner binary increases while its period remains roughly constant (Eggleton, 2006).

There is evidence to suggest that mass transfer via Roche lobe over flow could play a role in the formation of at least some BSs. It is difficult to account for the near zero eccentricities of some of the long-period BS binaries without at least one episode of mass transfer having occurred. This is because none of the normal MS-MS binaries with similar periods have such small eccentricities (Mathieu & Geller, 2009). On the other hand, it may not be unreasonable to expect that some collision products left in binaries undergo mass transfer since they are expected to expand adiabatically post-collision, and will sooner

or later evolve to ascend the giant branch. As a result of conservation of energy and angular momentum, the mass transfer process will usually act to increase the orbital periods of these binaries provided it is conservative (Iben, 1991). Interestingly, the cut-off period for Roche lobe overflow is $\sim$ 1000 days for low-mass stars (Eggleton, 2006), which is in rough agreement with the long-period peak in the observed period-eccentricity distribution of the BS binary population in NGC 188. Therefore, mass transfer could also be contributing to the period gap observed for the BS binaries.

According to the results of Geller at al. (2009), the number of giant-MS binaries with $P \lesssim 1000$ days is comparable to the number of BS binaries (A. Geller, private communication). It is unlikely that every giant-MS binary will form a BS from mass transfer, however, suggesting that at most a few of the long-period BS binaries in NGC 188 were formed via this mechanism. Finally, if the outer companion of a triple system evolves to over-fill its Roche lobe it could transfer mass to both of the components of the close inner binary. This mechanism could therefore also produce two BSs in a close binary, although it predicts the presence of an orbiting triple companion. For these reasons, a better understanding of triple evolution, as well as binary evolution in binaries containing merger products, is needed.

The dissipational effects of tides tend to convert stars' bulk translational kinetic energies into internal or thermal energy within the stars, leading to an increase in the total gravitational binding energy of the stellar configuration (e.g. McMillan, Hut & Makino, 1990). By increasing the terms $U_{ii}$ in Equation 2.1, the initial orbital energies of any binaries going into an encounter can increase accordingly in order to conserve energy. A higher orbital energy corresponds to a larger semi-major axis and hence cross section for

collision. This suggests that the derived encounter time-scales can be taken as upper limits in the limit that tidal dissipation is negligible. We expect tides to be particularly effective during encounters for which the total energy is very negative as a result of one or more very hard binaries being involved.

We have argued in Section 2.2.2 that the average stellar mass is expected to be comparable to (but slightly less than) the mass of the MSTO in old OCs and low-mass GCs. We have also argued that most encounters will involve stars having masses slightly larger than the average stellar mass. We might therefore expect to find that a high proportion of merger products have masses that exceed that of the MSTO in very dynamically-evolved clusters that have lost a large fraction of their low-mass stars. Consequently, a larger number of merger products could appear sufficiently bright to end up in the BS region of the cluster CMD in these clusters than in their less dynamically-evolved counterparts. This is consistent with the results of Knigge, Leigh & Sills (2009) and Leigh, Sills & Knigge (2009) who found that the number of BSs in the cores of GCs scales sub-linearly with the core mass. In particular, since the cluster relaxation time increases with increasing cluster mass, it is the lowest mass GCs that should have lost the largest fraction of their low-mass stars. Therefore, if a larger fraction of merger products do indeed end up more massive than the MSTO in these clusters, this could be a contributing factor to the observed sub-linear dependence on core mass. It is also interesting to note that, since BSs are among the most massive cluster members and many are thought to have a binary companion, BSs should be preferentially retained in clusters as they evolve dynamically compared to low-mass MS stars. This could also contribute to the observed sub-linear dependence on core mass.

The exchange or conversion of energies that occurs during an encounter

takes place over a finite period of time, so it is important to specify whether or not the system has fully relaxed post-encounter when discussing the remaining stellar configuration. For one thing, Sills et al. (2001) showed that, although collision products may be in hydrodynamic equilibrium, they are not in thermal equilibrium upon formation and so contract on a thermal time-scale. Simulations also suggest that most merger products should be rapid rotators (Sills et al., 2002, 2005). However, at least in the case of blue stragglers, this is rarely supported by the observations. Some mechanism for angular momentum loss must therefore be operating either during or after the merger takes place in order to spin down the remnant. The time-scale considered must also be sufficiently short that subsequent dynamical interactions are unlikely to have occurred since these could affect the total energy and momentum of the system.

With this last point in mind, N-body simulations considering BS formation have shown that after they are formed, BSs are often exchanged into other multiple star systems (Hurley et al., 2005). This suggests that for multiple star systems containing more than one BS, the BSs could have first been formed separately or in parallel, and then exchanged into their presently observed configuration. For the case of S1082, this would require at least 3 separate dynamical interactions. Given that the derived times between encounters are relatively long and the fact that the most likely formation scenario is usually that for which the number of encounters is minimized, the current state of M67 suggests that the probability of S1082 having formed from a scenario involving 3 encounters is low. Conversely, the derived encounter time-scales in NGC 188 are sufficiently short that many of the BS binaries could have experienced a subsequent dynamical interaction after their formation. BSs

tend to be more massive than normal MS stars, contributing to an increase in their gravitationally-focussed cross section for collision. This suggests that the encounter time-scale for multiple star systems containing BSs is slightly shorter than for otherwise identical systems composed only of normal MS stars. This contributes to a slight increase in the probability that a BS will experience an exchange encounter after it is formed. Interestingly, it could also contribute to an increase in the probability that a close binary containing two BSs will form during an encounter between two different multiple star systems each containing their own BSs (Mathieu & Geller (2009); R. Mathieu, private communication). This is because it is the heaviest stars that will experience the strongest gravitational focussing and are therefore the most likely to experience a close encounter, end up in a closely bound configuration, or even merge.

Most exchange interactions will involve wide binaries for which the cross section for collision is large. Since wide binaries are typically relatively soft and the hardest binary involved in the interaction will usually determine the orbital energy of the left-over BS binary, most exchange interactions will leave the periods of BS binaries relatively unaffected. This need not be the case, of course, provided one or more stars are ejected from the system with a very high escape velocity. With these last points in mind, we have assumed throughout our analysis that all binaries and triples are dynamically hard. This is a reasonable assumption since the hard-soft boundary corresponds to a period of $\sim 10^6$ days in both M67 and NGC 188, for which the cross section for collision is sufficiently large that we do not expect such binaries to survive for very long. Nonetheless, considerations such as these must be properly taken into account when isolating a preferred formation scenario and predicting the

final distribution of energies.

We have presented an analytic technique to constrain the dynamical origins of multiple star systems containing one or more BSs. Our results suggest that, in old open clusters, most dynamical interactions resulting in mergers involve triple stars. If most triples are formed dynamically, this could suggest that many stellar mergers are the culmination of a hierarchical build-up of dynamical interactions. Consequently, this mechanism for BS formation should be properly included in future N-body simulations of cluster evolution. A better understanding of the interplay between the cluster dynamics and the internal evolution of triple systems is needed in order to better understand the expected period distribution of BS binaries formed from triples. Simulations will therefore need to track both the formation and destruction of triples as well as their internal evolution via Kozai cycles, stellar and binary evolution, etc. On the observational front, our results highlight the need for a more detailed knowledge of binary and especially triple populations in clusters.

## Acknowledgments

We would like to thank Bob Mathieu for many helpful comments and suggestions. We would also like to thank Aaron Geller, Evert Glebbeek, Hagai Perets, David Latham, Daniel Fabrycky and Maureen van den Berg for useful discussions. This research has been supported by NSERC as well as the National Science Foundation under Grant No. PHY05-51164 to the Kavli Institute for Theoretical Physics.

# Bibliography

Binney J., Tremaine S., 1987, Galactic Dynamics (Princeton: Princeton University Press)

Bonatto C., Bica E., Santos J. F. C. Jr., 2005, A&A, 433, 917

Chandrasekhar S., 1939, An Introduction to the Study of Stellar Structure. Univ. of Chicago Press, Chicago, IL

Chen X. Han Z., 2008, MNRAS, 384, 1263

Chen X. Han Z., 2008, MNRAS, 387, 1416

Claret A., Gimenez A., 1989, A&AS, 81, 37

Cleary P. W., Monaghan J. J., 1990, ApJ, 349, 150

Davenport J. R. A., Sandquist E. L., 2010, ApJ, 711, 559

De Angeli F., Piotto G., Cassisi S., Busso G., Recio-Blanco A., Salaris M., Aparicio A., Rosenberg A. 2005, AJ, 130, 116

de Grijs R., Goodwin S. P., Kouwenhoven M. B. N., Kroupa P., 2008, A&A, 492, 685

de Marchi G., Paresce F., Portegies Zwart S., 2010, ApJ, 718, 105

Eggleton P., 2006, Evolutionary Processes in Binary and Multiple Stars. Cambridge Univ. Press, Cambridge, MA

Eggleton P., Tokovinin A. A., 2008, MNRAS, 389, 869

Fabrycky D., Tremaine S., 2007, ApJ, 669, 1298

Fan X., Burstein D., Chen J.-S. et al., 1996, AJ, 112, 628

Fregeau J. M., Cheung P., Portegies Zwart S. F., Rasio F. A., 2004, MNRAS, 352, 1

Geller A. M., Mathieu R. D., Harris H. C., McClure R. D., 2008, AJ, 135, 2264

Geller A. M., Mathieu R. D., Harris H. C., McClure R. D., 2009, AJ, 137, 3743

Giersz M., Heggie D. C., Hurley J. R., 2008, MNRAS, 388, 429

Girard T. M., Grundy, W. M., Lopez C. E., van Altena W. F. 1989, AJ, 98, 227

Harris W. E., 1996, AJ, 112, 1487

Heggie D. C., 1975, MNRAS, 173, 279

Hills J. G., Day C. A., 1976, ApJL, 17, 87

Hurley J. R., Pols O. R., Aarseth S. J., Tout C. A., 2005, MNRAS, 363, 293

Hut P., Bahcall J. N., 1983, ApJ, 268, 319

Hut P., Verbunt F., 1983, Nature, 301, 587

Iben I. Jr., 1991, ApJS, 76, 55

Ivanova N., Heinke C. O., Rasio F. A., Belczynski K., Fregeau J. M., 2008, MNRAS, 386, 553

Knigge C., Leigh N., Sills A., 2009, Nature, 457, 288

Knigge C., Dieball A., Maiz Apellaniz J., Long K. S., Zurek D. R., Shara M. M., 2008, ApJ, 683, 1006

Latham D. W., 2005, Highlights of Astronomy, 14, 444

Leigh N., Sills A., Knigge C., 2009, MNRAS, 399, L179

Leonard P. J. T., 1989, AJ, 98, 217

Leonard P. J. T., Linnell A. P., 1992, AJ, 103, 1928

Mardling R. A., 2001, in Podsiadlowski P., Rappaport S., King A. R., D'Antona F., Burderi L., eds, ASP Conf. Ser. Vol. 229, Evolution of Binary and Multiple Star Systems. Astron. Soc. Pac., San Francisco, p. 101

Mathieu R. D., Geller A. M., 2009, Nature, 462, 1032

Mathieu R. D., Latham D. W., 1986, AJ, 92, 1364

Mathieu R. D., Latham D. W., Griffin R. F., 1990, AJ, 100, 1859

Mathieu R. D., Meibom S., Dolan C. J., 2004, ApJ, 602, L121

McMillan S. L. W., 1986, ApJ, 306, 552

McMillan S. L. W., McDermott P. N., Taam R. E., 1987, ApJ, 318, 261

McMillan S., Hut P., Makino J., 1990, ApJ, 362, 522

Meibom S., Mathieu R. D., 2005, ApJ, 620, 970

Mikkola S., 1983, MNRAS, 203, 1107

Perets H. B., Fabrycky D. C., 2009, ApJ, 697, 1048

Platais I., Kozhurina-Platais V., Mathieu R. D., Girard T. M., van Altena W. F., 2003, AJ, 126, 2922

Podsiadlowski P., 1996, MNRAS, 279, 1104

Pols O. R., Schroder K., Hurley J. R., Tout C. A., Eggleton P. P., 1998, MNRAS, 298, 525

Sandquist E. L., Latham D. W., Shetrone M. D., Milone A. A. E., 2003, AJ, 125, 810

Shara M. M., Saffer R. A., Livio M., 1997, ApJ, 489, L59

Sigurdsson S., Phinney E. S., 1993, ApJ, 415, 631

Sills A., Faber J. A., Lombardi J. C. Jr., Rasio F. A., Warren A. R., 2001, ApJ, 548, 323

Sills A., Adams T., Davies M. B., Bate M. R., 2002, MNRAS, 332, 49

Sills A., Adams T., Davies M. B., 2005, MNRAS, 358, 716

Spitzer, L. 1987, Dynamical Evolution of Globular Clusters (Princeton: Princeton University Press)

Tokovinin A. A., 1997, A&AS, 124, 75

van den Berg M., Orosz J., Verbunt F., Stassun K., 2001, A&A, 375, 375

von Hippel T., Sarajedini A., 1998, AJ, 116, 1789

Chapter 3

# Stellar Populations in Globular Cluster Cores: Evidence for a Peculiar Trend Among Red Giant Branch Stars

## 3.1 Introduction

Studying the radial distributions of the various stellar populations (red giant branch, horizontal branch, main-sequence, etc.) found in globular clusters (GCs) can provide useful hints regarding their dynamical histories. As clusters evolve, they are expected to undergo relatively rapid mass stratification as a consequence of two-body relaxation, with the heaviest stars quickly sinking to the central cluster regions (Spitzer, 1987). The shorter the relaxation time (typically evaluated at the half-mass radius), the quicker this process occurs. Clusters tend towards dissolution as two-body relaxation progresses and

they lose mass due to stellar evolution and the preferential escape of low-mass stars. External effects like tidal perturbations, encounters with giant molecular clouds, and passages through the Galactic disk serve only to speed up the process (e.g. Baumgardt & Makino, 2003; Küpper et al., 2008). Stellar evolution complicates this otherwise simple picture of GC evolution, however. Stars are expected to change in size and lose mass as they evolve, often dramatically, and this could significantly impact the outcomes of future dynamical interactions with other stars. For instance, a typical star in a GC is expected to expand by up to a few orders of magnitude as it ascends the red giant branch (RGB) and will shed up to a quarter of its mass upon evolving from the tip of the RGB to the horizontal-branch (HB) (e.g. Caloi & D'Antona, 2008; Lee et al., 1994).

Red giant branch stars have been reported to be deficient in the cores of some Milky Way (MW) GCs. For instance, Bailyn (1994) found that the morphology of the giant branch in the dense core of 47 Tuc differs markedly from that in the cluster outskirts. In particular, there appear to be fewer bright RGB stars in the core as well as an enhanced asymptotic giant branch (AGB) sequence. While a similar deficiency of bright giants has been observed in the cores of the massive GCs NGC 2808 and NGC 2419, better agreement between the observations and theoretical luminosity functions obtained with the Victoria-Regina isochrones was found for M5 (Sandquist & Martel, 2007; Sandquist & Hess, 2008). Sandquist & Martel (2007) speculate that the giant star observations in NGC 2808 could be linked to its unusually blue horizontal branch if a fraction of the stars near the tip of the RGB experience sufficiently enhanced mass loss that they leave the RGB early. Alternatively, Beer & Davies (2004) suggest that RGB stars could be depleted in dense stel-

lar environments as a result of collisions between red giants and binaries.

While stellar populations have been studied and compared on an individual cluster basis, a statistical analysis in which their core populations are compared over a large sample of GCs is ideal for isolating trends in their differences. Though a handful of studies of this nature have been performed (e.g. Piotto et al., 2004), we present an alternative method by which quantitative constraints can be found for the relative sizes of different stellar populations. Specifically, a cluster-to-cluster variation in the central stellar mass function can be looked for by comparing the core masses to the sizes of their various stellar populations. Since stellar evolution is the principal factor affecting their relative numbers in the core, we expect the size of each stellar population to scale linearly with the core mass. If not, this could be evidence that other factors, such as stellar dynamics, are playing an important role. In this chapter, we present a comparison of the core RGB, main-sequence (MS) and HB populations of 56 GCs. In particular, we use star counts for each stellar population to show that RGB stars are either over-abundant in the least massive cores or under-abundant in the most massive cores, and that this effect is not seen for MS stars. We present the data in Section 3.2 and our methodology and results in Section 3.3. In Section 3.4, we discuss the implications of our results and explore various possibilities for the source of the observed discrepancy between RGB and MS stars. Concluding remarks are presented in Section 3.5.

## 3.2 The Data

Colour-magnitude diagrams (CMDs) taken from Piotto et al. (2002) are used to obtain star counts for the RGB, HB, MS and blue straggler (BS) populations

in the cores of 56 GCs. We apply the same selection criterion as outlined in Leigh, Sills & Knigge (2007) to derive our sample as well as to define the location of the main-sequence turn-off (MSTO) in the (F439W-F555W)-F555W plane. An example of this selection criterion, applied to the CMD of NGC 362, is shown in Figure 3.1. We include all stars in the Piotto et al. (2002) database. Since Piotto et al. (2002) took their HST snapshots with the centre of the PC chip aligned with the cluster centre, a portion of the cluster core was not sampled for most GCs. We have therefore applied a geometric correction factor to the star counts in these clusters in order to obtain numbers that are representative of the entire core (Leigh, Sills & Knigge, 2007, 2008). The total number of stars in the core is found by summing over all stars brighter than 1 mag below the MSTO and then multiplying by the appropriate geometric correction factor.

Errors on the number of stars for each stellar population were calculated using Poisson statistics. Core radii, distance moduli, extinction corrections, central luminosity densities and central surface brightnesses were taken from the Harris Milky Way Globular Cluster catalogue (Harris, 1996, 2010 update). Calibrated apparent magnitudes in the F555W, F439W and Johnson V bands were taken from Piotto et al. (2002).

## 3.3 Results

This chapter focuses on the core RGB, MS and HB populations of 56 GCs, comparing their numbers to the core masses. Note that we are focusing on the total number of stars in the core as a proxy for the core mass instead of the total luminosity in the core in order to avoid concerns regarding cluster-

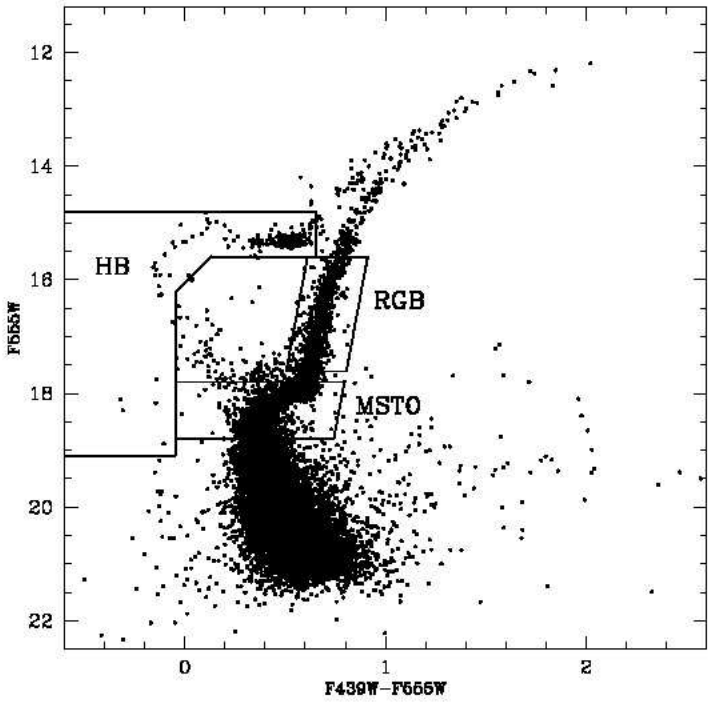



Figure 3.1 Colour-magnitude diagram for NGC 362 in the (F439W-F555W)-F555W plane. Boundaries enclosing the selected RGB, HB and MSTO populations are shown.

to-cluster variations in the central stellar mass function and selection effects. Given that a single bright HB star can be as luminous as 100 regular MS stars, a small surplus of bright stars could have a dramatic impact on the total luminosity. Therefore, the total number of stars in the core is a more direct and reliable estimate for the core mass than is the core luminosity.

Upon plotting the logarithm of the number of core RGB stars versus the logarithm of the total number of stars in the core and performing a weighted least-squares fit, we find a relation of the form:

$$\log(N_{RGB}) = (0.89 \pm 0.03)\log(N_{core}/10^3) + (2.04 \pm 0.02) \qquad (3.1)$$

The sub-linear slope is either indicative of a surplus of RGB stars in the least massive cluster cores or a deficiency in the most massive cores. Errors for lines of best fit were found using a bootstrap methodology in which we generated 1,000 fake data sets by randomly sampling (with replacement) RGB counts from the observations. We obtained lines of best fit for each fake data set, fit a Gaussian to the subsequent distribution and extracted its standard deviation. In order to avoid the additional uncertainty introduced into our RGB number counts from trying to distinguish AGB stars from RGB stars, as well as the difficulty in creating a selection criterion that is consistent from cluster-to-cluster when including the brightest portion of the RGB, stars that satisfy the RGB selection criterion shown in Figure 3.1 are referred to as RGB stars throughout this chapter. Note that it is the brightest portion of the RGB that should be the most affected by stellar evolution effects such as mass-loss. If we extend our selection criterion to include the entire RGB, however, our results remain unchanged.

Interestingly, MS plus sub-giant branch stars (hereafter collectively referred to as MSTO stars, the selection criterion for which is shown in Figure 1) show a more linear relationship than do RGB stars and appear to dominate the central star counts. If we count only those stars having a F555W mag within half a magnitude above and below the turn-off, we obtain a relation of the form:

$$\log(N_{MSTO}) = (1.02 \pm 0.01)\log(N_{core}/10^3) + (2.66 \pm 0.01) \qquad (3.2)$$

A nearly identical fit is found when counting only those stars having a F555W mag between the turn-off and one magnitude fainter than the turn-off.

We also tried plotting the logarithm of the number of core helium-burning stars (labeled HB in Figure 3.1) versus the logarithm of the number of stars in the core, yielding a relation of the form:

$$\log(N_{HB}) = (0.91 \pm 0.10)\log(N_{core}/10^3) + (1.58 \pm 0.05) \tag{3.3}$$

Note the large uncertainty associated with the fit, indicating that the slope is consistent with both those of the RGB and MSTO samples. We will discuss this stellar population further in Section 3.4.

The number of MSTO, RGB and HB stars are shown as a function of the total number of stars in the core in Figure 3.2. Interestingly, the blue stragglers in our sample also scale sub-linearly with core mass, albeit more dramatically, obeying a relation of the form $\mathrm{N}_{BS} \sim \mathrm{M}_{core}^{0.38\pm0.04}$ (Knigge, Leigh & Sills, 2009). Note that $\mathrm{N}_{core}$ can be used interchangeably with $\mathrm{M}_{core}$. In this case, we obtain a fit of:

$$\log(N_{BS}) = (0.47 \pm 0.06)\log(N_{core}/10^3) + (1.22 \pm 0.02) \tag{3.4}$$

In an effort to explore the influence of selection effects, we re-did our plots having removed from our sample clusters denser than $\log \rho > 10^5$ $\mathrm{L}_\odot$ $\mathrm{pc}^{-3}$ since we are the most likely to be under-counting stars in the most crowded cluster cores where blending of the stellar light is the most severe. This cut also removes from our sample the post-core collapse (PCC) clusters for which the core radii are poorly defined since King models are known to provide a poor fit to the observed surface brightness profiles in these clusters. Similarly, we applied a cut in the central surface brightness, removing from our sample

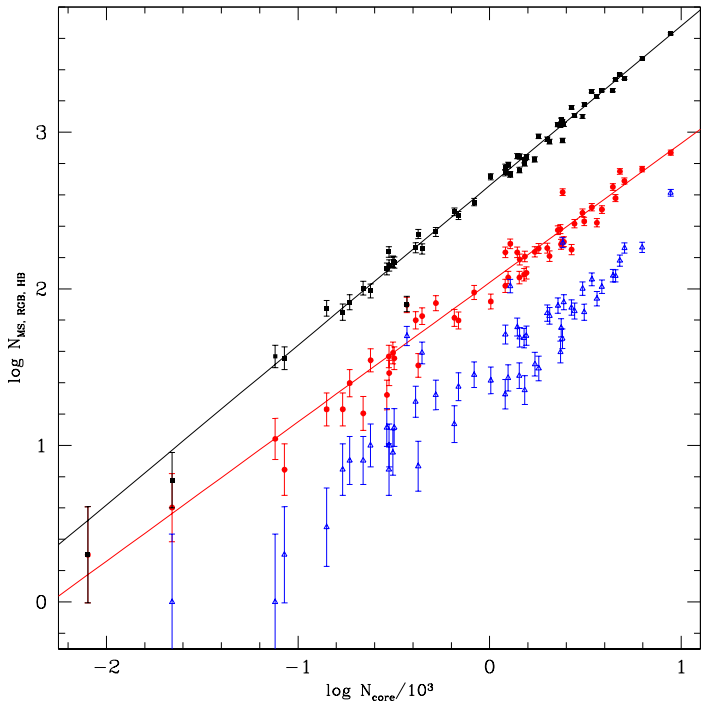



Figure 3.2 The number of RGB (red circles), MSTO (black squares) and HB (blue triangles) stars found within the cluster core plotted versus the total number of stars in the core brighter than 1 mag below the MSTO, along with the corresponding lines of best fit for the RGB and MSTO samples.

clusters satisfying $\Sigma_0 < 15.1$ V mag arcsec$^{-2}$. Finally, since clusters having both high surface brightnesses and small cores are the most likely to suffer from selection effects, we also tried adding to the aforementioned cut in $\Sigma_0$ a cut in the angular core radius, removing clusters with $r_c \leq 0.05$'. In all cases, the sub-linear power-law index reported for the RGB remains unchanged to within one standard deviation of our original result. Selection effects do not appear to be the source of the observed sub-linearity, though it is clear that its effects must properly be accounted for in future studies.

In order to assess the effects of age-related cluster-to-cluster variations

in the stellar mass function, as well as to test our assumption that the number of stars in the core provides a reliable estimate for the core mass, we have obtained MSTO masses for most of the GCs in our sample. We fit theoretical isochrones provided in Pols et al. (1998) to the cluster CMDs, using the bluest point along the MS of a given isochrone as a proxy for the MSTO mass. Isochrones were calculated using the metallicities of Piotto et al. (2002) and cluster ages were taken from De Angeli et al. (2005) using the Zinn & West (1984) metallicity scale. Core masses were estimated by multiplying the mass corresponding to the MSTO ($m_{MSTO}$) by the number of stars in the core brighter than 1 mag below the turn-off. This is a reasonable assumption given the very small dispersion in the ages of MW GCs (De Angeli et al., 2005) and the fact that we are only considering stars brighter than 1 mag below the TO. Consequently, the range of stellar masses upon which we are basing our number counts is very small. Our results remain entirely unchanged upon using $M_{core} \sim N_{core} m_{MSTO}$ as a proxy for the core mass instead of pure number counts.

In order to further check the sensitivity of our results to our estimate for the core masses, we re-did all plots shown in Figure 3.2 using various approximations for the total core luminosity instead of pure number counts. Core luminosities are calculated in the Johnson V band directly from the stellar fluxes which are summed over all stars in the core and then multiplied by the appropriate geometric correction factor. We also adopted $L_{core} = \frac{4}{3}\pi r_c^3 \rho_0$, where $\rho_0$ is the central luminosity density in $L_\odot$ $pc^{-3}$ taken from Harris (1996, 2010 update). Additionally, since the number of core RGB stars is in reality a projected quantity, we tried plotting $N_{RGB}$ versus $L_{core} = \pi r_c^2 \Sigma_0$, where $\Sigma_0$ is the central surface brightness in $L_\odot$ $pc^{-2}$, so that we are consistently comparing two projected quantities. Finally, we can adopt slightly

more realistic estimates for the total core luminosity by integrating over King density profiles. We fit single-mass King models calculated using the method of Sigurdsson & Phinney (1995) to the surface brightness profiles of the majority of the clusters in our sample using the concentration parameters of McLaughlin & van den Marel (2005) and the central luminosity densities of Harris (1996, 2010 update). We then integrated the derived luminosity density profiles numerically in order to estimate the total stellar light contained within the core. After removing clusters labelled as post-core collapse in Harris (1996, 2010 update) for which King models are known to provide a poor fit, we once again compared the integrated core luminosities to the number of RGB stars in the core. For all four of these estimates for the total core luminosity, we find that our fundamental results remain unchanged, with the power-law index for RGB stars remaining sub-linear at the 3-$\sigma$ level. Therefore, we conclude that our result is robust to changes in choices of cluster and population parameters.

## 3.4 Discussion

We have shown that the number of RGB stars in globular cluster cores does not directly trace the total stellar population in those cores. In particular, the number of RGB (but not MSTO) stars scales sub-linearly with core mass at the 3-$\sigma$ level. Given that the MS lifetime is expected to be a factor of 10-100 longer than that of the RGB sample (Iben, 1991), the ratio $\mathrm{N}_{MSTO}/\mathrm{N}_{RGB}$ indicates that the relative sizes of these stellar populations are in better agreement with the expectations of stellar evolution theory in the most massive cores. This suggests that our results are consistent with a surplus of RGB stars in

the least massive cores. We discuss below some of the key considerations in understanding the evolution of GC cores and the stars that populate them in an effort to explain our result.

### 3.4.1 Stellar evolution

Could this trend be a reflection of a stellar evolution process? The evolution and distribution of stellar populations can be thought of as the sum of many single stellar evolution tracks, which depend only on a star's mass and composition. Since there is no relation between a cluster's mass and its metallicity (Harris, 1996, 2010 update) and the dispersion in the relative ages of MW GCs is quite small (De Angeli et al., 2005), there is no reason to expect the RGB lifetime to depend on the cluster mass. On the other hand, recent studies suggest that the chemical self-enrichment of GCs during their early evolutionary stages could help to explain many of the population differences observed among them (e.g. Caloi & D'Antona, 2007). In particular, many of the most massive GCs are thought to be enriched in helium and this is expected to reduce the time scale for stellar evolution (e.g. Romano et al., 2007). While this scenario predicts a deficiency of RGB stars in the most massive cores, it would contribute to depressing the slope of the RGB sample relative to that of the MSTO population in Figure 3.2.

### 3.4.2 Single star dynamics

Two-body relaxation is the principal driving force behind the dynamical evolution of present-day GCs, slowly steering them towards a state of increased mass stratification as predominantly massive stars fall into the core and typi-

cally low-mass stars are ejected via dynamical encounters. The relaxation time increases with the cluster mass (Spitzer, 1987) and the variance in the relative ages (and hence MSTO masses) of MW GCs is quite small (De Angeli et al., 2005). Therefore, it is the least massive clusters that should show signs of being the most dynamically evolved. This assumes that cluster-to-cluster variations in the initial mass function and the degree of initial mass segregation are small. In general, however, proportionately fewer massive stars should have had sufficient time to migrate into the most massive cores, while fewer low-mass stars should have been ejected out. While qualitatively correct, this effect should contribute little to the observed difference between the core RGB and MSTO populations since RGB stars are only slightly more massive (e.g. De Marchi & Pulone, 2007).

Stars expand considerably as they ascend the RGB. Both the increase in collisional cross-section and the change in the average stellar density could have an important bearing on the outcomes of dynamical interactions involving RGB stars. Indeed, Bailyn (1994) suggests that interactions between giants and other cluster members in the core could strip the outer envelope of the giant before it has a chance to fully ascend the RGB. Since our adopted RGB selection criterion does not include the brightest giants, we are only considering giants that are larger than MSTO stars by a factor of $\sim 10$ (Iben, 1991). This small degree of expansion will have only a minor effect on the collision rate. Any scenario that relies on dynamical encounters to explain a depletion of RGB stars should be operating in very dense cores. Our results are consistent with some of the densest clusters in our sample having a surplus of giants, however.

### 3.4.3 Binary effects

Stripping of the envelopes of large stars could also be mediated by a binary companion as the expanding giant overfills its Roche lobe (Bailyn, 1994). While this process should preferentially occur in the centres of clusters where binaries will congregate as a result of mass segregation, two-body relaxation progresses more slowly in the most massive clusters. Binaries should therefore sink to the cluster core more quickly in the least massive clusters, contributing to an increase in the core binary fraction at a rate that decreases with increasing cluster mass. Observational evidence has been found in support of this, most notably by Sollima et al. (2007) and Milone et al. (2008) who found an anti-correlation between the cluster mass and the core binary fraction. Any mechanism for RGB depletion that relies on binary stars should therefore operate more efficiently in the least massive cores where the binary fraction is expected to be the highest. Our results are consistent with a surplus of giants in the least massive cores, however. This therefore argues against a binary mass-transfer origin for RGB depletion in massive GC cores. For similar reasons, it seems unlikely that our result can be explained by collisions between RGB stars and binaries. If, on the other hand, RGB stars are more commonly found in binaries than are MS stars, perhaps as a result of their larger cross-sections for tidal capture, binary stars could still be contributing to the observed trend. Note that in the cluster outskirts where the velocity dispersion has dropped considerably from its central value, individual encounters are more likely to result in tidal capture. Since mass segregation should deliver binaries to the core faster in the least massive clusters, a larger fraction of their RGB stars could have hitched a ride to the core as a binary companion. How-

ever, both the average half-mass relaxation time of MW GCs and the RGB lifetime tend to be on the order of a Gyr (Harris, 1996, 2010 update; Iben, 1991). This does not leave much time for giants to be captured into binaries and subsequently fall into the core before evolving away from the RGB.

### 3.4.4 Core helium-burning stars

The fit for the HB sample is consistent with those of the RGB and MSTO samples at the 3-sigma level so that we are unable to draw any reliable conclusions for this stellar population. The high uncertainty stems from a number of outlying clusters. Selection effects and contamination from the Galaxy are likely to be playing a role in this, in addition to our formulaic selection criterion which may not be as suitable to the varying morphology of the HB as it is to other stellar populations. That is, the creation of a purely photometry-based cluster-independent selection criterion may not be possible for HB stars. Given that stellar evolution effects are expected to be the most dramatic at the end of the RGB lifetime, an interplay with the cluster dynamics could also be contributing. In particular, if the central relaxation time is shorter than the HB lifetime, significant numbers of HB stars could be ejected from the core via dynamical encounters as a result of having lost around a quarter of their mass upon evolving off the tip of the RGB. Moreover, since stars expand considerably as they ascend the RGB, many of the dynamical arguments presented in Section 3.4.2 may more strongly affect the size of the HB sample if they are the direct evolutionary descendants of RGB stars. Since at most a handful of studies have been performed comparing the radial HB and RGB distributions in GCs (e.g. Iannicola et al., 2009), more data is needed before

any firm constraints can be placed on the source of the poor fit found for the HB sample.

### 3.4.5 An evolutionary link with blue stragglers?

The addition of a small number of extra RGB stars to every cluster is one way to account for the observed sub-linear dependence on core mass since the fractional increase in the size of the RGB population will be substantially larger in the least massive cores. In log-log space, the result is a reduction of the slope. Since blue stragglers will evolve into RGB and eventually HB stars (Sills, Karakas & Lattanzio, 2009), evolved BSs could be the cause of a surplus of RGB (and possibly core helium-burning) stars in these clusters. This scenario also predicts that MSTO stars should scale slightly more linearly with core mass since there should be a smaller contribution from evolved BSs, as we have shown. Given the fits for the RGB and BS samples presented in Section 3.3 and their corresponding uncertainties, we find that the addition of evolved BSs to the RGB populations could inflate the slope enough that the dependence on core mass becomes linear. Upon subtracting the BS sample from the RGB sample, we find that the new fit is consistent with being linear:

$$\log(N_{RGB}) = (0.94 \pm 0.04)\log(N_{core}/10^3) + (1.97 \pm 0.02) \qquad (3.5)$$

The slope becomes larger if we have under-estimated the number of BSs, perhaps as a result of selection effects, our adopted selection criterion or a larger population size having existed in the past.

## 3.5 Summary

In this chapter, we have performed a cluster-to-cluster comparison between the number of core RGB, MSTO & HB stars and the total core mass. We have introduced a technique for comparing stellar populations in clusters that is well suited to studies of both cluster and stellar evolution, in addition to the interplay thereof. Using a sample of 56 GCs taken from Piotto et al.'s 2002 HST database, we find a sub-linear scaling for RGB stars at the 3-$\sigma$ level, whereas the relation is linear for MSTO stars. While the preferential self-enrichment of massive GCs, two-body relaxation, and evolved BSs could all be contributing to the observed sub-linear dependence, further studies with an emphasis on selection effects are needed in order to better constrain the source of this curious observational result.

## Acknowledgments

We would like to thank an anonymous referee for a number of helpful suggestions, as well as Bill Harris, David Chernoff, Barbara Lanzoni and Francesco Ferraro for useful discussions. This research has been supported by NSERC as well as the National Science Foundation under Grant No. PHY05-51164 to the Kavli Institute for Theoretical Physics.

# Bibliography


Bailyn, C. D. 1994, AJ, 107, 1073

Baumgardt, H., & Makino, J. 2003, MNRAS, 340, 227

Beer, M. E. & Davies, M. B. 2004, MNRAS, 348, 679

Caloi, V. & D'Antona, F. 2008, ApJ, 673, 847

Caloi, V. & D'Antona, F. 2007, A&A, 463, 949

De Angeli, F., Piotto, G., Cassisi, S., Busso, G., Recio-Blanco, A., Salaris, M., Aparicio, A., & Rosenberg, A. 2005, AJ, 130, 116

De Marchi, G., & Pulone, L. 2007, A&A, 467, 107

Harris, W. E. 1996, AJ, 112, 1487

Iannicola, G., Monelli, M., Bono, G., Stetson, P. B., Buonanno, R., Calamida, A., Zoccali, M., Caputo, F., Castellani, M., Corsi, C. E., Dall'Ora, M., Cecco, A. Di, Deg'Innocenti, S., Ferraro, I., Nonino, M., Peitrinferni, A., Pulone, L., Moroni, P. G., Prada, R., M., Sanna, N., & Walker, A. R. 2009, ApJL, 696, L120

Iben, I., Jr. 1991, ApJS, 76, 55

Knigge, C., Leigh, N., & Sills, A. 2009, Nature, 457, 288

Küpper, A. H. W., MacLeod, A., & Heggie, D. C. 2008, MNRAS, 387, 1248

Lee, Y., Demarque, P., & Zinn, R. 1994, ApJ, 423, 248

Leigh, N., Sills, A., Knigge, C. 2007, ApJ, 661, 210

Leigh, N., Sills, A., Knigge, C. 2008, ApJ, 678, 564

McLaughlin, D. E., & van der Marel, R. P. 2005, ApJS, 161, 304

Milone, A. P., Piotto, G., Bedin, L. R., & Sarajedini, A. 2008, MmSAI, 79, 623

Piotto, G., King, I. R., Djorgovski, S. G., Sosin, C., Zoccali, M., Saviane, I., De Angeli, F., Riello, M., Recio-Blanco, A., Rich, R. M., Meylan, G., & Renzini, A. 2002, A&A, 391, 945

Piotto, G., De Angeli, F., King, I. R., Djorgovski, S. G., Bono, G., Cassisi, S., Meylan, G., Recio-Blanco, A., Rich, R. M., & Davies, M. B. 2004, ApJL, 604, L109

Pols, O. R., Schroder, K., Hurley, J. R., Tout, C. A., & Eggleton, P. P. 1998, MNRAS, 298, 525

Romano, D., Matteucci, F., Tosi, M., Pancino, E., Bellazzini, M., Ferraro, F. R., Limongi, M., & Sollima, A. 2007, MNRAS, 376, 405

Sandquist, E. L. & Martel, A. R. 2007, ApJ, 654, L65

Sandquist, E. L. & Hess, J. M. 2008, AJ, 136, 2259

Sigurdsson, S. & Phinney, E. S. 1995, ApJS, 99, 609

Sills, A., Karakas, A., & Lattanzio, J. 2009, ApJ, 692, 1411

Sollima, A., Beccari, G., Ferraro, F. R., Fusi Pecci, F., & Sarajedini, A. 2007, MNRAS, 380, 781

Spitzer, L. 1987, Dynamical Evolution of Globular Clusters (Princeton: Princeton University Press)

Zinn, R. & West, M. J. 1984, ApJS, 55, 45

Chapter 4

# Dissecting the Colour-Magnitude Diagram: A Homogeneous Catalogue of Stellar Populations in Globular Clusters

## 4.1 Introduction

Colour-magnitude diagrams (CMDs) are one of the most important tools available to astronomers for studying stellar evolution, stellar populations and star clusters. And yet, there remain several features found in CMDs whose origins are still a mystery. Examples include horizontal branch (HB) morphology, the presence of extended horizontal branch (EHB) stars, and blue stragglers (BSs) (e.g. Sandage, 1953; Zinn & Barnes, 1996; Peterson et al., 2003; Dotter et al., 2010). Previous studies have shown that the observed differences in the HBs of Milky Way globular clusters (GCs) are related to metal-

licity (Sandage & Wallerstein, 1960), however at least one additional parameter is required to explain the spread in their colours. Many cluster properties have been suggested as possible Second and Third Parameters, including age, central density and cluster luminosity, although no definitive candidates have been identified (e.g. Rood, 1973; Fusi Pecci et al., 1993). An explanation to account for the existence of BSs has proved equally elusive. Many BS formation mechanisms have been proposed, including stellar collisions (e.g. Leonard, 1989; Sills & Bailyn, 1999) and binary mass-transfer (McCrea, 1964; Mathieu & Geller, 2009). However, no clear evidence has yet emerged in favour of a dominant formation mechanism.

In short, we still do not understand how many of the physical processes operating within star clusters should affect the appearance of CMDs (e.g. Fusi Pecci et al., 1992; Buonanno et al., 1997; Ferraro et al., 1999; Beccari et al., 2006). In general, the importance of these processes can be constrained by looking for correlations between particular features in CMDs and cluster properties that serve as proxies for different effects. For example, the central density can be used as a rough proxy for the frequency with which close dynamical encounters occur. Similarly, the cluster mass can be used as a proxy for the rate of two-body relaxation. Once the relevant effects are accounted for, CMDs can continue to provide an ideal tool to further our understanding of stellar evolution, stellar populations and star clusters.

It is now clear that an important interplay occurs in clusters between stellar dynamics and stellar evolution. For example, dynamical models have shown that star clusters expand in response to mass-loss driven by stellar evolution, particularly during their early evolutionary phases when massive stars are still present (e.g. Chernoff & Weinberg, 1990; Portegies Zwart et al.,

1998; Gieles et al., 2010). Mass-loss resulting from stellar evolution has also been proposed to cause horizontal branch stars to exhibit more extended radial distributions relative to red giant branch and main-sequence turn-off (MSTO) stars in globular clusters having short central relaxation times relative to the average HB lifetime (e.g. Sigurdsson & Phinney, 1995; Leigh, Sills & Knigge, 2009). This can be understood as follows. Red giant branch (RGB) stars should be more mass segregated than other stellar populations since they are among the most massive stars in GCs. HB stars, on the other hand, are much less massive since RGB stars experience significant mass loss upon evolving into HB stars. Consequently, two-body relaxation should act to re-distribute HB stars to wider orbits within the cluster potential relative to RGB and MSTO stars (Spitzer & Shull, 1975), provided the average HB lifetime is shorter than the central relaxation time. Studies have shown that the radial distributions of the HB populations in some GCs could differ from those of other stellar populations. For instance, Saviane et al. (1998) presented evidence that blue HB stars could be more centrally concentrated than red HB and sub-giant branch stars in the GC NGC 1851. Conversely, Cohen et al. (1997) showed that blue HB stars could be centrally depleted relative to other stellar types in the GC NGC 6205. To date, no clear evidence has been found linking the spatial distributions of HB stars to any global cluster properties.

Peculiar trends have also been reported for the radial distributions of RGB stars. For example, a deficiency of bright red giants has been observed in the GC NGC 1851 (e.g. Iannicola et al., 2009). Sandquist & Martel (2007) discussed the possibility that this deficiency could be the result of strong mass loss on the RGB. Alternatively, some authors have suggested that dynamical effects could deplete red giants. For instance, giants could experience collisions

more frequently than other stellar populations due to their larger cross-sections for collision (Beers & Davies, 2004).

One important example of the interplay that occurs in clusters between stellar evolution and stellar dynamics can be found in the study of blue stragglers. Found commonly in both open and globular clusters, BSs are thought to be produced by the addition of hydrogen to the cores of low-mass main-sequence (MS) stars, and therefore appear as an extension of the MSTO in cluster CMDs (Sandage, 1953). This can occur via multiple channels, most of which involve the mergers of low-mass MS stars since a significant amount of mass is typically required to reproduce the observed locations of BSs in CMDs (e.g. Sills & Bailyn, 1999). Stars in close binaries can merge if enough orbital angular momentum is lost, which can be mediated by dynamical interactions with other stars, magnetized stellar winds, tidal dissipation or even an outer triple companion (e.g. Leonard & Linnell, 1992; Li & Zhang, 2006; Perets & Fabrycky, 2009; Dervisoglu, Tout & Ibanoglu, 2010). Alternatively, MS stars can collide directly, although this is also thought to usually be mediated by multiple star systems (e.g. Leonard, 1989; Fregeau et al., 2004; Leigh & Sills, 2010). Finally, BSs have also been hypothesized to form by mass-transfer from an evolving primary onto a normal MS companion via Roche lobe overflow (McCrea, 1964).

Whatever the dominant BS formation mechanism(s) operating in dense star clusters, it is now thought to somehow involve multiple star systems. This was shown to be the case in even the dense cores of GCs (Knigge, Leigh & Sills, 2009) where collisions between single stars are thought to occur frequently (Leonard, 1989). In Knigge, Leigh & Sills (2009), we showed that the numbers of BSs in the cores of a large sample of GCs correlate with the core masses.

We argued that our results are consistent with what is expected if BSs are descended from binary stars. Mathieu & Geller (2009) also showed that at least 76% of the BSs in the old open cluster NGC 188 have binary companions. Although the nature of these companions remains unknown, it is clear that binaries played a role in the formation of these BSs. Dynamical interactions occur frequently enough in dense clusters that they are also expected to be at least partly responsible for the observed properties of BSs. It follows that the current properties of BS populations should reflect the dynamical histories of their host clusters. As a result, BSs could provide an indirect means of probing the physical processes that drive star cluster evolution.

In this chapter, we present a homogeneous catalogue for red giant branch, main-sequence turn-off, horizontal branch and blue straggler stars in a sample of 35 Milky Way (MW) GCs taken from the Advanced Camera for Surveys (ACS) Survey for Globular Clusters (Sarajedini et al., 2007). With this catalogue, we investigate two important issues related to stellar populations in GCs. First, we test the observational correlation found for BSs presented in Knigge, Leigh & Sills (2009) by re-doing the study with newer and more accurate photometry. The larger spatial coverage considered in our new sample offers an important additional constraint for the origin of this correlation. Second, we perform the same statistical comparison for RGB, HB and MSTO stars in order to study their radial distributions. This will allow us to test some of the results and hypotheses introduced in Leigh, Sills & Knigge (2009), where we first presented this technique for studying stellar populations. In particular, we found evidence for a surplus of RGB stars in low-mass GC cores relative to MSTO stars. However, we concluded that the study needed to be re-done with better photometry. The ACS data are of sufficiently high

quality to address this issue.

In Section 4.2, we present our selection criteria to determine the numbers of BS, RGB, HB and MSTO stars located in the central cluster regions. The spatial coverage of the photometry extends out to several core radii from the cluster centre for most of the clusters in our sample. For these clusters, we have obtained number counts within several circles centred on the cluster centres provided in Goldsbury et al. (2010) for various multiples of the core radius. This catalogue is presented in Section 4.3. In this section, we also present a comparison between the sizes of the different stellar populations and the total stellar masses contained within each circle and annulus. Finally, we discuss our results for both BSs and the other stellar populations in Section 4.4.

## 4.2 Method

In this section, we present our sample of CMDs and define our selection criteria for each of the different stellar populations. We also discuss the spatial coverage offered by the ACS sample, and describe how we obtain estimates for several different fractions of the total cluster mass from King models.

### 4.2.1 The Data

The data used in this study consists of a sample of 35 MW GCs taken from the ACS Survey for Globular Clusters (Sarajedini et al., 2007).[1] The ACS Survey provides unprecedented deep photometry in the F606W ($\sim$ V) and F814W ($\sim$ I) filters that is nearly complete down to $\sim 0.2$ $M_{\odot}$. In other words, the CMDs extend reliably from the HB all the way down to about 7 magnitudes below

[1]The data can be found at http://www.astro.ufl.edu/ ata/public_hstgc/.

the MSTO. We have confirmed that the photometry is nearly complete above at least 0.5 magnitudes below the MSTO for every cluster in our sample. This was done using the results of artificial star tests taken from Anderson et al. (2008), and confirms that the photometric quality of the stellar population catalogue presented in this chapter is very high.[2] We have also considered foreground contamination by field stars, and it is negligible.

Each cluster was centred in the ACS field, which extends out to several core radii from the cluster centre in most clusters and, in a few cases, beyond even 15 core radii. Coordinates for the cluster centres were taken from Goldsbury et al. (2010). These authors found their centres by fitting a series of ellipses to the density distributions within the inner 2' of the cluster centre, and computing an average value. The core radii were taken from Harris (1996, 2010 update).

### 4.2.2 Stellar Population Selection Criteria

In order to select the number of stars belonging to each stellar population, we define a series of lines in the (F606W-F814W)-F814W plane that act as boundaries enclosing each of the different stellar populations. To do this, we fit theoretical isochrones taken from Dotter et al. (2007) to the CMDs of every cluster in our sample. Each isochrone was generated using the metallicity and age of the cluster, and fit to its CMD using the corresponding distance modulus and extinction provided in Dotter et al. (2010). The MSTO was then defined using our isochrone fits by selecting the bluest point along the MS. This acts as our primary point of reference for defining the boundaries in the CMD for

[2]Artificial star tests were obtained directly from Ata Sarajedini via private communication.

the different stellar populations. Consequently, the selection criteria provided in this chapter are a significant improvement upon the criteria presented in Leigh, Sills & Knigge (2007), and our new catalogue for the different stellar populations is highly homogeneous.

Two additional points of reference must also be defined in order for our selection criteria to be applied consistently from cluster-to-cluster. First, the selection criteria for the HB are determined by fitting a line through the approximate mid-point of the points that populate it in the CMD. This line is then used to define upper and lower boundaries for the HB. Theoretical isochrones become highly uncertain at the HB, so it is necessary to specify this additional criterion by eye. Second, the lower boundary of the RGB is defined for each cluster as the point along its isochrone corresponding to a helium core mass of 0.08 $M_{\odot}$. We do not include RGB stars brighter than the HB since the tilt of the upper RGB varies significantly from cluster-to-cluster, presenting a considerable challenge for the consistency of our selection criteria. Moreover, the distinction between RGB and asymptotic giant branch stars in the CMD is often ambiguous.

Example selection criteria for each of the different stellar populations are shown in Figure 4.1. Formal definitions for the boundaries in the cluster CMD that define the BS, RGB, HB and MSTO populations are provided in Appendix B. We note that the sizes of our selection boxes have been chosen to accommodate the photometric errors, which contribute to broadening the various evolutionary sequences in the CMD. With superior photometry, the sizes of our selection boxes could therefore be reduced. This would further decrease contamination from field stars in our samples.

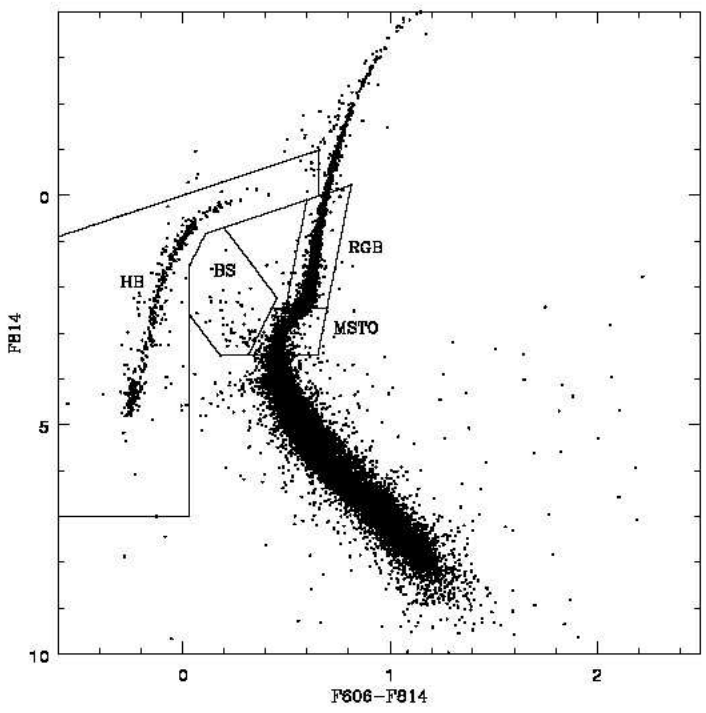



Figure 4.1 Colour-magnitude diagram for the Milky Way globular cluster NGC 6205. Boundaries enclosing the parameter space in the (F606W-F814W)-F814W plane that define each of the different stellar populations are indicated with solid lines, as described in the text. Absolute magnitudes are shown, converted from apparent magnitudes using the distance moduli and extinctions provided in Dotter et al. (2010). Labels for blue straggler, red giant branch, horizontal branch and main-sequence turn-off stars are indicated. Stars with large photometric errors have been omitted from this plot.

### 4.2.3 Spatial Coverage

The ACS field of view extends out to several core radii from the cluster centre for nearly every cluster in our sample. Consequently, we have obtained estimates for the number of stars contained within four different circles centred on the central cluster coordinates provided in Goldsbury et al. (2010). We list these numbers only for clusters for which the indicated circle is completely sampled by the field of view. The radii of the circles were taken to be integer

multiples of the core radius, and we focus our attention on the inner four core radii since the field of view extends beyond this for only a handful of the clusters in our sample. An example of this is shown in Figure 4.2. The numbers we list are cumulative, so that entries for each circle include stars contained within all smaller circles.

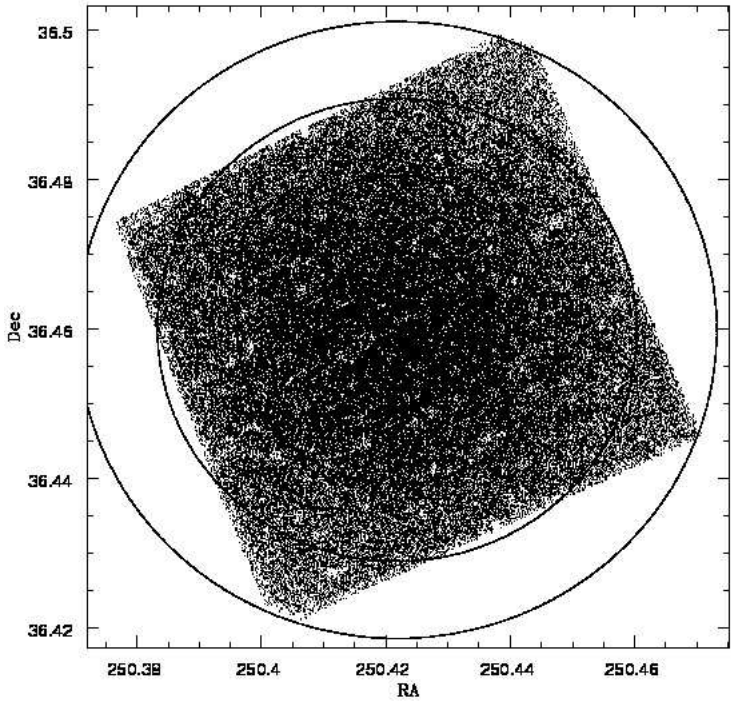



Figure 4.2 RA and Dec coordinates for all stars in the GC NGC 6205. Circles corresponding to one, two, three and four core radii are shown.

### 4.2.4 King Models

In order to obtain accurate estimates for the total stellar mass contained within each circle, we generated single-mass King models calculated using the method of Sigurdsson & Phinney (1995) to obtain luminosity density profiles

for the majority of the clusters in our sample. The profiles were obtained using the concentration parameters of McLaughlin & van den Marel (2005) and the central luminosity densities of Harris (1996, 2010 update) for each cluster in McLaughlin & van den Marel (2005) that overlaps with our sample. We then integrated the derived luminosity density profiles numerically in order to estimate the total stellar light contained within each circle. After removing clusters with high concentration parameters (Harris, 1996, 2010 update) for which King models are known to provide a poor fit, we multiplied the total stellar light by a mass-to-light ratio of 2 in order to obtain estimates for the total stellar mass contained within each circle. Calculating the total stellar mass contained within each circle from King models requires a number of assumptions that we will discuss fully in Section 4.4.

## 4.3 Results

In this section, we present our catalogue along with the results of our comparisons between the sizes of the different stellar populations and the total stellar mass contained within each circle and annulus.

### 4.3.1 Catalogue

The numbers of BS, RGB, HB and MSTO stars found within several different circles are shown for all clusters in Table 4.1, along with the total number of stars with magnitudes brighter than 0.5 mag below the MSTO. Number counts are only shown whenever the spatial coverage is complete within the indicated circle.

Table 4.1 Stellar Population Catalogue

| Cluster ID | Alternate ID | Core Radius (in arcmin) | $N_{BS}$ | | | | $N_{HB}$ | | | | $N_{RGB}$ | | | | $N_{MSTO}$ | | | | $N_{TOT}$ | | | |
|---|---|---|---|---|---|---|---|---|---|---|---|---|---|---|---|---|---|---|---|---|---|---|
| | | | $< r_c$ | $< 2r_c$ | $< 3r_c$ | $< 4r_c$ | $< r_c$ | $< 2r_c$ | $< 3r_c$ | $< 4r_c$ | $< r_c$ | $< 2r_c$ | $< 3r_c$ | $< 4r_c$ | $< r_c$ | $< 2r_c$ | $< 3r_c$ | $< 4r_c$ | $< r_c$ | $< 2r_c$ | $< 3r_c$ | $< 4r_c$ |
| 104 | 47 Tuc | 0.36 | 62 | 100 | 120 | 128 | 172 | 344 | 486 | 615 | 397 | 944 | 1454 | 1798 | 2190 | 5004 | 7300 | 9080 | 4874 | 11430 | 16985 | 21183 |
| 1261 | | 0.35 | 56 | 79 | 95 | 104 | 73 | 170 | 216 | 250 | 241 | 481 | 664 | 755 | 1102 | 2268 | 2953 | 3369 | 2713 | 5576 | 7347 | 8429 |
| 1851 | | 0.09 | 34 | 58 | 74 | 90 | 33 | 107 | 161 | 213 | 93 | 223 | 307 | 385 | 178 | 692 | 1128 | 1524 | 417 | 1418 | 2421 | 3400 |
| 2298 | | 0.31 | 27 | 32 | 37 | 38 | 16 | 41 | 56 | 63 | 61 | 120 | 158 | 186 | 208 | 429 | 568 | 662 | 549 | 1117 | 1490 | 1753 |
| 3201 | | 1.30 | 40 | – | – | – | 43 | – | – | – | 160 | – | – | – | 635 | – | – | – | 1691 | – | – | – |
| 4147 | | 0.09 | 16 | 26 | 30 | 34 | 7 | 18 | 35 | 44 | 23 | 61 | 93 | 120 | 89 | 206 | 316 | 400 | 234 | 569 | 844 | 1064 |
| 4590 | M 68 | 0.58 | 29 | 59 | – | – | 33 | 66 | – | – | 152 | 269 | – | – | 480 | 977 | – | – | 1321 | 2623 | – | – |
| 5024 | M 53 | 0.35 | 57 | 103 | 133 | 149 | 114 | 235 | 333 | 387 | 293 | 704 | 1059 | 1260 | 1215 | 2864 | 4106 | 4891 | 3118 | 7504 | 10730 | 12827 |
| 5139 | Ω Cen | 2.37 | 49 | 87 | – | – | 408 | 762 | – | – | 1441 | 2592 | – | – | 4643 | 8637 | – | – | 12652 | 23178 | – | – |
| 5272 | M 3 | 0.37 | 74 | 111 | 127 | 135 | 153 | 311 | 379 | 413 | 496 | 995 | 1277 | 1387 | 1909 | 3828 | 5052 | 5512 | 4971 | 10020 | 13195 | 14429 |
| 5286 | | 0.28 | 82 | 120 | 138 | 144 | 218 | 413 | 530 | 599 | 442 | 970 | 1308 | 1535 | 1723 | 3666 | 4983 | 5876 | 4016 | 8934 | 12448 | 14826 |
| 5466 | | 1.43 | 30 | – | – | – | 37 | – | – | – | 123 | – | – | – | 487 | – | – | – | 1276 | – | – | – |
| 5904 | M 5 | 0.44 | 37 | 57 | 64 | 68 | 97 | 212 | 291 | 338 | 233 | 516 | 729 | 885 | 997 | 2260 | 3190 | 3843 | 2483 | 5700 | 8123 | 9846 |
| 5927 | | 0.42 | 28 | 71 | 93 | 122 | 91 | 207 | 294 | 358 | 188 | 513 | 748 | 922 | 1214 | 3043 | 4528 | 5667 | 2619 | 6714 | 10108 | 12688 |
| 5986 | | 0.47 | 57 | 88 | – | – | 220 | 386 | – | – | 614 | 1136 | – | – | 2359 | 4549 | – | – | 5756 | 11255 | – | – |
| 6093 | M 80 | 0.15 | 79 | 114 | 133 | 135 | 94 | 199 | 269 | 331 | 252 | 543 | 773 | 984 | 1045 | 2176 | 3090 | 3790 | 2008 | 4627 | 6840 | 8637 |
| 6101 | | 0.97 | 26 | – | – | – | 68 | – | – | – | 173 | – | – | – | 681 | – | – | – | 1798 | – | – | – |
| 6121 | M 4 | 1.16 | 11 | 18 | – | – | 21 | 46 | – | – | 52 | 126 | – | – | 243 | 574 | – | – | 553 | 1350 | – | – |
| 6171 | M 107 | 0.56 | 19 | 43 | 54 | – | 16 | 37 | 56 | – | 63 | 153 | 223 | – | 264 | 667 | 933 | – | 677 | 1688 | 2414 | – |
| 6205 | M 13 | 0.62 | 41 | 58 | – | – | 207 | 416 | – | – | 527 | 1162 | – | – | 1960 | 4250 | – | – | 5015 | 10973 | – | – |
| 6218 | M 12 | 0.79 | 28 | 50 | – | – | 32 | 68 | – | – | 114 | 245 | – | – | 447 | 1118 | – | – | 1127 | 2680 | – | – |
| 6254 | M 10 | 0.77 | 36 | 52 | – | – | 93 | 169 | – | – | 257 | 540 | – | – | 955 | 1985 | – | – | 2483 | 5165 | – | – |
| 6304 | | 0.21 | 19 | 36 | 51 | 67 | 27 | 65 | 95 | 112 | 82 | 207 | 313 | 397 | 453 | 1112 | 1657 | 2143 | 994 | 2584 | 3864 | 5008 |
| 6341 | M 92 | 0.26 | 41 | 73 | 84 | 91 | 60 | 126 | 177 | 217 | 140 | 367 | 540 | 684 | 543 | 1290 | 1896 | 2376 | 1409 | 3341 | 4943 | 6252 |
| 6362 | | 1.13 | 35 | – | – | – | 61 | – | – | – | 165 | – | – | – | 716 | – | – | – | 1844 | – | – | – |
| 6535 | | 0.36 | 7 | 11 | 12 | 12 | 8 | 18 | 24 | 26 | 21 | 42 | 56 | 72 | 54 | 107 | 174 | 227 | 165 | 338 | 493 | 629 |
| 6584 | | 0.26 | 36 | 54 | 63 | – | 52 | 95 | 135 | – | 217 | 386 | 482 | – | 788 | 1499 | 1863 | – | 2023 | 3810 | 4830 | – |
| 6637 | M 69 | 0.33 | 50 | 85 | 96 | 106 | 80 | 148 | 204 | 239 | 200 | 443 | 592 | 702 | 1067 | 2257 | 3063 | 3605 | 2413 | 5209 | 7129 | 8414 |
| 6652 | | 0.10 | 16 | 19 | 24 | 27 | 10 | 21 | 34 | 40 | 32 | 61 | 87 | 122 | 127 | 272 | 417 | 536 | 286 | 619 | 919 | 1218 |
| 6723 | | 0.83 | 39 | – | – | – | 113 | – | – | – | 354 | – | – | – | 1594 | – | – | – | 3777 | – | – | – |
| 6779 | M 56 | 0.44 | 21 | 41 | 48 | 49 | 44 | 99 | 133 | 158 | 128 | 302 | 435 | 528 | 411 | 993 | 1495 | 1875 | 1126 | 2679 | 3982 | 4912 |
| 6838 | M 71 | 0.63 | 17 | 45 | – | – | 10 | 30 | – | – | 36 | 95 | – | – | 144 | 385 | – | – | 355 | 960 | – | – |
| 6934 | | 0.22 | 35 | 54 | 57 | 60 | 50 | 100 | 137 | 163 | 150 | 322 | 431 | 508 | 612 | 1240 | 1681 | 1974 | 1528 | 3208 | 4308 | 5088 |
| 6981 | M 72 | 0.46 | 31 | 49 | 56 | – | 52 | 78 | 103 | – | 140 | 285 | 354 | – | 652 | 1272 | 1596 | – | 1594 | 3159 | 4000 | – |
| 7089 | M 2 | 0.32 | 83 | 129 | 143 | 150 | 277 | 551 | 729 | 838 | 535 | 1205 | 1652 | 1960 | 2264 | 4832 | 6603 | 7795 | 5394 | 12038 | 16669 | 19851 |

### 4.3.2 Population Statistics

How can we use our catalogue to learn which, if any, cluster properties affect the appearance of CMDs? One way to accomplish this is by plotting the size of a given stellar population in a particular circle versus the total stellar mass contained within it. From this, lines of best fit can be found that provide equations relating the size of each stellar population to the total stellar mass contained within each circle. As described below, this is ideal for probing the effects of the cluster dynamics on the appearance of CMDs.

The rate of two-body relaxation for a cluster can be approximated using the half-mass relaxation time (Spitzer, 1987):

$$t_{rh} = 1.7 \times 10^5 [r_h(pc)]^{3/2} N^{1/2} [m/M_\odot]^{-1/2} years, \tag{4.1}$$

where $r_h$ is the half-mass radius, $N$ is the total number of stars within $r_h$ and $m$ is the average stellar mass. The half-mass radii of MW GCs are remarkably similar independent of mass, and simulations have shown that $r_h$ changes by a factor of at most a few over the course of a cluster's lifetime (Murray, 2009; Henon, 1973). The GCs that comprise our sample show a range of masses spanning roughly 3 orders of magnitude, and have comparably old ages (De Angeli et al., 2005). Therefore, Equation 4.1 suggests that the degree of dynamical evolution (due to two-body relaxation) experienced by a cluster is primarily determined by the total cluster mass for the GCs in our sample. In particular, more massive clusters are less dynamically evolved, and vice versa. Consequently, if the size of a given stellar population is affected by two-body relaxation, the effects should be the most pronounced in the least massive clusters in our sample. Additionally, the rate of (direct) stellar colli-

sions increases with increasing cluster mass (e.g. Davies, Piotto & De Angeli, 2004). This suggests that, if a given stellar population is affected by collisions, the effects should be the most pronounced in the most massive clusters in our sample. Therefore, by comparing the size of each stellar population to the total stellar mass contained within a given circle, the effects of the cluster dynamics can be quantified. This technique also ensures a normalized and consistent comparison since it accounts for cluster-to-cluster differences in the fractional area sampled by the ACS field of view. That is, we are consistently comparing the same structural area for each cluster. The validity and implications of all of these assumptions will be discussed further in Section 4.4.

Plots showing the number of stars belonging to each stellar population as a function of the total stellar mass contained within each circle are shown in Figure 4.3. Uncertainties for the number of stars belonging to each stellar population were calculated using Poisson statistics. We also plot in Figure 4.4 the number of stars belonging to each stellar population as a function of the total stellar mass contained in each annulus outside the core. That is, we considered the populations for each annulus individually, as opposed to considering every star with a distance from the cluster centre smaller than the radius of the outer-most circles. Recall that we have neglected clusters for which our theoretical King models provide a poor description of the true density distributions. This was the case for clusters in our sample having a high concentration parameter, most of which are labelled as post-core collapse in Harris (1996, 2010 update).

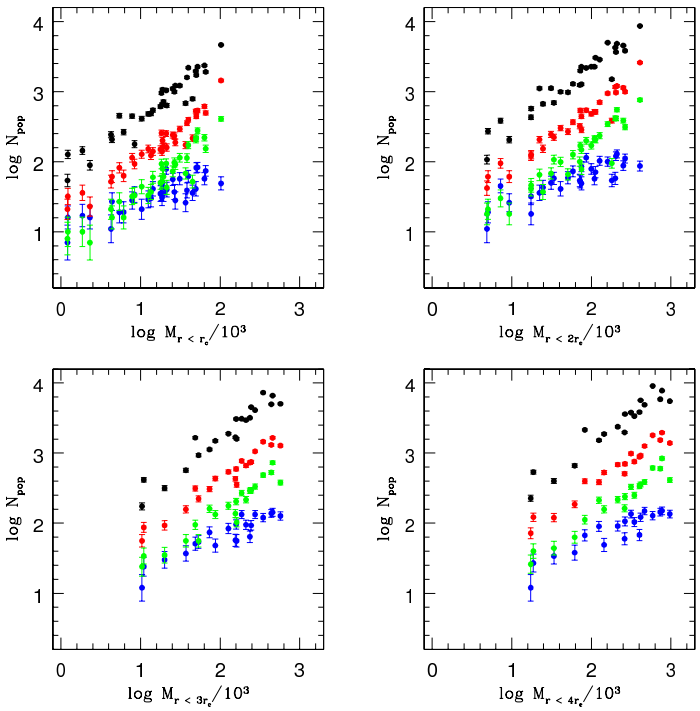



Figure 4.3 The logarithm of the number of stars belonging to each stellar population is shown for each circle as a function of the logarithm of the total stellar mass. From left to right and top to bottom, each frame corresponds to number counts contained within a circle having a radius of $r_c$, $2r_c$, $3r_c$ and $4r_c$. Blue corresponds to blue stragglers, red to red giant branch stars, green to horizontal branch stars and black to main-sequence turn-off stars. Estimates for the total stellar mass contained within each circle were found using single-mass King models, as described in Section 4.2.4.

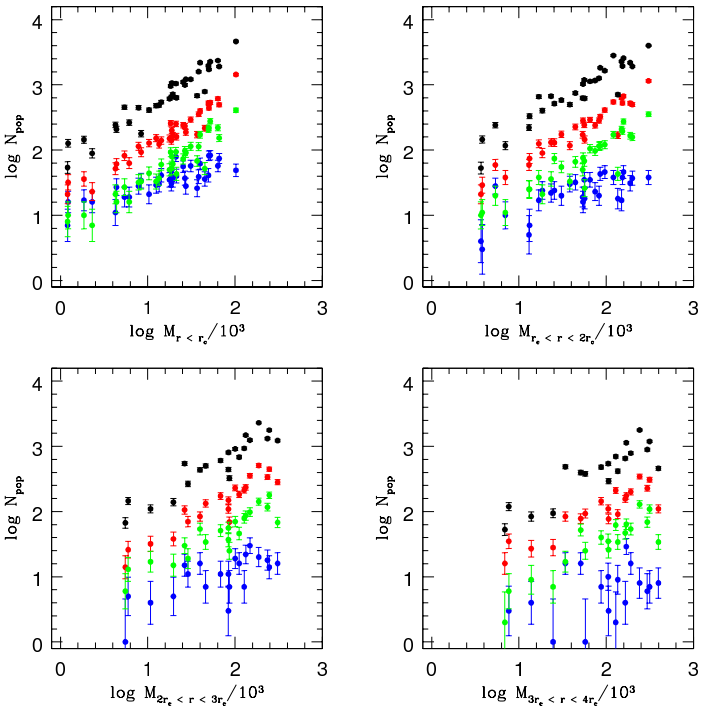



Figure 4.4 The logarithm of the number of stars belonging to each stellar population is shown for each annulus as a function of the logarithm of the total stellar mass. The annulus and colour corresponding to each inset and stellar population, respectively, are the same as in Figure 4.3.

Table 4.2 Lines of Best Fit for $\log(M_{circle}/10^3)$ Versus $\log(N_{pop})$

| Circle | BS | RGB | HB | MSTO |
|---|---|---|---|---|
| $< r_c$ | $\log(N_{BS})$ = (0.39 ± 0.05)$\log(M_{<r_c}/10^3)$ + (1.22 ± 0.05) | $\log(N_{RGB})$ = (0.95 ± 0.11)$\log(M_{<r_c}/10^3)$ + (1.36 ± 0.11) | $\log(N_{HB})$ = (0.95 ± 0.06)$\log(M_{<r_c}/10^3)$ + (0.92 ± 0.06) | $\log(N_{MSTO})$ = (0.90 ± 0.07)$\log(M_{<r_c}/10^3)$ + (2.03 ± 0.07) |
| $< 2r_c$ | $\log(N_{BS})$ = (0.36 ± 0.05)$\log(M_{<2r_c}/10^3)$ + (1.26 ± 0.08) | $\log(N_{RGB})$ = (0.87 ± 0.08)$\log(M_{<2r_c}/10^3)$ + (1.27 ± 0.12) | $\log(N_{HB})$ = (0.85 ± 0.06)$\log(M_{<2r_c}/10^3)$ + (0.84 ± 0.09) | $\log(N_{MSTO})$ = (0.82 ± 0.06)$\log(M_{<2r_c}/10^3)$ + (1.98 ± 0.09) |
| $< 3r_c$ | $\log(N_{BS})$ = (0.47 ± 0.04)$\log(M_{<3r_c}/10^3)$ + (1.02 ± 0.08) | $\log(N_{RGB})$ = (0.80 ± 0.06)$\log(M_{<3r_c}/10^3)$ + (1.26 ± 0.12) | $\log(N_{HB})$ = (0.79 ± 0.08)$\log(M_{<3r_c}/10^3)$ + (0.83 ± 0.14) | $\log(N_{MSTO})$ = (0.82 ± 0.11)$\log(M_{<3r_c}/10^3)$ + (1.86 ± 0.20) |
| $< 4r_c$ | $\log(N_{BS})$ = (0.45 ± 0.05)$\log(M_{<4r_c}/10^3)$ + (1.01 ± 0.12) | $\log(N_{RGB})$ = (0.75 ± 0.07)$\log(M_{<4r_c}/10^3)$ + (1.28 ± 0.15) | $\log(N_{HB})$ = (0.75 ± 0.09)$\log(M_{<4r_c}/10^3)$ + (0.83 ± 0.19) | $\log(N_{MSTO})$ = (0.78 ± 0.12)$\log(M_{<4r_c}/10^3)$ + (1.86 ± 0.25) |

Table 4.3 Lines of Best Fit for $\log(M_{annulus}/10^3)$ Versus $\log(N_{pop})$

| Annulus | BS | RGB | HB | MSTO |
|---|---|---|---|---|
| $r_c < r < 2r_c$ | $\log(N_{BS}) = (0.27 \pm 0.08)\log(M_{r_c<r<2r_c}/10^3) + (1.04 \pm 0.13)$ | $\log(N_{RGB}) = (0.80 \pm 0.06)\log(M_{r_c<r<2r_c}/10^3) + (1.22 \pm 0.08)$ | $\log(N_{HB}) = (0.77 \pm 0.06)\log(M_{r_c<r<2r_c}/10^3) + (0.79 \pm 0.09)$ | $\log(N_{MSTO}) = (0.76 \pm 0.05)\log(M_{r_c<r<2r_c}/10^3) + (1.91 \pm 0.08)$ |
| $2r_c < r < 3r_c$ | $\log(N_{BS}) = (0.39 \pm 0.09)\log(M_{2r_c<r<3r_c}/10^3) + (0.52 \pm 0.16)$ | $\log(N_{RGB}) = (0.79 \pm 0.11)\log(M_{2r_c<r<3r_c}/10^3) + (0.97 \pm 0.17)$ | $\log(N_{HB}) = (0.68 \pm 0.10)\log(M_{2r_c<r<3r_c}/10^3) + (0.67 \pm 0.16)$ | $\log(N_{MSTO}) = (0.78 \pm 0.12)\log(M_{2r_c<r<3r_c}/10^3) + (1.64 \pm 0.20)$ |
| $3r_c < r < 4r_c$ | $\log(N_{BS}) = (0.15 \pm 0.21)\log(M_{3r_c<r<4r_c}/10^3) + (0.77 \pm 0.35)$ | $\log(N_{RGB}) = (0.63 \pm 0.11)\log(M_{3r_c<r<4r_c}/10^3) + (1.04 \pm 0.18)$ | $\log(N_{HB}) = (0.69 \pm 0.18)\log(M_{3r_c<r<4r_c}/10^3) + (0.45 \pm 0.31)$ | $\log(N_{MSTO}) = (0.69 \pm 0.16)\log(M_{3r_c<r<4r_c}/10^3) + (1.60 \pm 0.27)$ |

We performed a weighted least-squares fit for every relation in Figure 4.3 and Figure 4.4. Slopes and y-intercepts for these lines are shown in Table 4.2 and Table 4.3, respectively. Uncertainties for the slopes and y-intercepts were found using a bootstrap methodology in which we generated 1,000 fake data sets by randomly sampling (with replacement) number counts from the observations. We obtained lines of best fit for each fake data set, fit a Gaussian to the subsequent distribution and extracted its standard deviation.

As shown in Table 4.2, the power-law index is sub-linear for BSs within the core at much better than the $3-\sigma$ confidence level, and it is consistent with the slope obtained in our earlier analysis presented in Knigge, Leigh & Sills (2009). The slopes for the BSs are also sub-linear at better than the $3-\sigma$ confidence level for all circles outside the core. This is also the case for all annuli outside the core, as shown in Table 4.3. Note, however, that the uncertainties for the BS slopes are very large for all annuli outside the core, whereas this is not always the case for corresponding circles outside the core. This is the result of the fact that the number of BSs drops off rapidly outside the core in several clusters so that the corresponding Poisson uncertainties, which are given by the square-root of the number of BSs, are significant. The rapid decline of BS numbers with increasing distance from the cluster centre in these clusters has also contributed to an increased degree of scatter in the relations for annuli outside the core relative to the corresponding relations for circles outside the core.

The slopes are consistent with being linear for all other stellar populations in the core within their respective $3-\sigma$ confidence intervals. This agrees with the results of our earlier analysis presented in Leigh, Sills & Knigge (2009) when we performed the comparison using the total core masses. The

slopes are also consistent with being linear for all circles outside the core for both HB and MSTO stars. The power-law indices are sub-linear at the $3-\sigma$ confidence level only for RGB stars, and this is only the case for circles outside the core. The power-law index is nearly unity for the core RGB population, yet the associated uncertainty is very large. Upon closer inspection, the distribution of power-law indices obtained from our bootstrap analysis for RGB stars in the core is strongly bi-modal, with comparably-sized peaks centred at $\sim 0.82$ and $\sim 1.0$. This bi-modality is most likely an artifact of our bootstrap analysis caused by a chance alignment of data points in the log $M_{core}$-log $N_{RGB}$ plane. Upon performing the comparison for only those stars found within particular annuli, our results suggest that the slopes are consistent with being sub-linear for all stellar populations at the $3-\sigma$ confidence level in only the annulus immediately outside the core (i.e. $r_c < r < 2r_c$). The slopes are consistent with being linear for RGB, HB and MSTO stars in all other annuli.

We also tried performing the same comparisons using the total number of stars in each circle and annulus as a proxy for the total stellar mass. In this case, the slopes are sub-linear for BSs within all circles and annuli at the $3-\sigma$ confidence level. Once again, the uncertainties are very large for all annuli outside the core, whereas this is not the case for corresponding circles outside the core. The slopes are consistent with being linear within the $1-\sigma$ confidence interval for all other stellar populations in all circles and annuli. Our results are therefore inconsistent with those presented in Leigh, Sills & Knigge (2009) for the core RGB populations, in which we found that RGB numbers scale sub-linearly with the number of stars in the core at the $3-\sigma$ confidence level. We will discuss the implications of these new results in Section 4.4.

### 4.3.3 Blue Stragglers and Single-Single Collisions

As a check of our previous results reported in Knigge, Leigh & Sills (2009), we also looked for a correlation between the observed number of BSs in the cluster core and the number predicted from single-single (1+1) collisions. The results of this comparison are shown in Figure 4.5. We define the predicted number of BSs formed from 1+1 collisions as $N_{1+1} = \tau_{BS}/\tau_{1+1}$, where $\tau_{BS}$ is the average BS lifetime and $\tau_{1+1}$ is the average time between 1+1 collisions in the cluster core. We adopt the same definition for $\tau_{1+1}$ as used in Knigge, Leigh & Sills (2009), and assume $\tau_{BS} = 1.5$ Gyrs as well as an average stellar mass and radius of 0.5 $M_{\odot}$ and 0.5 $R_{\odot}$, respectively. We also adopt a constant mass-to-light ratio of $M/L = 2$ for all clusters. Central luminosity densities and velocity dispersions were taken from Harris (1996, 2010 update) and Webbink (1985), respectively.

Upon performing a weighted line of best fit for every cluster in our sample that overlaps with the catalogue of Webbink (1985), we find a power-law index of $0.15 \pm 0.03$ (the uncertainty was found using the bootstrap methodology described in Section 4.3.2). For the subset of dense clusters having a central luminosity density satisfying $\log \rho_0 > 4$, we find a power-law index of $0.36 \pm 0.14$. As before, we find no significant correlation with collision rate, even for the subset of dense clusters. Although we do find a weak dependence of BS numbers on collision rate for the entire sample, this is not unexpected since the collision rate and the core mass are themselves correlated, and our results suggest that there exists a strong correlation between BS numbers and the core masses.

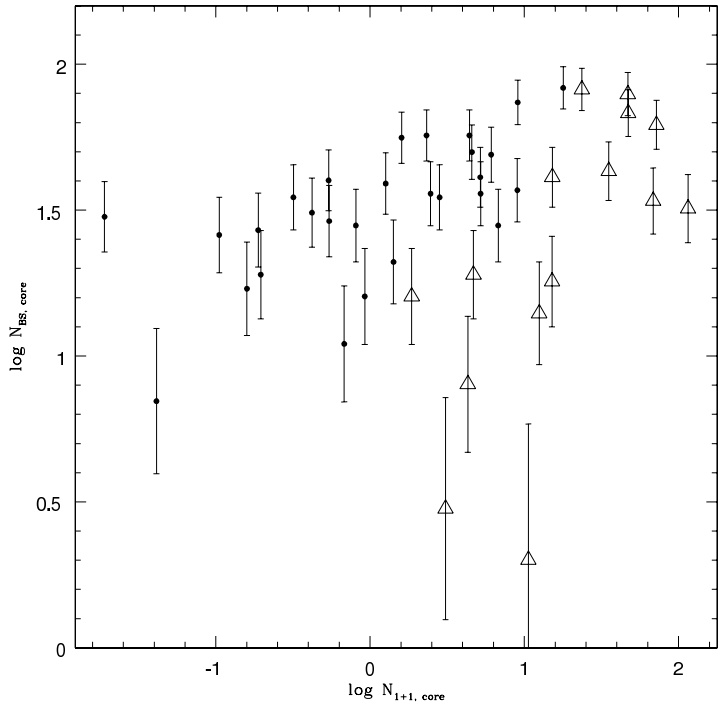



Figure 4.5 The logarithm of the number of BSs predicted to have formed in the core from single-single collisions $N_{1+1}$ versus the logarithm of the observed number of BSs in the core $N_{BS}$. Filled circles correspond to clusters having central luminosity densities satisfying $\log \rho_0 < 4$, whereas open triangles correspond to dense clusters for which $\log \rho_0 > 4$. The adopted definition for $N_{1+1}$ has been provided in the text.

## 4.4 Summary & Discussion

In this chapter, we have presented a catalogue for BS, RGB, HB and MSTO stars in a sample of 35 GCs. Our catalogue provides number counts for each stellar population within several different circles centred on the cluster centre. The radii of the circles were taken to be integer multiples of the core radius, and we have focussed on the inner four core radii since the field of view extends beyond this for only a handful of the clusters in our sample. Particular consideration was given to our selection criteria for the different stellar populations in order to ensure that they were applied consistently from

cluster-to-cluster. In particular, we have improved upon our previous selection criteria (Leigh, Sills & Knigge, 2007) by fitting theoretical isochrones to the cluster CMDs. This provides an unambiguous definition for the location of the MSTO, which acts as the primary point of reference for the application of our selection criteria. As a result, our new catalogue is highly homogeneous.

We have used our catalogue to quantify the dependence of the size of each stellar population on the total stellar mass enclosed within the same radius. As described in Section 4.3.2, this provides a means of quantifying the effects, if any, had by the cluster dynamics in shaping the appearance of CMDs above the MSTO. Below, we summarize the implications of our results for each of the different stellar populations.

### 4.4.1 Blue Stragglers

We have confirmed our previous result that the numbers of BSs in the cores of GCs scale sub-linearly with the core masses (Knigge, Leigh & Sills, 2009). That is, we find proportionately larger BS populations in low-mass GCs. There exist several possibilities that could explain the origin of this sub-linear dependence. First, we previously suggested that this could be an artifact of an anti-correlation between the binary fraction and the cluster (or core) mass (Knigge, Leigh & Sills, 2009). This assertion stems from the fact that, if BSs have a binary origin, we expect their numbers to scale with the core mass as $N_{BS} \sim f_b M_{core}$, where $f_b$ is the binary fraction in the core. As before, we find that $N_{BS} \sim M_{core}^{0.4-0.5}$. Our result could therefore be explained if $f_b \sim M_{core}^{-(0.5-0.6)}$. Second, we suggested in Leigh, Sills & Knigge (2009) that the fact that the least massive GCs in our sample should be more dynamically

evolved than their more massive counterparts could be contributing to the observed sub-linearity for BSs. In particular, the low-mass clusters in our sample should have experienced a significant depletion of their very low-mass stars as a result of stellar evaporation induced by two-body relaxation (e.g. Spitzer, 1987; Heggie & Hut, 2003; De Marchi, Paresce & Portegies Zwart, 2010). In turn, this could contribute to a higher fraction of merger products having masses that exceed that of the MSTO in low-mass GCs. As a result, more merger products would appear brighter and bluer than the MSTO in these clusters' CMDs, leading to more merger products being identified as BSs. Finally, mass segregation could also be contributing to the observed sub-linear dependence for BSs. Again, this is the result of the fact that the rate of two-body relaxation, and therefore dynamical friction, is in general the fastest in low-mass clusters. BSs are among the most massive stars in GCs, so they should rapidly migrate into the core via dynamical friction in clusters for which the half-mass relaxation time is shorter than the average BS lifetime. It follows that proportionately more BSs could have drifted into the core via dynamical friction in low-mass GCs. This would also contribute to the observed sub-linear dependence of BS numbers on the core masses.

This last hypothesis can be tested by comparing our scaling relations for progressively larger circles outside the core. If mass segregation is indeed the cause of the observed sub-linear dependence of BS numbers on the core masses, then we might expect the power-law index to systematically increase as we consider progressively larger circles. That is, we could be including more BSs that have not yet migrated into the core via dynamical friction, particularly in the most massive clusters in our sample. However, our results suggest that the power-law index remains roughly constant for all circles. This

is the case for both the comparison to the total stellar masses as well as to the total number of stars contained in each circle. The fact that these relations are comparably sub-linear within all circles can be interpreted as evidence that mass segregation is not the dominant effect contributing to the observed sub-linear dependence of BS numbers on the total stellar masses (or the total number of stars). We note that for many of the clusters in our sample, the spatial coverage is comparable to or exceeds the half-mass radius. This is a sufficiently large fraction of the total cluster area for our comparison to be sensitive to the effects of mass segregation.

On the other hand, several GCs are known to show evidence for a bi-modal BS radial distribution (e.g. Mapelli et al., 2006; Lanzoni et al., 2007). That is, in these clusters the number of BSs is highest in the central cluster regions and decreases with increasing distance from the cluster centre until a second rise in BS numbers occurs in the cluster outskirts. This secondary outer peak has been shown to occur at a distance from the cluster centre that exceeds 20 core radii in several cases. Consequently, the spatial coverage provided by the ACS data likely does not extend sufficiently far in most clusters to detect any bi-modality in the BS radial distribution. Nonetheless, if applied to a statistically-significant sample for which the spatial coverage is complete out to the tidal radius, the technique we have presented in this chapter could provide a powerful constraint for the origin of the bi-modal BS radial distribution observed in several MW GCs by addressing the role played by mass segregation.

We also tried to correlate the number of BSs observed in the cluster core with the number predicted from single-single collisions. As in Knigge, Leigh & Sills (2009), we find that BS numbers depend strongly on core mass, but not on

collision rate. This also proved to be the case for the subset of dense clusters satisfying $\log \rho_0 > 4$. Our previous interpretation that our results provide strong evidence for a binary, as opposed to a collisional, origin for BSs in GCs therefore remains the same.

### 4.4.2 Red Giant Branch Stars

The technique used in this chapter to compare the sizes of the different stellar populations was first presented in Leigh, Sills & Knigge (2009). In that study, we introduced our method and applied it to a sample of 56 GCs taken from Piotto et al. (2002) in order to study their RGB populations. Our results were consistent with a sub-linear dependence of RGB numbers on the core masses. In particular, we found evidence for a surplus of RGB stars relative to MSTO stars in the cores of low-mass GCs. We considered several possible causes for this result, but concluded that our analysis should ideally be repeated with superior photometry in order to properly assess effects such as completeness. Given the high-quality of the ACS data, we are now in a position to reassess our previous result for RGB stars.

Upon applying our technique to the ACS sample, we find that the numbers of RGB stars scale linearly with the core masses to within one standard deviation. This is also the case for our comparison to the total number of stars in the core. This suggests that we should reject our previous conclusions for this stellar population reported in Leigh, Sills & Knigge (2009). Specifically, if we take a strict $3-\sigma$ limit as our criterion for whether or not the slopes are sub-linear at a statistically significant level, then the core RGB slope reported in this chapter is consistent with being linear whereas this was not the case

for the core RGB slope reported in Leigh, Sills & Knigge (2009). However, if we take a more stringent criterion for statistical significance, then there is no inconsistency between our new and old results for RGB stars, and both slopes are consistent with being linear.

We also tried comparing the RGB catalogue presented in this chapter with the one presented in Leigh, Sills & Knigge (2009). This showed that the old RGB numbers are slightly deficient relative to the new numbers at the high-mass end. Although this difference is not sufficiently large to completely account for the difference in slopes (for the comparison with the core mass) found between our new and old RGB catalogues, it works in the right direction and is likely a contributing factor. If our uncertainties are also factored in, then our new and old slopes agree to within one standard deviation (due mainly to the large uncertainty for the new slope). The source of the disagreement between our old and new RGB catalogues is unclear, and we cannot say whether or not incompleteness (in the old data set) is the culprit. The results of our artificial star tests have at least confirmed that incompleteness is not an issue for our new catalogue, however it could certainly have contributed to the lower RGB numbers reported in Leigh, Sills & Knigge (2009). Indeed, the central cluster density tends to be higher in more massive clusters, which should negatively affect completeness. It is not clear, however, why this would have affected RGB stars more than MSTO stars in the old data set. Given all of these considerations, we feel that our new results show that this issue needs to be looked at in more detail before any firm conclusions can be drawn.

The evidence in favour of RGB numbers scaling linearly with the core masses is interesting. For one thing, it suggests that two-body relaxation does not significantly affect RGB population size relative to other stellar popula-

tions of comparable mass in even the dense central regions of GCs. This is not surprising, since two-body relaxation is a long-range effect for which the stellar radius plays a negligible role. Second, it suggests that collisions do not significantly deplete RGB stars relative to other stellar populations despite their much larger radii. This is because the collision rate increases with increasing cluster mass, so we would expect RGB stars to appear preferentially depleted in massive clusters if they are significantly affected by collisions (e.g. Beers & Davies, 2004; Davies, Piotto & De Angeli, 2004). Third, it suggests that the sub-linear relation found for BSs does not contribute to a sub-linear relation for RGB stars despite the fact that BSs should eventually evolve to occupy our RGB selection box, as discussed in Leigh, Sills & Knigge (2009). This is likely the result of the relatively small sizes of the BS populations in our sample when compared to the numbers of RGB stars since the rate at which evolved BSs ascend the RGB is thought to be comparable to the RGB lifetimes of regular MSTO stars (Sills, Karakas & Lattanzio, 2009). Alternatively, this result could, at least in part, be explained if a smaller fraction of BSs end up sufficiently bright and blue to be identified as BSs in the CMDs of massive GCs. In other words, it could be that a larger fraction of BSs are hidden along the MS in massive clusters, as discussed in Section 4.4.1. In this case, the contributions to RGB populations from evolved BSs could be comparable in all clusters, in which case a linear relationship between RGB numbers and the core masses would be expected. Finally, evolved BSs would be expected to have a negligible impact on RGB population size if the average BS lifetime is considerably longer than the lifetimes of RGB stars. This effect is difficult to quantify, however, given that BS lifetimes are poorly constrained in the literature (e.g. Sandquist, Bolte & Hernquist, 1997; Sills et al., 2001).

### 4.4.3 Horizontal Branch Stars

Our results suggest that HB numbers scale linearly with the core masses. This can be interpreted as evidence that two-body relaxation does not significantly affect the radial distributions of HB stars in GCs relative to the other stellar populations above the MSTO. One reason to perhaps expect that two-body relaxation should affect the spatial distributions of HB stars stems from the fact that RGB stars are among the most massive stars in clusters, and they undergo significant mass loss upon evolving into HB stars. Consequently, the progenitors of HB stars should be heavily mass segregated. HB stars themselves, however, have relatively low-masses so that two-body relaxation and strong dynamical encounters should act to re-distribute them to wider orbits within the cluster potential. The HB lifetime is roughly constant at $10^8$ years (Iben, 1991) and it is comparable to or exceeds the core relaxation times for most of the low-mass clusters in our sample (Harris, 1996, 2010 update). Therefore, we might expect the HB populations in these clusters to exhibit more extended radial profiles relative to more massive clusters. This would contribute to a sub-linear relationship between the numbers of HB stars and the core masses. Our uncertainties are sufficiently large that this possibility cannot be entirely ruled out, however our results are consistent with a linear relationship between HB numbers and the core masses.

### 4.4.4 Additional Considerations

Recent observations have revealed the presence of multiple stellar populations in a number of MW GCs (e.g. Pancino et al., 2003). The majority of these cases have been reported in very massive clusters. Moreover, their existence

is thought to be related to the chemical properties of GCs, in particular an observed anti-correlation between their sodium and oxygen abundances. In turn, these chemical signatures have been argued to be linked to the cluster metallicity, mass and age (Carretta et al., 2010).

We identified clusters in our sample currently known to host multiple stellar populations, but none of these were clear outliers in our plots. Consequently, the effects had on our results by multiple stellar populations remains unclear. It is certainly possible that multiple stellar populations have contributed to the uncertainties for the weighted lines of best fit performed for the relations in Figure 4.3 and Figure 4.4. It is difficult to quantify the possible severity of this effect, however, given the limited evidence linking multiple stellar populations to cluster properties.

Although the uncertainties are sufficiently large that the slopes are consistent with being linear at the $3-\sigma$ confidence level for all stellar populations when performing the comparisons with the total stellar mass, the reported slopes are typically less than unity within the $1-\sigma$, and often even the $2-\sigma$, confidence interval. This does not appear to result from the fact that we have obtained our estimates for the total stellar masses by numerically integrating 3-dimensional density distributions and are comparing to number counts, which are projected quantities. To address this, we also tried obtaining the total stellar masses by numerically integrating 2-dimensional surface brightness profiles so that we are consistently comparing only projected quantities. Despite this, our results remain unchanged and the new slopes agree with the old ones to within one standard deviation for all stellar populations. Another possibility to account for this trend that is perhaps worth considering is a systematic dependence of the mass-to-light ratios of clusters on their to-

tal mass. There are two ways this could have affected our analysis. First, stellar remnants have been shown to affect the dynamical evolution of clusters, and therefore the sizes of their cores (e.g. Lee, Fahlman & Richer, 1991; Trenti, Vesperini & Pasquato, 2010). It follows that, if the number of stellar remnants depends on the cluster mass, then this could contribute to an additional underlying dependence of the core radius on the cluster mass. This could perhaps arise as a result of the fact that the ratio of the rate of stellar evolution to the rate of dynamical evolution is larger in more massive clusters, since in general the rate of two-body relaxation decreases with increasing cluster mass whereas the rate of stellar evolution is independent of the cluster mass. Coupled with their deeper gravitational potential wells, this could contribute to more massive clusters retaining more stellar remnants. Second, variations in the mass-to-light ratios of clusters can also occur as a result of changes in the average stellar mass (not including stellar remnants) (Kruijssen & Mieske, 2009). That is, we can approximate the total stellar mass contained in the core as:

$$M_{core} \sim \frac{4}{3}\pi\frac{M}{L}\rho_0 r_c^3 \sim mN_{core}, \tag{4.2}$$

where $M/L$ is the mass-to-light ratio, $\rho_0$ is the central luminosity density, $m$ is the average stellar mass and $N_{core}$ is the total number of stars in the core. Based on our results, $M_{core} \propto N_{core}^{0.9}$, where we have used the total number of stars in the core with magnitudes brighter than 0.5 mag below the MSTO as a proxy for $N_{core}$. This could suggest that $m \propto N_{core}^{-0.1} \propto M_{core}^{-0.1}$. In other words, the average stellar mass in the core decreases weakly with increasing core mass. This could in part be due to the fact that more massive clusters should be less dynamically evolved than their less massive counterparts, and should

therefore be less depleted of their low-mass stars due to stellar evaporation induced by two-body relaxation (e.g. Ambartsumian, 1938; Spitzer & Harm, 1958; Henon, 1960; De Marchi, Paresce & Portegies Zwart, 2010). Similarly, mass segregation should also tend to operate more rapidly in low-mass clusters, which acts to migrate preferentially massive stars into the core (Spitzer, 1969; Spitzer & Hart, 1971; Farouki & Salpeter, 1982; Shara et al., 1995; King, Sosin & Cool, 1995; Meylan & Heggie, 1997). Alternatively, differences in the stellar mass function in the core could result from variations in the degree of primordial mass segregation, or even variations in the initial stellar mass function.

We have assumed throughout our analysis that the core mass is a suitable proxy for the total cluster mass. We have checked that these two quantities are indeed correlated, however this does not tell the whole story since we are also using the total cluster mass as a proxy for the degree of dynamical evolution. The central concentration parameter, defined as the logarithm of the ratio of the tidal to core radii, describes the degree to which a cluster is centrally concentrated. Previous studies have shown that there exists a weak correlation between the concentration parameter and the total cluster mass (e.g. Djorgovski & Meylan, 1994; McLaughlin, 2000). In order to better use our technique to reliably probe the effects of the cluster dynamics on the sizes and radial distributions of the different stellar populations, the concentration parameter should ideally be accounted for when applying our normalization technique in future studies. It is not yet clear how the concentration parameter can be properly absorbed into the normalization, however its effect on our analysis should be small given the weak dependence on cluster mass.

The assumption that the degree of dynamical evolution experienced by a given cluster depends only on its mass is also incorrect. Two-body re-

laxation has been shown to dominate cluster evolution for a significant fraction of the lives of old MW GCs (e.g. Gieles, Heggie & Zhao, 2011), however other effects can also play a significant role. For example, stellar evolution is known to affect the dynamical evolution of star clusters, although its primary role is played during their early evolutionary phases (e.g. Applegate, 1986; Chernoff & Weinberg, 1990; Fukushige & Heggie, 1995). Tidal effects from the Galaxy have also been shown to play an important role in deciding the dynamical fates of clusters by increasing the rate of mass loss across the tidal boundary (e.g. Heggie & Hut, 2003). Consequently, clusters with small perigalacticon distances should appear more dynamically evolved than their total mass alone would suggest. This effect can be significant, and has likely contributed to increasing the uncertainties found for the comparisons to the total stellar mass. Therefore, tidal effects from the Galaxy should also ideally be absorbed into our normalization technique in future studies. This can be done by using the perigalacticon distances of clusters as a rough proxy for the degree to which tides from the Galaxy should have affected their internal dynamical evolution (Gieles, Heggie & Zhao, 2011).

Interestingly, tides could also help to explain why the uncertainties for the comparisons to the total number of stars in each circle are considerably smaller than for the comparisons to the total stellar mass. We have used the number of stars with magnitudes brighter than 0.5 mag below the MSTO as a proxy for the total number of stars. Consequently, we are comparing stars within a very narrow mass range, so that all populations of interest should have been comparably affected by two-body relaxation (except, perhaps, for HB stars) independent of tidal effects from the Galaxy. In other words, tides should affect all stars above the MSTO more or less equally, and this is consistent with

our results. It is also worth mentioning here that our King models consider only a single stellar mass. This assumption is not strictly true and could also be contributing to increasing the uncertainties found for the comparisons to the total stellar masses.

An additional concern is that we do not know if the clusters in our sample are currently in a phase of core contraction or expansion. This has a direct bearing on the recent history of the stellar density in the core, and therefore the degree to which stars in the core should have been affected by close dynamical interactions. These effects are independent of two-body relaxation and occur on a time-scale that is typically much shorter than the half-mass relaxation time (Heggie & Hut, 2003). The effects could be significant in clusters that were recently in a phase of core-collapse but have since rebounded back out of this highly concentrated state. This could occur, for example, as a result of binary formation induced by 3-body interactions combined with their subsequent hardening via additional encounters (Hut, 1983; Heggie & Hut, 2003). In general, binaries play an important role in the dynamical evolution of clusters, and could have affected our results in a number of ways. This is a difficult issue to address even qualitatively given how little is currently known about the binary populations in globular clusters. Theoretical models suggest, however, that the time-scale for core contraction is often longer than a Hubble time, and that this evolutionary phase will only come to an end once the central density becomes sufficiently high for hardening encounters involving binaries to halt the process (Fregeau, Ivanova & Rasio, 2009). It follows that the cores of most MW GCs are expected to currently be in a phase of core contraction. This process is ultimately driven by two-body relaxation, so that our assumption that the total cluster mass provides a suitable proxy for the

degree of dynamical evolution is still valid.

In summary, our results suggest that effects related to the cluster dynamics do not significantly affect the relative sizes of the different stellar populations above the MSTO. This is the case for at least RGB, HB and MSTO stars. BSs, on the other hand, show evidence for a sub-linear dependence of population size on the total stellar mass contained within the same radius. Whether or not the cluster dynamics is responsible for this sub-linearity is still not clear. Notwithstanding, our results have provided evidence that mass segregation is not the dominant cause for this result, although it will be necessary to redo the comparison performed in this study with a larger spatial coverage in order to fully address this question. Further insight into the origin of the sub-linearity found for BSs will be provided by reliable binary fractions for the clusters in our sample, which are forthcoming (Sarajedini 2010, private communication).

## Acknowledgments

We would like to thank Ata Sarajedini, Aaron Dotter and Roger Cohen for providing the data on which this study was based and for their extensive support in its analysis. We would also like to thank Evert Glebbeek for useful discussions. This research has been supported by NSERC and OGS.

# Bibliography

Ambartsumian V. A. 1938, Ann. Leningrad State Univ., 22, 19; English translation: Ambartsumian V.A., 1985, in Dynamics of Star Clusters, IAU Symp. 113, eds. Goodman J. & Hut P. (Dordrecht: Reidel), 521

Anderson J., Sarajedini A., Bedin L. R., King I. R., Piotto G., Reid I. N., Siegel M., Majewski S. R., Paust N. E. Q., Aparicio A., Milone A. P., Chaboyer B., Rosenberg A. 2008, AJ, 135, 2055

Applegate J. H. 1986, ApJ, 301, 132

Beccari G., Ferraro F. R., Possenti A., Valenti E., Origlia L., Rood R. T. 2006, AJ, 131, 2551

Beers M. E., Davies M. B. 2004, MNRAS, 348, 679

Buonanno R., Corsi C., Bellazzini M., Ferraro F. R., Fusi Pecci F. 1997, AJ, 113, 706

Carretta E., Bragaglia A., Gratton R. G., Recio-Blanco A., Lucatello S., D'Orazi V., Cassisi S. 2010, A&A, 516, 55

Chernoff D. F., Weinberg M. D. 1990, ApJ, 351, 121

Cohen R. L., Guhathakurta P., Yanny B., Schneider D. P., Bahcall J. N. 1997, AJ, 113, 669

Davies M. B., Piotto G., De Angeli F. 2004, MNRAS, 348, 129

De Angeli F., Piotto G., Cassisi S., Busso G., Recio-Blanco A., Salaris M., Aparicio A., Rosenberg A. 2005, AJ, 130, 116

De Marchi G., Paresce F., Portegies Zwart S. 2010, ApJ, 718, 105

Dervisoglu A., Tout C. A., Ibanoglu C. 2010, MNRAS, 406, 1071

Djorgovski S., Meylan G. 1994, AJ, 108, 1292

Dotter A., Chaboyer B., Jevremovic D., Baron E., Ferguson J. W., Sarajedini A., Anderson J. 2007, AJ, 134, 376

Dotter, A., Sarajedini A., Anderson J., Aparicio A., Bedin L. R., Chaboyer B., Majewski S., Marin-Franch A., Milone A., Paust N., Piotto G., Reid N., Rosenberg A., Siegel M. 2010, ApJ, 708, 698

Farouki R. T., Salpeter E. E. 1982, ApJ, 253, 512

Ferraro F. R., Messineo M., Fusi Pecci F., de Palo M. A., Straniero O., Chieffi A., Limongi M. 1999, AJ, 118, 1738

Fregeau J. M., Cheung P., Portegies Zwart S. F., Rasio F. A. 2004, MNRAS, 352, 1

Fregeau J. M., Ivanova N., Rasio F. A. 2009, ApJ, 707, 1533

Fukushige T., Heggie D. C. 1995, MNRAS, 276, 206

Fusi Pecci F., Ferraro F. R., Corsi C. E., Cacciari C., Buonanno R. 1992, AJ, 104, 1831

Fusi Pecci F., Ferraro F. R., Bellazzini M., et al. 1993, AJ, 105, 1145

Gieles M., Baumgardt H., Heggie D., Lamers H. 2010, MNRAS, 408, L16

Gieles M., Heggie D., Zhao H. 2011, MNRAS, accepted

Goldsbury R., Richer H. B., Anderson J., Dotter A., Sarajedini A., Woodley K. 2010, AJ, 140, 1830

Harris, W. E. 1996, AJ, 112, 1487 (2010 update)

Heggie D. C., Hut P. 2003, The Gravitational Million-Body Problem: A Multidisciplinary Approach to Sar Cluster Dynamics (Cambridge: Cambridge University Press)

Henon M. 1960, Annales d'Astrophysique, 23, 668

Henon M. 1973, Dynamical Structure and Evolution of Dense Stellar Systems, ed. L. Martinet & M. Mayor (Geneva Obs.)

Hut P., Bahcall J. N. 1983, ApJ, 268, 319

Iannicola G., Monelli M., Bono G., Stetson P. B., Buonanno R., Calamida A., Zoccali M., Caputo F., Castellani M., Corsi C. E., Dall'Ora M., Cecco A. Di, Degl'Innocenti S., Ferraro I., Nonino M., Pietrinferni A., Pulone L., Moroni P. G. Prada, Romaniello M., Sanna N., Walker A. R. 2009, ApJ, 696, L120

Iben I. Jr. 1991, ApJS, 76, 55

King I. R., Sosin C., Cool A. M. 1995, ApJ, 452, L33

Knigge C., Leigh N. W., Sills A. 2009, Nature, 457, 288

Kruijssen J. M. D., Mieske S. 2009, A&A, 500, 785

Lanzoni B., Dalessandro E., Perina S., Ferraro F. R., Rood R. T., Sollima A. 2007, ApJ, 670, 1065

Lee H. M., Fahlman G. G., Richer H. B. 1991, ApJ, 366, 455

Leigh N. W., Sills A., Knigge C. 2007, ApJ, 661, 210

Leigh N. W., Sills A., Knigge C. 2008, ApJ, 678, 564

Leigh N. W., Sills A., Knigge C. 2009, MNRAS, 399, L179

Leigh N. W., Sills A. 2010, MNRAS, 410, 2370

Leonard P. J. T. 1989, AJ, 98, 217

Leonard P. J. T., Linnell A. P. 1992, AJ, 103, 1928

Li L., Zhang F. 2006, MNRAS, 369, 2001

Mapelli M., Sigurdsson S., Ferraro F. R., Colpi M., Possenti A., Lanzoni B. 2006, MNRAS, 373, 361

Mathieu R. D., Geller A. R. 2009, Nature, 462, 1032

McCrea W. H. 1964, MNRAS, 128, 147

McLaughlin D. E. 2000, ApJ, 539, 618

McLaughlin D. E., van der Marel R. P. 2005, ApJS, 161, 304

Meylan G., Heggie D. C. 1997, A&AR, 8, 1

Murray N. 2009, ApJ, 691, 946

Pancino E., Seleznev A., Ferraro F. R., Bellazzini M., Piotto G. 2003, MNRAS, 345, 683

Perets H. B., Fabrycky D. C. 2009, ApJ, 697, 1048

Peterson R. C., Carney B. W., Dorman B., Green E. M., Landsman W., Liebert J., O'Connell R. W., Rood R. T. 2003, ApJ, 588, 299

Piotto G., King I. R., Djorgovski S. G., Sosin C., Zoccali M., Saviane I., De Angeli F., Riello M., Recio-Blanco A., Rich R. M., Meylan G., Renzini A. 2002, A&A, 391, 945

Portegies Zwart S. F., Hut P., Makino J., McMillan S. L. W. 1998, A&A, 337, 363

Rood R. T. 1973, ApJ, 184, 815

Sandage A. R. 1953, AJ, 58, 61

Sandage A., Wallerstein G. 1960, ApJ, 131, 598

Sandquist E. L., Bolte M., Hernquist L. 1997, ApJ, 477, 335

Sandquist E. L., Martel A. R. 2007, ApJL, 654, L65

Sarajedini A., Bedin L. R., Chaboyer B., Dotter A., Siegel M., Anderson J., Aparicio A., King I., Majewski S., Marin-Franch A., Piotto G., Reid I. N., Rosenberg A., Steven M. 2007, AJ, 133, 1658

Saviane I., Piotto G., Fagotto F., Zaggia S., Capaccioli M., Aparicio A. 1998, A&A, 333, 479

Shara M. M., Drissen L., Bergeron L. E., Paresce F. 1995, ApJ, 441, 617

Sigurdsson S., Phinney E. S. 1995, ApJS, 99, 609

Sills A., Bailyn C. D. 1999, ApJ, 513, 428

Sills A. R., Faber J. A., Lombardi J. C., Rasio F. A., Waren A. R. 2001, ApJ, 548, 323

Sills A., Karakas A., Lattanzio J. 2009, ApJ, 692, 1411

Spitzer L. Jr., Harm R. 1958, ApJ, 127, 544

Spitzer L. Jr. 1969, ApJ, 168, L139

Spitzer L. Jr., Hart M. H. 1971, ApJ, 166, 483

Spitzer L. Jr., Shull J. M. 1975, ApJ, 200, 339

Spitzer L. 1987, Dynamical Evolution of Globular Clusters (Princeton: Princeton University Press)

Trenti M., Vesperini E., Pasquato M. 2010, ApJ, 708, 1598

Webbink R. F. Structure parameters of galactic globular clusters. In Goodman, J. & Hut, P. (eds.) Dynamics of Star Clusters, vol. 113 of IAU Symposium, 541-577 (1985).

Zinn R., Barnes S. 1996, AJ, 112, 1054

Chapter 5

# An Analytic Model for Blue Straggler Formation in Globular Clusters

## 5.1 Introduction

Commonly found in both open and globular clusters (GCs), blue stragglers (BSs) appear as an extension of the main-sequence (MS) in cluster colour-magnitude diagrams (CMDs), occupying the region that is just brighter and bluer than the main-sequence turn-off (MSTO) (Sandage, 1953). BSs are thought to be produced via the addition of hydrogen to low-mass MS stars (e.g. Sills et al., 2001; Lombardi et al., 2002). This can occur via multiple channels, most of which involve the mergers of low-mass MS stars since a significant amount of mass is typically required to reproduce the observed locations of BSs in CMDs (e.g. Sills & Bailyn, 1999). Stars in close binaries can merge if enough orbital angular momentum is lost, which can be mediated by dynam-

ical interactions with other stars, magnetized stellar winds, tidal dissipation or even an outer triple companion (e.g. Leonard & Linnell, 1992; Li & Zhang, 2006; Perets & Fabrycky, 2009; Dervisoglu, Tout & Ibanoglu, 2010). Alternatively, MS stars can collide directly, although this is also thought to usually be mediated by multiple star systems (e.g. Leonard, 1989; Leonard & Livio, 1995; Fregeau et al., 2004; Leigh & Sills, 2011). First proposed by McCrea (1964), BSs have also been hypothesized to form by mass-transfer from an evolving primary onto a normal MS companion via Roche lobe overflow.

Despite numerous formation mechanisms having been proposed, a satisfactory explanation to account for the presence of BSs in star clusters eludes us still. Whatever the dominant BS formation mechanism(s) operating in dense clusters, it is now thought to somehow involve multiple star systems. This was shown to be the case in even the dense cores of GCs (Leigh, Sills & Knigge, 2007, 2008; Knigge, Leigh & Sills, 2009) where collisions between single stars are thought to occur frequently (Leonard, 1989). In Knigge, Leigh & Sills (2009), we showed that the numbers of BSs in the cores of a large sample of GCs correlate with the core masses. We argued that our results are consistent with what is expected if BSs are descended from binary stars since this would imply a dependence of the form $N_{BS} \sim f_b M_{core}$, where $N_{BS}$ is the number of BSs in the core, $f_b$ is the binary fraction in the core and $M_{core}$ is the total stellar mass contained within the core. Mathieu & Geller (2009) also showed that at least 76% of the BSs in the old open cluster NGC 188 have binary companions. Although the nature of these companions remains unknown, it is clear that binaries played a role in the formation of these BSs.

Blue stragglers are typically concentrated in the dense cores of globular clusters where the high stellar densities should result in a higher rate

of stellar encounters (e.g. Leonard, 1989). Whether or not this fact is directly related to BS formation remains unclear, since mass segregation also acts to migrate BSs (or their progenitors) into the core (e.g. Saviane et al., 1998; Guhathakurta et al., 1998). Additionally, numerous BSs have been observed in more sparsely populated open clusters (e.g. Andrievsky et al., 2000) and the fields of GCs where collisions are much less likely to occur and mass-transfer within binary systems is thought to be a more likely formation scenario (e.g. Mapelli et al., 2004).

Several studies have provided evidence that BSs show a bimodal spatial distribution in some GCs (Ferraro et al., 1997, 1999; Lanzoni et al., 2007). In these clusters, the BS numbers are the highest in the central cluster regions and decrease with increasing distance from the cluster centre until a second rise occurs in the cluster outskirts. This drop in BS numbers at intermediate cluster radii is often referred to as the "zone of avoidance". Some authors have suggested that it is the result of two separate formation mechanisms occurring in the inner and outer regions of the cluster, with mass-transfer in primordial binaries dominating in the latter and stellar collisions dominating in the former (Ferraro et al., 2004; Mapelli et al., 2006). Conversely, mass segregation could also give rise to a "zone of avoidance" for BSs if the time-scale for dynamical friction exceeds the average BS lifetime in only the outskirts of GCs that exhibit this radial trend (e.g. Leigh, Sills & Knigge, 2011).

Dynamical interactions occur frequently enough in dense clusters that they are expected to be at least partly responsible for the observed properties of BSs (e.g. Stryker, 1993; Leigh & Sills, 2011). It follows that the current properties of BS populations should reflect the dynamical histories of their host clusters. As a result, BSs could provide an indirect means of probing the

physical processes that drive star cluster evolution (e.g. Heggie & Hut, 2003; Hurley et al., 2005; Leigh & Sills, 2011).

In this chapter, our goal is to constrain the dominant BS formation mechanism(s) operating in the dense cores of GCs by analyzing the principal processes thought to influence their production. To this end, we use an analytic treatment to obtain predictions for the number of BSs expected to be found within one core radius of the cluster centre at the current cluster age. Predicted numbers for the core are calculated for a range of free parameters, and then compared to the observed numbers in order to find the best-fitting model parameters. In this way, we are able to quantify the degree to which each of the considered formation mechanisms should contribute to the total predicted numbers in order to best reproduce the observations.

In Section 5.2, we describe the BS catalogue used for comparison to our model predictions. In Section 5.3, we present our analytic model for BS formation as well as the statistical technique we have developed to compare its predictions to the observations. These predictions are then compared to the observations in Section 5.4 for a range of model parameters. In Section 5.5, we discuss the implications of our results for BS formation, as well as the role played by the cluster dynamics in shaping the current properties of BS populations.

## 5.2 The Data

The data used in this study was taken from Leigh, Sills & Knigge (2011). In that chapter, we presented a catalogue for blue straggler, red giant branch (RGB), horizontal branch (HB) and main-sequence turn-off stars obtained

from the colour-magnitude diagrams of 35 Milky Way GCs taken from the ACS Survey for Globular Clusters (Sarajedini et al., 2007). The ACS Survey provides unprecedented deep photometry in the F606W ($\sim$ V) and F814W ($\sim$ I) filters that extends reliably from the HB all the way down to about 7 magnitudes below the MSTO. The clusters in our sample span a range of total masses (by nearly 3 orders of magnitude) and central concentrations (Harris, 1996, 2010 update). We have confirmed that the photometry is nearly complete in the BS region of the CMD for every cluster in our sample. This was done using the results of artificial star tests taken from Anderson et al. (2008).

Each cluster was centred in the ACS field, which extends out to several core radii from the cluster centre in most of the clusters in our sample. Only the core populations provided in Leigh, Sills & Knigge (2011) are used in this chapter. We have taken estimates for the core radii and central luminosity densities for the clusters in our sample from Harris (1996, 2010 update), whereas central velocity dispersions were taken from Webbink (1985). Estimates for the total stellar mass contained within the core were obtained from single-mass King models, as described in Leigh, Sills & Knigge (2011). All of the clusters in our sample were chosen to be non-post-core collapse, and have surface brightness profiles that provide good fits to our King models.

## 5.3 Method

In this section, we present our model and outline our assumptions. We also present the statistical technique used to compare the observed number counts to our model predictions in order to identify the best-fitting model parameters.

### 5.3.1 Model

Consider a GC core that is home to $N_{BS,0}$ BSs at some time $t = t_0$. At a specified time in the future, the number of BSs in the core can be approximated by:

$$N_{BS} = N_{BS,0} + N_{coll} + N_{bin} + N_{in} - N_{out} - N_{ev}, \tag{5.1}$$

where $N_{coll}$ is the number of BSs formed from collisions during single-single (1+1), single-binary (1+2) and binary-binary (2+2) encounters, $N_{bin}$ is the number formed from binary evolution (either partial mass-transfer between the binary components or their complete coalescence), $N_{in}$ is the number of BSs that migrate into the core due to dynamical friction, $N_{out}$ is the number that migrate out of the core via kicks experienced during dynamical encounters, and $N_{ev}$ is the number of BSs that have evolved away from being brighter and bluer than the MSTO in the cluster CMD due to stellar evolution.

We adopt an average stellar mass of $m = 0.65 M_{\odot}$ and an average BS mass of $m_{BS} = 2m = 1.3 M_{\odot}$. The mass of a BS can provide a rough guide to its lifetime, although a range of lifetimes are still possible for any given mass. For instance, Sandquist, Bolte & Hernquist (1997) showed that a 1.3 $M_{\odot}$ blue straggler will have a lifetime of around 0.78 Gyrs in unmixed models, or 1.57 Gyrs in completely mixed models. Combined with the results of Sills et al. (2001), Lombardi et al. (2002) and Glebbeek & Pols (2008), we expect a lifetime in the range 1-5 Gyrs for a 1.3 $M_{\odot}$ BS. As a first approximation, we choose a likely value of $\tau_{BS} = 1.5$ Gyrs for the average BS lifetime (e.g. Sills et al., 2001). The effects had on our results by changing our assumption for the average BS lifetime will be explored in Section 5.4 and discussed in Section 5.5.

We consider only the last $\tau_{BS}$ years. This is because we are comparing our model predictions to current observations of BS populations, so that we are only concerned with those BSs formed within the last few Gyrs. Any BSs formed before this would have evolved away from being brighter and bluer than the MSTO by the current cluster age. Consequently, we set $\mathrm{N}_{BS,0} = \mathrm{N}_{ev}$ in Equation 5.1. We further assume that all central cluster parameters have not changed in the last $\tau_{BS}$ years, including the central velocity dispersion, the central luminosity density, the core radius and the core binary fraction. It follows that the rate of BS formation is constant for the time-scale of interest. This time-scale is comparable to the half-mass relaxation time but much longer than the central relaxation time for the majority of the clusters in our sample (Harris, 1996, 2010 update). This suggests that core parameters such as the central density and the core radius will typically change in a time $\tau_{BS}$ since the time-scale on which these parameters vary is the central relaxation time (Heggie & Hut, 2003). Therefore, our assumption of constant rates and cluster parameters is not strictly correct, however it provides a suitable starting point for our model. We will discuss the implications of our assumption of time-independent cluster properties and rates in Section 5.5.

In the following sections, we discuss each of the remaining terms in Equation 5.1.

#### 5.3.1.1 Stellar Collisions

We can approximate the number of BSs formed in the last $\tau_{BS}$ years from collisions during dynamical encounters as:

$$N_{coll} = f_{1+1}N_{1+1} + f_{1+2}N_{1+2} + f_{2+2}N_{2+2}, \tag{5.2}$$

where $N_{1+1}$, $N_{1+2}$ and $N_{2+2}$ are the number of single-single, single-binary and binary-binary encounters, respectively. The terms $f_{1+1}$, $f_{1+2}$ and $f_{2+2}$ are the fraction of 1+1, 1+2 and 2+2 encounters, respectively, that will produce a BS in the last $\tau_{BS}$ years. We treat these three variables as free parameters since we do not know what fraction of collision products will produce BSs (i.e. stars with an appropriate combination of colour and brightness to end up in the BS region of the CMD), nor do we know what fraction of 1+2 and 2+2 encounters will result in a stellar collision. Numerical scattering experiments have been performed to study the outcomes of 1+2 and 2+2 encounters (e.g. Hut, 1983; McMillan, 1986; Fregeau et al., 2004), however a large fraction of the relevant parameter space has yet to be explored.

In terms of the core radius $r_c$ (in parsecs), the central number density $n_0$ (in $pc^{-3}$), the root-mean-square velocity $v_m$ (in km $s^{-1}$), the average stellar mass $m$ (in $M_\odot$) and the average stellar radius $R$ (in $R_\odot$), the mean time-scale between single-single collisions in the core of a GC is (Leonard, 1989):

$$\tau_{1+1} = 1.1 \times 10^{10}(1-f_b)^{-2}\Big(\frac{1pc}{r_c}\Big)^3\Big(\frac{10^3 pc^{-3}}{n_0}\Big)^2 \Big(\frac{v_m}{5km/s}\Big)\Big(\frac{0.5M_\odot}{m}\Big)\Big(\frac{0.5R_\odot}{R}\Big) \text{ years} \tag{5.3}$$

The additional factor $(1\text{-}f_b)^{-2}$ comes from the fact that we are only considering interactions between single stars and the central number density of single stars is given by $(1\text{-}f_b)n_0$, where $f_b$ is the binary fraction in the core (i.e. the fraction of objects that are binaries). For our chosen mass, we assume a corresponding average stellar radius using the relation $M/M_\odot = R/R_\odot$ (Iben, 1991). The number of 1+1 collisions expected to have occurred in the last $\tau_{BS}$ years is

then approximated by:

$$N_{1+1} = \frac{\tau_{BS}}{\tau_{1+1}}. \tag{5.4}$$

The rate of collisions between single stars and binaries, as well as between two binary pairs, can be roughly approximated in the same way as for single-single encounters (Leonard, 1989; Sigurdsson & Phinney, 1993; Bacon et al., 1996; Fregeau et al., 2004). We adopt the time-scales derived in Leigh & Sills (2011) for the average times between 1+2 and 2+2 encounters. These are:

$$\begin{aligned}\tau_{1+2} = 3.4 \times 10^7 f_b^{-1}(1-f_b)^{-1}\Big(\frac{1pc}{r_c}\Big)^3\Big(\frac{10^3 pc^{-3}}{n_0}\Big)^2 \\ \Big(\frac{v_m}{5km/s}\Big)\Big(\frac{0.5M_\odot}{m}\Big)\Big(\frac{1AU}{a}\Big) \text{ years}\end{aligned} \tag{5.5}$$

and

$$\begin{aligned}\tau_{2+2} = 1.3 \times 10^7 f_b^{-2}\Big(\frac{1pc}{r_c}\Big)^3\Big(\frac{10^3 pc^{-3}}{n_0}\Big)^2 \\ \Big(\frac{v_m}{5km/s}\Big)\Big(\frac{0.5M_\odot}{m}\Big)\Big(\frac{1AU}{a}\Big) \text{ years,}\end{aligned} \tag{5.6}$$

where $a$ is the average binary semi-major axis in the core in AU and we have assumed that the average binary mass is equal to twice the average single star mass. The numbers of 1+2 and 2+2 encounters expected to have occurred in the last $\tau_{BS}$ years are given by, respectively:

$$N_{1+2} = \frac{\tau_{BS}}{\tau_{1+2}} \tag{5.7}$$

and

$$N_{2+2} = \frac{\tau_{BS}}{\tau_{2+2}}. \tag{5.8}$$

The outcomes of 1+2 and 2+2 encounters will ultimately contribute

to the evolution of the binary fraction in the core. How and with what frequency binary hardening/softening as well as capture, exchange and ionization interactions affect the binary fraction in the dense cores of GCs is currently a subject of debate (e.g. Ivanova et al., 2005; Hurley, Aarseth & Shara, 2007). Observations are also lacking for binary fractions in the dense cores of GCs, however rough constraints suggest that they range from a few to a few tens of a percent (e.g. Rubenstein & Bailyn, 1997; Cool et al., 2002; Sollima et al., 2008; Davis et al., 2008). The situation is even worse for the distribution of binary orbital parameters observed in dense stellar environments. Our best constraints come from radial velocity surveys of moderately dense open clusters (Latham, 2005; Geller at al., 2009), however whether or not the properties of the binary populations in these clusters should differ significantly from those in the much denser cores of GCs is unclear. As an initial assumption, we assume a time-independent core binary fraction of 10% for all clusters, and an average semi-major axis of 2 AU. This semi-major axis corresponds roughly to the hard-soft boundary for most of the clusters in our sample, defined by setting the average binary orbital energy equal to the kinetic energy of an average star in the cluster (e.g. Heggie & Hut, 2003). We treat both the core binary fraction and the average binary semi-major axis as free parameters, and explore a range of possibilities using the available observations as a guide for realistic values. We will return to these assumptions in Section 5.5.

#### 5.3.1.2 Binary Star Evolution

Although we do not know the rate of BS formation from binary star evolution, we expect a general relation of the form $N_{bin} = \tau_{BS}/\tau_{mt}$ for the number of BSs produced from binary mergers in the last $\tau_{BS}$ years, where $\tau_{mt}$ is the

average time between BS formation events due to binary star evolution. We can express the number of BSs formed from binary star evolution in the last $\tau_{BS}$ years as:

$$N_{bin} = f_{mt} f_b N_{core}, \tag{5.9}$$

where $N_{core}$ is the total number of objects (i.e. single and binary stars) in the core and $f_{mt}$ is the fraction of binary stars that evolved internally to form BSs within the last $\tau_{BS}$ years. We treat $f_{mt}$ as a free parameter since it is likely to depend on the mass-ratio, period and eccentricity distributions characteristic of the binary populations of evolved GC cores, for which data is scarce at best.

#### 5.3.1.3 Migration Into and Out of the Core

Due to the relatively small sizes of the BS populations considered, the migration of BSs into or out of the core is an important consideration when calculating the predicted numbers. In other words, we are dealing with relatively small number statistics and every blue straggler counts. In order to approximate the number of stars in the core as a function of time, two competing effects need to be taken into account: (1) mass stratification/segregation (or, equivalently, dynamical friction) and (2) kicks experienced during dynamical interactions. These effects are accounted for with the variables $N_{in}$ and $N_{out}$ in Equation 5.1, respectively.

Blue stragglers are among the most massive stars in clusters (e.g. Shara, Saffer & Livio, 1997; van den Berg et al., 2001; Mathieu & Geller, 2009), so they should typically be heavily mass segregated relative to other stellar populations (e.g. Spitzer, 1969; Shara et al., 1995; King, Sosin & Cool, 1995). The time-scale for this process to occur can be approximated using the dynamical friction

time-scale (Binney & Tremaine, 1987):

$$\tau_{dyn} = \frac{3}{4ln\Lambda G^2(2\pi)^{1/2}} \frac{\sigma(r)^3}{m_{BS}\rho(r)}, \tag{5.10}$$

where $\sigma(r)$ and $\rho(r)$ are, respectively, the velocity dispersion and stellar mass density at the given distance from the cluster centre $r$. Both $\sigma(r)$ and $\rho(r)$ are found from single-mass King models (Sigurdsson & Phinney, 1993), which are fit to each cluster using the concentration parameters provided in McLaughlin & van den Marel (2005). The Coulomb logarithm is denoted by $\Lambda$, and we adopt a value of $\ln\Lambda \sim 10$ throughout this chapter (e.g. Spitzer, 1987; Heggie & Hut, 2003). If $\tau_{dyn} > \tau_{BS}$ at a given distance from the cluster centre, then any BSs formed at this radius in the last $\tau_{BS}$ years will not have had sufficient time to migrate into the core by the current cluster age. The maximum radius $\mathrm{r}_{max}$ at which BSs can have formed in the last $\tau_{BS}$ years and still have time to migrate into the core via dynamical friction is given by setting $\tau_{dyn} = \tau_{BS}$. Therefore, $\mathrm{N}_{in}$ depends only on the number of BSs formed in the last $\tau_{BS}$ years at a distance from the cluster centre smaller than $\mathrm{r}_{max}$.

In order to estimate the contribution to $\mathrm{N}_{BS}$ in Equation 5.1 from BSs formed outside the core, we calculate the number of BSs formed in radial shells between the cluster centre and $\mathrm{r}_{max}$. Each shell is taken to be one core radius thick, and we calculate the contribution from each formation mechanism in every shell. This is done by assuming a constant (average) density and velocity dispersion in each shell. Specifically, we estimated the density and velocity dispersion at the half-way point in each shell using our single-mass King models, and used these to set average values. The number of BSs expected to have

migrated into the core within the last $\tau_{BS}$ years can be written:

$$N_{in} = \sum_{i=2}^{N} \Big( f_{1+1} N_{(1+1),i} + f_{1+2} N_{(1+2),i} + f_{2+2} N_{(2+2),i} + f_{mt} N_{(bin),i} \Big) \times \Big( 1 - \frac{\tau_{(dyn),i}}{\tau_{BS}} \Big), \tag{5.11}$$

where $i = 1$ refers to the core, $i = 2$ refers to the shell immediately outside the core, etc. and N is taken to be the integer nearest to $\mathrm{r}_{max}/\mathrm{r}_c$. We let the terms with $\mathrm{N}_{(1+1),i}$, $\mathrm{N}_{(1+2),i}$, $\mathrm{N}_{(2+2),i}$ and $\mathrm{N}_{(bin),i}$ represent the number of BSs formed in shell $i$ from single-single collisions, single-binary collisions, binary-binary collisions and binary star evolution, respectively. The time-scale for dynamical friction in shell $i$ is denoted by $\tau_{(dyn),i}$, and the factor (1 - $\tau_{(dyn),i}/\tau_{BS}$) is included to account for the fact that we are assuming a constant formation rate for BSs, so that not every BS formed in shells outside the core will have sufficient time to fall in by the current cluster age.

It is typically the least massive stars that are ejected from 1+2 and 2+2 interactions as single stars (e.g. Sigurdsson & Phinney, 1993). Combined with conservation of momentum, this suggests that BSs are the least likely to be ejected from dynamical encounters with velocities higher than the central velocity dispersion due to their large masses. This has been confirmed by several studies of numerical scattering experiments (e.g. Hut, 1983; Fregeau et al., 2004). Based on this, we expect that $\mathrm{N}_{out}$ should be very small and so, as a first approximation, we take $\mathrm{N}_{out} = 0$. However, we also explore the effects of a non-zero $\mathrm{N}_{out}$ by assigning a kick velocity to all BSs at birth. If dynamical interactions play a role in BS formation, we might naturally expect BSs to be imparted a recoil velocity at birth (or shortly before) due to momentum conservation. We will return to this assumption in Section 5.4.

### 5.3.2 Statistical Comparison with Observations

Our model contains 4 free parameters, which correspond to the fraction of outcomes that produce a blue straggler for each formation mechanism (1+1 collisions, 1+2 collisions, 2+2 collisions, and binary star evolution). These are the $f$ values described in the previous section: $f_{1+1}, f_{1+2}, f_{2+2}, f_{mt}$. We assume that these values are constant throughout each cluster, and are also constant between clusters. By fitting the predictions of our model to the observational data, we can determine best-fit values for each of these $f$ parameters, and therefore make predictions about which blue straggler formation processes are more important.

In order to determine the best values for these $f$ parameters, we need an appropriate statistical test. For this, we follow the approach of Verbunt, Pooley & Bassa (2008). The number of BSs seen in the core of a globular cluster can be described by Poisson statistics. In particular, the probability of observing $N$ sources when $\mu$ are expected is:

$$P(N, \mu) = \frac{\mu^N}{N!} e^{-\mu} \tag{5.12}$$

We can calculate a probability for each cluster, and then calculate an overall probability $P'$ for the model by multiplying the individual $P$ values. We can then vary the $f$ values to maximize this value.

In practice, these $P$ values are typically of order ten percent per cluster, and with 35 clusters, the value of $P'$ quickly becomes extremely small. Therefore we chose to work with a modified version of this value: the deviance of our model to the saturated model. A saturated model is one in which the observed number of sources is exactly equal to the expected number in each

cluster. In other words, this is the best that we can possibly do. However, because of the nature of Poisson statistics, the probability $P$ of such a model (calculated by setting $N = \mu$ in Equation 5.12) is not equal to 1, but in fact has some smaller value. For the numbers of blue stragglers in our clusters, the $P$ values for the saturated model run from 0.044 to 0.149, and the value of $P'$ is $2.08 \times 10^{-41}$.

The deviance of any model from the saturated model is given by

$$D = 2.0(\ln(P'_{saturated}) - \ln(P'_{model})) \tag{5.13}$$

The model which minimizes this quantity will be our best-fit model. Ideally, the scaled deviance $(D/(N_{data} - N_{parameters})$ should be equal to 1 for a best fit. Given the simplicity of our model, we expect that our values will not provide this kind of agreement, and we simply look for the model which provides the minimum of the scaled deviance.

## 5.4 Results

In this section, we present the results of comparing our model predictions to the observations. After presenting the results for a constant core binary fraction for all clusters, we explore the implications of adopting a core binary fraction that depends on the cluster luminosity, as reported in Sollima et al. (2007) and Milone et al. (2008).

### 5.4.1 Initial Assumptions

The predictions of our model for our initial choice of assumptions are shown in Figure 5.1. These numbers are plotted against the total stellar mass in the core along with the number of BSs observed in the core (blue triangles). We plot both the total number of BSs predicted to have formed within $r_{max}$ in the last $\tau_{BS}$ years ($N_{BS}$ in Equation 5.1; green circles), as well as the total number formed only in the core ($N_{coll} + N_{bin}$; red circles). Upon comparing $N_{BS}$ to the observed number of BSs in the core, the best-fitting model parameters predict that most BSs are formed from binary star evolution, with a small contribution from 2+2 collisions being needed in order to obtain the best possible match to the observations. The ideal contribution from 2+2 collisions constitutes at most a few percent of the predicted total for most of the clusters in our sample. Even for our best-fitting model parameters, our initial choice of assumptions predicts too few BSs in clusters with small core masses.

### 5.4.2 Binary Fraction

We tried changing our assumption of a constant $f_b$ for all clusters to one for which the core binary fraction varies with the total cluster magnitude. First, we adopted a dependence of the form:

$$f_b = 0.13 M_V + 1.07, \tag{5.14}$$

where $M_V$ is the total cluster V magnitude. This relation comes from fitting a line of best-fit to the observations of Sollima et al. (2007), who studied the binary fractions in a sample of 13 low-density GCs (we calculated an average

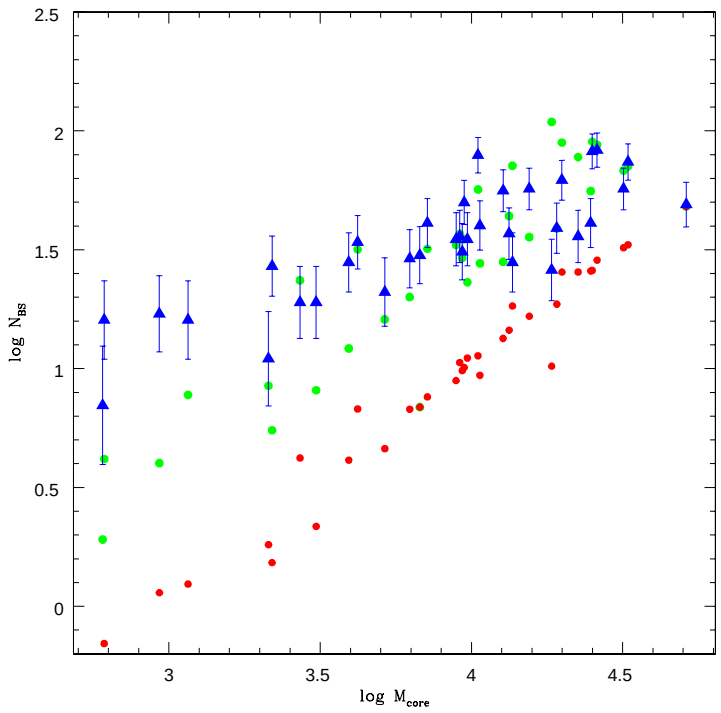



Figure 5.1 The predicted number of BSs plotted versus the total stellar mass in the core for the best-fitting model parameters found for our initial choice of assumptions. The filled blue triangles correspond to the observed numbers, the filled green circles to the number of BSs predicted to have formed within $r_{max}$, and the filled red circles to the number predicted to have formed in only the core. The best-fitting model parameters used to calculate the predicted numbers are $f_{1+1} = 0$, $f_{1+2} = 0$, $f_{2+2} = 7.3 \times 10^{-3}$, and $f_{mt} = 1.7 \times 10^{-3}$. Estimates for the total stellar masses in the core were obtained from single-mass King models, as described in Leigh, Sills & Knigge (2011). Error bars have been indicated for the observed numbers using Poisson statistics.

of columns 3 and 4 in their Table 3 and used these binary fractions to obtain Equation 5.14). In order to prevent negative binary fractions, we impose a minimum binary fraction of $f_b^{min} = 0.01$. In other words, we set $f_b = f_b^{min}$ if Equation 5.14 gives a binary fraction less than $f_b^{min}$. As before, we adopt an average semi-major axis of 2 AU. The results of this comparison are presented in Figure 5.2. As in Figure 5.1, both the numbers of observed (blue triangles)

and predicted (green circles) BSs in the core are plotted versus the total stellar mass in the core. Once again, the predicted numbers include all BSs formed within $r_{max}$ in the last $\tau_{BS}$ years. The best-fitting model parameters for this comparison suggest that both single-single collisions and binary star evolution are significant contributors to BS formation. Single-single collisions contribute up to several tens of a percent of the predicted total in several clusters. We obtain a deviance in this case that is significantly larger than that obtained for the best-fitting model parameters assuming a constant $f_b$ of 10% for all clusters. Equation 5.14 gives higher binary fractions in low-mass clusters relative to our initial assumption of a constant $f_b$. This increases the number of BSs formed from binary star evolution and improves the agreement between our model predictions and the observations in low-mass clusters. This is consistent with the results of Sollima et al. (2008). However, adopting Equation 5.14 for $f_b$ also causes our model to under-predict the number of BSs in several high-mass clusters.

The best fit to the observations is found by adopting the relation for $f_b$ provided in Equation 5.14 and setting $f_b^{min} = 0.1$ (however we note that a comparably good agreement is found with a slightly lower $f_b^{min} = 0.05$). This improves the agreement between our model predictions and the observations by increasing the number of BSs formed from binary star evolution in massive clusters. The result is a good agreement between our model predictions and the observations in both low- and high-mass cores, as shown in Figure 5.3. In this case, the best-fitting model parameters yield the lowest deviance of any of the assumptions so far considered. These best-fitting values suggest that most BSs are formed from binary star evolution, with a small contribution from 2+2 collisions being needed in order to obtain the best possible match

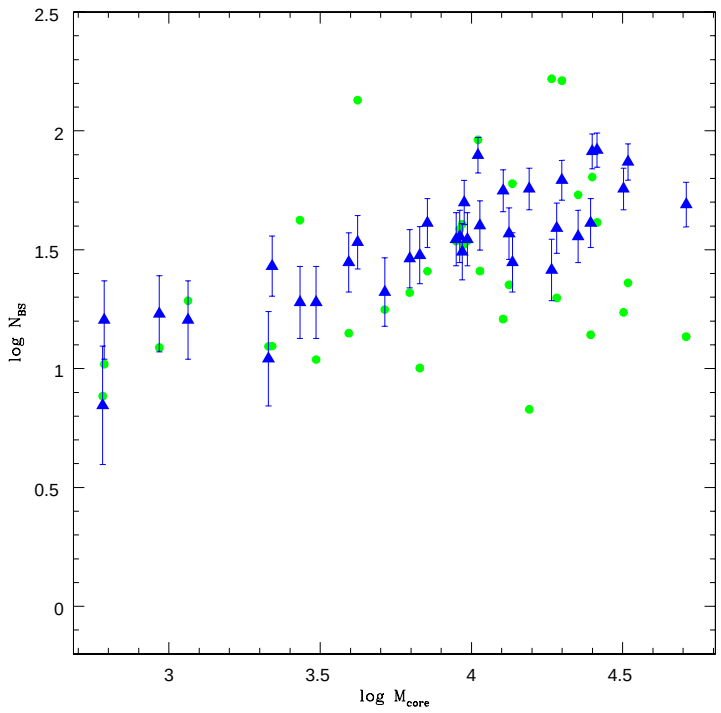



Figure 5.2 The number of BSs predicted in the cluster core using the binary fractions of Sollima et al. (2007) with $f_b^{min} = 0.01$ plotted against the total stellar mass contained within the core. The colours used to indicate the observed and predicted numbers are the same as in Figure 5.1. The predicted numbers correspond to the best-fitting model parameters, which are $f_{1+1} = 0.41$, $f_{1+2} = 0$, $f_{2+2} = 0$, and $f_{mt} = 1.5 \times 10^{-3}$.

to the observations. Similarly to what was found for our initial assumptions, the ideal contribution from 2+2 collisions constitutes at most a few percent of the predicted total for most of the clusters in our sample. On the other hand, if we change our imposed minimum binary fraction to $f_b^{min} = 0.05$ we find that a non-negligible (i.e. up to a few tens of a percent) contribution from single-single collisions is needed in several clusters to obtain the best possible agreement with the observations (which is very nearly as good as was found using $f_b^{min} = 0.1$). All of this shows that, although binary star

evolution consistently dominates BS formation in our best-fitting models, at least some contribution from collisions (whether it be 1+1 or 2+2 collisions, or some combination of 1+1, 1+2 and 2+2 collisions) also consistently improves the agreement with the observations. Moreover, it is interesting to note that an improved agreement with the observations could alternatively be obtained if we keep $f_b^{min} = 0.01$ but all or some of $f_{1+1}$, $f_{1+2}$ and $f_{2+2}$ increase with increasing cluster mass. This would also serve to improve the agreement at the high-mass end. We will return to this in Section 5.5.

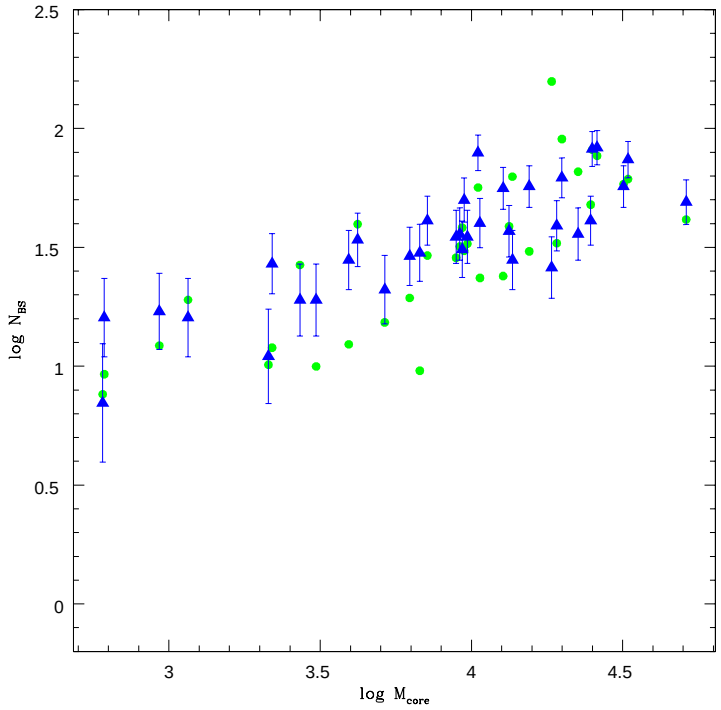



Figure 5.3 The number of BSs predicted in the cluster core using the binary fractions of Sollima et al. (2007) with $f_b^{min} = 0.1$ plotted against the total stellar mass contained within the core. The colours used to indicate the observed and predicted numbers are the same as in Figure 5.1. The predicted numbers correspond to the best-fitting model parameters, which are $f_{1+1} = 0$, $f_{1+2} = 0$, $f_{2+2} = 3.6 \times 10^{-3}$, and $f_{mt} = 1.4 \times 10^{-3}$.

Finally, we also tried adopting the observed dependence of $f_b$ on $M_V$ reported in Milone et al. (2008), who also found evidence for an anti-correlation between the core binary fraction and the total cluster mass. Despite this change, we consistently find that our results are the same as found when using the empirical binary fraction relation provided in Equation 5.14.

### 5.4.3 Average BS Lifetime

We also tried changing our assumption for the average BS lifetime. We explored a range of plausible lifetimes based on values found throughout the literature. Specifically, we explored the range 0.5-5 Gyrs. We find that at the low end of this range, our model fits become increasingly poor. This is because lower values for $\tau_{BS}$ correspond to smaller values for $r_{max}$ and decrease the term (1 - $t_{(dyn),i}/\tau_{BS}$) in Equation 5.11. This reduces the contribution to the total predicted numbers from BSs formed outside the core that fall in via dynamical friction. Conversely, our model fits improve for $\tau_{BS} > 1.5$ Gyrs since this corresponds to a larger contribution to $N_{BS}$ from $N_{in}$. It is important to note, however, that this same effect can be had by increasing the number of BSs formed outside the core, since this would also serve to increase $N_{in}$ in Equation 5.1. This can be accomplished by, for instance, increasing the binary fraction outside the core (which would increase the number of BSs formed from binary star evolution outside the core that migrate in due to dynamical friction) relative to inside the core. This seems unlikely, however, given that observations of low-density globular clusters and open clusters suggest that their binary fractions tend to drop off rapidly outside the core (e.g. Sollima et al., 2007). We will return to this issue in Section 5.5.

The best possible match to the observations is found by adopting an average BS lifetime of 5 Gyrs along with the relation for $f_b$ provided in Equation 5.14 with $f_b^{min} = 0.1$. The predictions of our model are shown in Figure 5.4 for these best-fitting model parameters. As shown, the agreement between our model predictions and the observed numbers is excellent. The best agreement is found by adopting an average BS lifetime of 5 Gyrs, however the agreement is comparably excellent down to slightly less than $\tau_{BS} \sim 3$ Gyrs. Although increasing $\tau_{BS}$ does contribute to improving the agreement between our model predictions and the observations, the effect is minor compared to the improvement that can be found by changing our assumption for the binary fraction. This is apparent upon comparing Figure 5.4 to Figure 5.3.

### 5.4.4 Migration

In order to explore the sensitivity of our results to our assumption for $r_{max}$, we also tried setting $N_{in}$ equal to the total number of BSs expected to form within 10 $r_c$ for all clusters. For comparison, for an average BS lifetime of $\tau_{BS} = 1.5$ Gyrs, $r_{max}$ ranges from 2 - 15 $r_c$ for the clusters in our sample. Despite implementing this change, our results remained the same. This is because the largest contribution to the total number of BSs comes from those BSs formed in the first few shells immediately outside the core that migrate in due to dynamical friction.

Several GCs have been reported to show evidence for a decrease in their binary fractions with increasing distance from the cluster centre (e.g. Sollima et al., 2007; Davis et al., 2008). This effect is often significant, with binary fractions decreasing by up to a factor of a few within only a few core

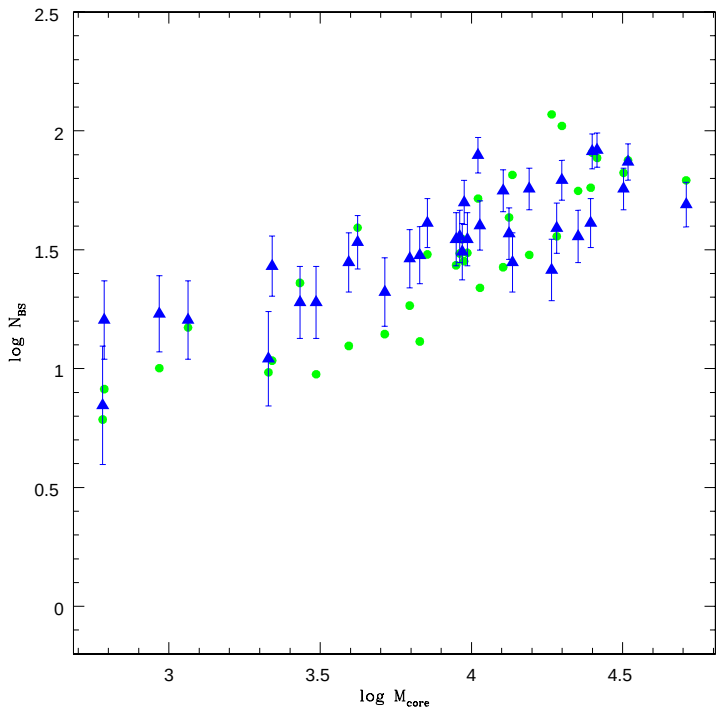



Figure 5.4 The predicted number of BSs plotted versus the total stellar mass in the core for the best-fitting model parameters found using an average BS lifetime of 5 Gyrs and the relation for the cluster binary fraction provided in Equation 5.14 with $f_b^{min} = 0.1$. The colours used to indicate the observed and predicted numbers are the same as in Figure 5.1. The best-fitting model parameters used to calculate the predicted numbers are $f_{1+1} = 0$, $f_{1+2} = 0$, $f_{2+2} = 1.6 \times 10^{-3}$, and $f_{mt} = 9.9 \times 10^{-4}$. The agreement with the observations is excellent for these best-fitting values.

radii from the cluster centre. Based on this, our assumption that $f_b$ is independent of the distance from the cluster centre likely results in an over-estimate of the true binary fraction at large cluster radii. In order to quantify the possible implications of this for our results, we tried setting $f_b = 0$ for all shells outside the core. Although this assumption is certainly an under-estimate for the true binary fraction outside the core, our results remain the same (albeit the agreement with the observations is considerably worse than for most of

our previous model assumptions). Once again, the best-fitting model parameters suggest that most BSs are formed from binary star evolution, with a non-negligible (i.e. up to a few tens of a percent in some clusters) contribution from binary-binary collisions. Our results indicate that, if the binary fraction is negligible outside the core, then the contribution from BSs that migrate into the core due to dynamical friction is also negligible. This is because the time between 1+1 collisions increases rapidly outside the core, and every other BS formation mechanism requires binary stars to operate.

We also explored the effects of assuming a non-zero value for $N_{out}$ in Equation 5.1 by imparting a constant kick velocity to all BSs at birth. Using conservation of energy, we calculated the cluster radius to which BSs should be kicked upon formation, and used the time-scale for dynamical friction at the kick radius to calculate the fraction of BSs expected to migrate back into the core within a time $\tau_{BS}$. Regardless of our assumption for the kick velocity, this did not improve the deviance for any of our best-fitting model parameters.

### 5.4.5 Average Binary Semi-Major Axis

We investigated the dependence of our results on our assumption for the average binary semi-major axis. However, this had a very small effect on our results. This is because only $N_{1+2}$ and $N_{2+2}$ depend on the average semi-major axis, and neither of these terms dominated BS production regardless of our model assumptions. Only $f_{2+2}$ is non-zero for our best-fitting models however, as before, it consistently suggests that far fewer BSs should be formed from 2+2 collisions than from binary star evolution.

## 5.5 Summary & Discussion

In this chapter, we have presented an analytic model to investigate BS formation in globular clusters. Our model predicts the number of BSs in the cluster core at the current cluster age by estimating the number that should have either formed there from stellar collisions and binary star evolution, or migrated in via dynamical friction after forming outside the core. We have compared the results of our model predictions for a variety of input parameters to observed BS numbers in 35 GCs taken from the catalogue of Leigh, Sills & Knigge (2011).

What has our model told us about BS formation in dense cluster environments? The agreement between the predictions of our model and the observations is excellent if we assume that:

- Binary star evolution dominates BS formation, however at least some contribution from 2+2 collisions (most of which occur in the core) must also be included in the total predicted numbers. Although it is clear that including a contribution from dynamical encounters gives the best possible match to the observations, it is not clear how exactly this is accomplished in real star clusters. Does the cluster dynamics increase BS numbers via direct collisions? Or do dynamical interactions somehow modify primordial binaries to initiate more mass-transfer events? We will return to this point below.

- The binary fraction in the core is inversely correlated with the total cluster luminosity, similar to the empirical relations found by Sollima et al. (2007) and Milone et al. (2008). We also require a minimum core binary

fraction of $5 - 10\%$. The inverse dependence of $f_b$ on the total cluster mass contributes to a better agreement with the observations at the low-mass end of the distribution of cluster masses, whereas the imposed condition that $f_b^{min} = 0.05 - 0.1$ contributes to improving the agreement at the high-mass end.

- BSs formed outside the core that migrate in by the current cluster age contribute to the total predicted numbers.

- The average BS lifetime is roughly a few ($\sim$ 3-5) Gyrs, since this increases the fraction of BSs formed outside the core that will have sufficient time to migrate in due to dynamical friction.

Our model can only provide a reasonable fit to the observations for all cluster masses if we assume that the cluster binary fraction is inversely proportional to the total cluster mass. It is interesting to consider the possibility that such an inverse proportionality could arise as a result of the fact that the rate of two-body relaxation is also inversely proportional to the cluster mass (Spitzer, 1987). Consequently, since binaries tend to be the most massive objects in GCs, they should quickly migrate into the core in low-mass clusters, contributing to an increase in the core binary fraction over time (Fregeau, Ivanova & Rasio, 2009). This process should operate on a considerably longer time-scale in very massive GCs since the time-scale for two-body relaxation is very long. Mass segregation could then contribute to the observed sub-linear dependence of BS numbers on the core masses by acting to preferentially migrate the binary star progenitors of BSs into the cores of low-mass clusters. This is one example of how a direct link could arise between the observed properties of BS populations and the dynamical histories of their host

clusters. Although this scenario is interesting to consider, we cannot rule out the possibility that an anti-correlation between the core binary fraction and the total cluster mass could be a primordial property characteristic of GCs at birth.

When interpreting our results, it is important to bear in mind that binary star evolution and dynamical interactions involving binaries may not always contribute to BS formation independently. For example, dynamics could play an important role in changing the distribution of binary orbital parameters so that mass-transfer occurs more commonly in some clusters. One way to perhaps compensate for this effect would be to include a factor of $1/a$ (where $a$ is the average binary semi-major axis) in Equation 5.9. This would serve to account for the fact that we might naively expect clusters populated by more close binaries to be more likely to have a larger fraction of their binary populations undergo mass-transfer. This does not, however, guarantee that more BSs will form since our poor understanding of binary star evolution prevents us from being able to predict the outcomes of these mass-transfer events, and whether or not they will form BSs. Moreover, little is known about the distribution of orbital parameters characteristic of the binary populations in globular clusters, and how they are typically modified by the cluster dynamics. For these reasons, the interpretation of our results must be done with care in order to ensure that reliable conclusions can be drawn.

In general, our results suggest that binary stars play a crucial role in BS formation in dense GCs. In order to obtain the best possible agreement with the observations, an enhancement in BS formation from dynamical encounters is required in at least some clusters relative to what is expected by assuming a simple population of binaries evolving in isolation. It is not

clear from our results, however, how exactly this occurs in real star clusters. Dynamics could enhance BS formation directly by causing stellar collisions, or this could also occur indirectly if the cluster dynamics somehow induces episodes of mass-transfer by reducing the orbital separations of binaries. But in which clusters is BS formation the most strongly influenced by the cluster dynamics? Unfortunately, no clear trends have emerged from our analysis that provide a straight-forward answer to this question. However, our results are consistent with dynamical interactions playing a more significant role in more massive clusters (although this does not imply that the cluster dynamics does not also contribute in low-mass clusters). This could be due to the fact that more massive clusters also tend to have higher central densities (e.g. Djorgovski & Meylan, 1994), and therefore higher collision rates. This picture is, broadly speaking, roughly consistent with the results of Davies, Piotto & De Angeli (2004). These authors considered the observed dependence (or lack thereof) of BS numbers on the total cluster masses presented in Piotto et al. (2004), and suggested that primordial binary evolution and stellar collisions dominate BS production in low- and high-mass clusters, respectively.

Our model neglects the dynamical evolution of GCs and the resulting changes to their global properties, including the central density, velocity dispersion, core radius and binary fraction. As a young cluster evolves, dynamical processes like mass segregation and stellar evaporation tend to result in a smaller, denser core. Within a matter of a few half-mass relaxation times, a gravothermal instability has set in and the collapse ensues on a time-scale determined by the rate of heat flow out of the core (e.g. Spitzer, 1987). We are focussing on the last $\tau_{BS}$ years of cluster evolution, a sufficiently late pe-

riod in the lives of most GCs that gravothermal collapse will have long since taken over as the primary driving force affecting the stellar concentration in the core. Most of the GCs in our sample should currently be in a phase of core contraction (Fregeau, Ivanova & Rasio, 2009; Gieles, Heggie & Zhao, 2011), and their central densities and core radii should have been steadily decreasing over the last $\tau_{BS}$ years. Therefore, by using the currently observed central cluster parameters and assuming that they remained constant over the last $\tau_{BS}$ years, we have effectively calculated upper limits for the encounter rates. This could suggest that we have over-estimated the importance of dynamical interactions for BS formation. On the other hand, some theoretical models of GC evolution suggest that the hard binary fraction in the core of a dense stellar system will generally increase with time (e.g. Hurley et al., 2005; Fregeau, Ivanova & Rasio, 2009). This can be understood as an imbalance between the migration of binaries into the core via mass segregation and the destruction of binaries in the core via both dynamical encounters and their internal evolution. This could suggest that our estimate for the number of BSs formed from binary star evolution should also be taken as an upper limit. The key point is that GC evolution can act to increase the number of BSs in the cluster core via several different channels. The effects we have discussed should typically be small, however, since $\tau_{BS}$ is much shorter than the cluster age (De Angeli et al., 2005) and any changes to global cluster properties that occur during this time will often be small.

Our model adopts the same values for all free parameters in all clusters. In particular, this is the case for several global cluster properties, including the average stellar mass, the average BS mass, the average BS lifetime, and the average binary semi-major axis. With the exception of the average stellar mass,

there is no conclusive observational or theoretical evidence to indicate that these parameters should differ from cluster-to-cluster, although we cannot rule out this possibility. For instance, the distribution of binary orbital parameters could depend on cluster properties like the total mass, density or velocity dispersion (e.g. Sigurdsson & Phinney, 1993). In particular, the central velocity dispersion should be higher in more massive GCs (e.g. Djorgovski & Meylan, 1994), which should correspond to a smaller binary orbital separation for the hard-soft boundary. This could contribute to massive GCs tending to have smaller average binary orbital separations since soft binaries should not survive for long in the dense cores of GCs (e.g. Heggie & Hut, 2003). In turn, this could affect the occurrence of mass-transfer events, or of mergers during 1+2 and 2+2 encounters. This last point follows from the fact that numerical scattering experiments have shown that the probability of mergers occurring during 1+2 and 2+2 interactions increases with decreasing binary orbital separation (e.g. Fregeau et al., 2004). Both the average stellar mass and the average BS mass (and hence lifetime) could also depend on the total cluster mass, as discussed in Leigh, Sills & Knigge (2009) and Leigh, Sills & Knigge (2011).

We have also neglected to consider the importance of triples for BS formation throughout our analysis (e.g. Perets & Fabrycky, 2009) since we are unaware of any observations of triples in GCs in the literature. Interestingly, however, our results for binary star evolution can be generalized to include the internal evolution of triples since they should have the same functional dependence on the core mass (i.e. $N_{te} \propto f_t M_{core}$, where $N_{te}$ is the number of BSs formed from triple star evolution and $f_t$ is the fraction of objects that are triples).

Finally, our model assumes that several parameters remain constant as a function of the distance from the cluster centre, including the binary fraction and the average semi-major axis. However, observations of GCs suggest that their binary fractions could fall off rapidly outside the core (e.g. Sollima et al., 2007; Davis et al., 2008). Our results suggest that, if the binary fraction is negligible outside the core, then the contribution from BSs that migrate into the core due to dynamical friction is also negligible. This is because the time between 1+1 collisions increases rapidly outside the core, and every other BS formation mechanism requires binary stars to operate. On the other hand, the presently observed binary fraction outside the core could be low as a result of binaries having previously migrated into the core due to dynamical friction (e.g. Fregeau, Ivanova & Rasio, 2009). If these are the binary star progenitors of the BSs currently populating the core, then dynamical friction remains an important effect in determining the number of BSs currently populating the core.

Despite all of these simplifying assumptions, we have shown that our model can reproduce the observations with remarkable accuracy. Notwithstanding, the effects we have discussed could be contributing to cluster-to-cluster differences in the observed BS numbers. Our model provides a well-suited resource for addressing the role played by these effects, however future observations will be needed in order to obtain the desired constraints (e.g. binary fractions, distributions of binary orbital parameters, etc.).

# Acknowledgments

We would like to thank Ata Sarajedini, Aaron Dotter and Roger Cohen for providing the observations to which we compared our model predictions, as well as for providing a great deal of guidance in analyzing the data. We would also like to thank Evert Glebbeek, Bob Mathieu and Aaron Geller for useful discussions. This research has been supported by NSERC and OGS.

# Bibliography

Anderson J., Sarajedini A., Bedin L. R., King I. R., Piotto G., Reid I. N., Siegel M., Majewski S. R., Paust N. E. Q., Aparicio A., Milone A. P., Chaboyer B., Rosenberg A. 2008, AJ, 135, 2055

Andrievsky S. M., Schonberner D., Drilling J. S. 2000, A&A, 356, 517

Bacon D., Sigurdsson S., Davies M. B. 1996, MNRAS, 281, 830

Binney J., Tremaine S. 1987, Galactic Dynamics (Princeton: Princeton University Press)

Cool A. M., Bolton A. S. 2002, in ASP Conference Series 263, Stellar Collisions, Mergers and their Consequences, ed. M. M. Shara (San Francisco: ASP), 163

Davies M. B., Piotto G., De Angeli F. 2004, MNRAS, 348, 129

Davis D. S., Richer H. B., Anderson J., Brewer J., Hurley J., Kalirai J. S., Rich R. M., Stetson P. B. 2008, AJ, 135, 2155

De Angeli F., Piotto G., Cassisi S., Busso G., Recio-Blanco A., Salaris M., Aparicio A., Rosenberg A. 2005, AJ, 130, 116

Dervisoglu A., Tout C. A., Ibanoglu C. 2010, MNRAS, 406, 1071

Djorgovski S., Meylan G. 1994, ApJ, 108, 1292

Ferraro F. R., Paltrinieri B., Fusi Pecci F., Cacciari C., Dorman B., Rood R. T., Buonanno R., Corsi C. E., Burgarella D., Laget M. 1997, A&A, 324, 915

Ferraro F. R., Paltrinieri B., Rood R. T., Dorman B. 1999, ApJ, 522, 983

Ferraro F. R., Beccari G., Rood, R. T., Bellazzini M., Sills A., Sabbi E. 2004, ApJ, 603, 127

Fregeau J. M., Cheung P., Portegies Zwart S. F., Rasio F. A. 2004, MNRAS, 352, 1

Fregeau J. M., Ivanova N., Rasio F. A. 2009, ApJ, 707, 1533

Geller A. M., Mathieu R. D., Harris H. C., McClure R. D., 2009, AJ, 137, 3743

Gieles M., Heggie D., Zhao H. 2011, MNRAS, accepted

Glebbeek E., Pols O. R. 2008, A&A, 488, 1017

Guhathakurta P., Webster Z. T., Yanny B., Schneider D. P., Bahcall J. N. 1998, AJ, 116, 1757

Harris W. E. 1996, AJ, 112, 1487; 2010 update

Heggie D. C., Hut P. 2003, The Gravitational Million-Body Problem: A Multidisciplinary Approach to Sar Cluster Dynamics (Cambridge: Cambridge University Press)

Hurley J. R., Pols O. R., Aarseth S. J., Tout C. A. 2005, MNRAS, 363, 293

Hurley J. R., Aarseth S. J., Shara M. M. 2007, ApJ, 665, 707

Hut P., Bahcall J. N. 1983, ApJ, 268, 319

Iben I. Jr. 1991, ApJS, 76, 55

Ivanova N., Belczynski K., Fregeau J. M., Rasio F. A. 2005, MNRAS, 358, 572

King I. R., Sosin C., Cool A. M. 1995, ApJ, 452, L33

Knigge C., Leigh N., Sills A. 2009, Nature, 457, 288

Latham D. W., 2005, Highlights of Astronomy, 14, 444

Lanzoni B., Dalessandro E., Perina S., Ferraro F. R., Rood R. T., Sollima A. 2007, ApJ, 670, 1065

Leigh N. W., Sills A., Knigge C. 2007, ApJ, 661, 210

Leigh N. W., Sills A., Knigge C. 2008, ApJ, 678, 564

Leigh N. W., Sills A., Knigge C. 2009, MNRAS, 399, L179

Leigh N. W., Sills A. 2011, MNRAS, 410, 2370

Leigh N. W., Sills A., Knigge C. 2011, MNRAS, accepted

Leonard P. J. T. 1989, AJ, 98, 217

Leonard P. J. T., Linnell A. P. 1992, AJ, 103, 1928

Leonard P. J. T., Livio M. 1995, ApJ, 447, L121

Li L., Zhang F. 2006, MNRAS, 369, 2001

Lombardi J. C., Warren J. S., Rasio F.A., Sills A., Warren A. R. 2002, ApJ, 568, 939

Mapelli M., Sigurdsson S., Colpi M., Ferraro F. R., Possenti A., Rood R. T., Sills A., Beccari G. 2004, ApJ, 605, L29

Mapelli M., Sigurdsson S., Ferraro F. R., Colpi M., Possenti A., Lanzoni B. 2006, MNRAS, 373, 361

Mathieu R. D., Geller A. R. 2009, Nature, 462, 1032

McCrea W. H. 1964, MNRAS, 128, 147

McLaughlin D. E., van der Marel R. P. 2005, ApJS, 161, 304

McMillan S. L. W. 1986, ApJ, 306, 552

Milone A. P., Piotto G., Bedin L. R., Sarajedini A. 2008, MmSAI, 79, 623

Piotto G., De Angeli F., King I. R., Djorgovski S. G., Bono G., Cassisi S., Meylan G., Recio-Blanco A., Rich R. M., Davies M. B. 2004, ApJ, 604, L109

Perets H. B., Fabrycky D. C. 2009, ApJ, 697, 1048

Rubenstein E. P., Bailyn C. D. 1997, ApJ, 474, 701

Sandage A. R. 1953, AJ, 58, 61

Sandquist E. L., Bolte M., Hernquist L. 1997, ApJ, 477, 335

Sarajedini A., Bedin L. R., Chaboyer B., Dotter A., Siegel M., Anderson J., Aparicio A., King I., Majewski S., Marin-Franch A., Piotto G., Reid I. N., Rosenberg A., Steven M. 2007, AJ, 133, 1658

Sigurdsson S., Phinney E. S. 1993, ApJ, 415, 631

Saviane I., Piotto G., Fagotto F., Zaggia S., Capaccioli M., Aparicio A. 1998, A&A, 333, 479

Shara M. M., Drissen L., Bergeron L. E., Paresce F. 1995, ApJ, 441, 617

Shara M. M., Saffer R. A., Livio M. 1997, ApJ, 489, L59

Sills A., Bailyn C. D. 1999, ApJ, 513, 428

Sills A. R., Faber J. A., Lombardi J. C., Rasio F. A., Waren A. R. 2001, ApJ, 548, 323

Sollima A., Beccari G., Ferraro F. R., Fusi Pecci F., Sarajedini A. 2008, MNRAS, 380, 781

MN-11-0613-MJ Sollima A., Beccari G., Ferraro F. R., Fusi Pecci F., Sarajedini A. 2007, A&A, 481, 701

Spitzer L. Jr. 1969, ApJ, 168, L139

Spitzer L. 1987, Dynamical Evolution of Globular Clusters (Princeton: Princeton University Press)

Stryker L. L. 1993, PASP, 105, 1081

van den Berg M., Orosz J., Verbunt F., Stassun K. 2001, A&A, 375, 375

Verbunt F., Pooley D., Bassa C. 2008, IAU Symposium 246, 301

Webbink R. F. 1985, in Dynamics of Star Clusters, IAU Symp. 113, ed. J. Goodman & P. Hut (Dordrecht: Reidel), 541

Chapter 6

# A New Quantitative Method for Comparing the Stellar Mass Functions in a Large Sample of Star Clusters: Evidence for a Universal Initial Mass Function in Massive Star Clusters in the Early Universe

## 6.1 Introduction

It is now known that most, if not all, of the stars in our Galaxy were born in star clusters (e.g. Lada & Lada, 1995, 2003; McKee & Ostriker, 2007). And

yet, there remain several key details of the star formation process that are still not understood. Part of the problem lies in the fact that populations of young stars are typically hidden by a dense veil of optically-thick gas and dust. This prevents the escape of most of the light produced by infant stars, and often renders these regions difficult to observe (e.g. Grenier, Casandijan & Terrier, 2005; Lada, Alves & Lombardi, 2007). Most of these clusters are sparsely populated and are of relatively low mass ($M \lesssim 10^4$ $M_\odot$) (e.g. Lada, 1985). They are also very young since these clusters are unlikely to survive for more than 1 Gyr (e.g. Portegies Zwart, McMillan & Gieles, 2010). At the other end of the mass spectrum, most massive star clusters ($M \gtrsim 10^4$ $M_\odot$) in our Galaxy tend to be at least a few Gyrs old, and in many cases are nearly as old as the Universe itself (e.g. Harris, 1996, 2010 update; De Angeli et al., 2005). Unfortunately, the conditions present at the time of their formation have been largely erased (e.g. Hurley et al., 2005; Murray, 2009). This presents a considerable challenge for studying star formation in the regime of cluster masses and metallicities that characterize Milky Way globular clusters. These old star clusters contain the fossil record of a very early episode of star formation in the Universe, and are the only means of studying it locally.

One of the primary observational tests for star formation theories is the stellar initial mass function (IMF). Current observational evidence suggests that the IMF is very similar in several different regions of our Galaxy, including the disk and young star clusters (e.g. Elmegreen, 1999), however this is still being debated throughout the literature (e.g. Scalo, 1998). The arguably "standard" IMF to come from these observations is that of Kroupa (2001), who fit a three-part power-law with breaks at 0.08 $M_\odot$ and 0.5 $M_\odot$.

This can be expressed as:

$$\frac{dN}{dlm} = \beta m^{-\alpha}, \tag{6.1}$$

where $\alpha$ is a constant given by $\alpha = 2.3$ for $0.5 < m/\mathrm{M}_{\odot} < 50$, $\alpha = 1.3$ for $0.08 < m/\mathrm{M}_{\odot} < 0.5$, and $\alpha = 0.3$ for $0.01 < m/\mathrm{M}_{\odot} < 0.08$, and $\beta$ is a constant determined by the total cluster mass. By considering the mass function up to only $\sim 1$ $\mathrm{M}_{\odot}$, Miller & Scalo (1979) found a good fit to the observed mass distribution using a log-normal functional form:

$$\frac{dN}{dlnm} \propto exp\Big[ - \frac{(lnm - lnm_c)^2}{2\sigma^2}\Big], \tag{6.2}$$

where $\mathrm{m}_c \sim 0.2$ $\mathrm{M}_{\odot}$ and $\sigma \sim 0.55$ (Chabrier, 2005).

Different star formation theories tend to predict different IMFs. These tend to vary with the properties of the gas clouds from which the stars are born (e.g. Elmegreen, 2001; Bonnell, Larson & Zinnecker, 2007). Given the sensitive nature of the observations, a large sample of IMFs spanning the entire range of cluster properties exhibited by star clusters in the Milky Way, including total mass and chemical composition, has yet to be compiled. This is a sorely needed step in order to advance our understanding of star formation by providing direct comparisons for theoretical predictions. This is especially true of massive ($\mathrm{M} \gtrsim 10^4$ $\mathrm{M}_{\odot}$), metal-poor star clusters since we are particularly lacking observations of IMFs in this regime of cluster masses and metallicites, especially in our own Galaxy (e.g. McKee & Ostriker, 2007; Portegies Zwart, McMillan & Gieles, 2010).

For the very first time, the ACS Survey for Globular Clusters has provided photometry that is nearly reliable all the way down to the hydrogen

burning limit in a large sample of Milky Way globular clusters. This offers a large sample of current stellar mass functions spanning the stellar mass range $\sim 0.2 - 0.8$ $M_{\odot}$. All of the clusters are massive and of very old age, with total masses and ages ranging from $\sim 10^4$ - $10^6$ $M_{\odot}$ and $\sim$ 10-12 Gyrs, respectively (Harris, 1996, 2010 update; De Angeli et al., 2005). This has allowed significant time for their stellar mass functions to have been modified from their primordial forms due to both stellar evolution and stellar dynamics. However, most of the processes responsible for this evolution are now largely understood. Therefore, in principle, it is possible to use current observations of old star clusters together with theoretical models for their evolution to indirectly probe their IMFs.

For most of the life of a star cluster, two-body relaxation is the dominant physical mechanism driving its evolution (e.g. Heggie & Hut, 2003; Gieles, Heggie & Zhao, 2011). The term describes the cumulative effects of long-range gravitational interactions that occur between pairs of stars, which act to alter their orbits within the cluster. Two-body relaxation also acts to slowly modify the distribution of stellar masses within clusters. Among other things, it results in a phenomenon known as mass segregation. This is the tendency for heavier stars to accumulate in the central cluster regions and low-mass stars to be dispersed to wider orbits. This same process also causes the continual escape of preferentially low-mass stars from the cluster, which has been confirmed to occur observationally in real star clusters (e.g. von Hippel & Sarajedini, 1998; De Marchi, Paresce & Portegies Zwart, 2010).

The time-scale for two-body relaxation to operate can range anywhere from several million years to the age of the Universe or longer. The rate at which it occurs can be roughly approximated using the half-mass relaxation

time, which provides a rough average for the entire cluster. This is given by (Spitzer, 1987):

$$t_{rh} = 1.7 \times 10^5 [r_h(pc)]^{3/2} N^{1/2} [m/M_\odot]^{-1/2} years, \tag{6.3}$$

where $r_h$ is the half-mass radius (i.e. the radius enclosing half the mass of the cluster), $N$ is the total number of stars within $r_h$ and $m$ is the average stellar mass. The half-mass radii of MW GCs are remarkably similar independent of mass, and simulations have shown that $r_h$ changes by a factor of at most a few over the course of a cluster's lifetime (Henon, 1973; Murray, 2009). The GCs that comprise the ACS sample show a range of masses spanning roughly 3 orders of magnitude ($10^4$-$10^6$ $M_\odot$), and have comparably old ages ($\sim$ 10-12 Gyrs) (De Angeli et al., 2005). Therefore, Equation 6.3 suggests that the total cluster mass provides a rough proxy for the degree of dynamical evolution (due to two-body relaxation). In other words, the effects of two-body relaxation on the evolution of the stellar mass function should be the most pronounced in the least massive clusters in the ACS sample. Said another way, dynamical age increases with decreasing cluster mass.

In this chapter, we present a new technique to quantify cluster-to-cluster variations in the observed stellar mass functions of a large sample of clusters spanning a diverse range of properties. Our sample consists of 33 Milky Way globular clusters taken from the ACS Survey for Globular Clusters (Sarajedini et al., 2007). With it, we constrain the universality of the IMF in a large sample of old, metal-poor star clusters spanning a wider range of masses than ever before considered. In Section 6.2, we present our sample of stellar mass functions and describe our technique. The results of our analysis

of the ACS observations are presented in Section 6.3. Finally, we discuss the implications of our results for the universality of the stellar IMF in Section 6.4, and describe how our results can be compared to theoretical models for GC evolution.

## 6.2 Method

In this section, we describe how we acquire our sample of mass functions from the ACS data.

### 6.2.1 The Data

The data used in this study consists of a sample of 33 MW GCs taken from the ACS Survey for Globular Clusters (Sarajedini et al., 2007).[1] The ACS Survey provides unprecedented deep photometry in the F606W ($\sim$ V) and F814W ($\sim$ I) filters that is nearly complete down to $\sim 0.2$ $M_{\odot}$. In other words, the colour-magnitude diagrams (CMDs) extend reliably from the HB all the way down to about 7 magnitudes below the main-sequence turn-off (MSTO).

Each cluster was centred in the ACS field, which extends out to several core radii from the cluster centre in most clusters. Coordinates for the cluster centres were taken from Goldsbury et al. (2010). These authors found their centres by fitting a series of ellipses to the density distributions within the inner 2' of the cluster centre, and computing an average value. The core radii were taken from Harris (1996, 2010 update).

[1]The data can be found at http://www.astro.ufl.edu/ ata/public_hstgc/.

### 6.2.2 Mass Bin Selection Criteria

In order to select the number of stars belonging to each mass bin, we fit theoretical isochrones taken from Dotter et al. (2007) to the CMDs of every cluster in our sample. Each isochrone was generated using the metallicity and age of the cluster, and fit to its CMD using the corresponding distance modulus and extinction provided in Dotter et al. (2010). The MSTO was then defined using our isochrone fits by selecting the bluest point along the MS.

We considered five mass bins along the main-sequence. These ranged from 0.25 - 0.75 $M_{\odot}$ in increments of 0.1 $M_{\odot}$. This range was chosen to ensure complete sampling in all bins since the lowest MSTO mass in our sample corresponds to $\sim 0.75$ $M_{\odot}$, and the photometric errors remain small ($\lesssim 0.05$ mag) within the corresponding magnitude range for each cluster. We have obtained number counts for all mass bins within the core, as well as for within two and three core radii. We do not consider circles outside this since the spatial coverage becomes incomplete for several clusters. This greatly reduces our sample size and causes the statistical significance of our analysis to suffer.

We have obtained completeness fractions for each mass bin in all three annuli for every cluster in our sample. This was done using the results of artificial star tests taken from Anderson et al. (2008).[2] Number counts for each mass bin were then multiplied by their corresponding completeness corrections. The field of view of the ACS images is about 200" on a side, which gives physical scales ranging between 1.5 and 16 pc (for the closest and furthest clusters in our sample). Based on this, we expect foreground contamination by field stars to be negligible for most of the clusters in our sample given their

[2]Artificial star tests were obtained directly from Ata Sarajedini via private communication.

current locations in the Galaxy. For example, Da Costa (1982) considered star count data in a similar area and over a comparable range of stellar masses for three nearby globular clusters. The author found that the corrections resulting from field contamination were always less than 10% over nearly the entire range of stellar masses we are considering.

### 6.2.3 Weighted Lines of Best-Fit

In order to quantify cluster-to-cluster differences in the current stellar mass functions of the clusters in our sample, we have obtained lines of best-fit for (the logarithm of) the number of stars belonging to each mass bin versus (the logarithm of) the total number of stars spanning all five mass bins (which provides a rough proxy for the total cluster mass). These lines have been weighted by adopting uncertainties for the number of stars in each mass bin using Poisson statistics. We have performed this comparison for all three circles (i.e. within one, two and three core radii). Our motivation for adopting this technique is as follows. If the fraction of stars belonging to each mass bin (relative to the total number of stars in all five mass bins), which we denote by $f_{m_1-m_2}$, is constant for all cluster masses, then we would expect the number of stars in each mass bin $N_{m_1-m_2}$ to scale linearly with the total number of stars spanning all five mass bins $N_{tot}$ (since $f_{m_1-m_2} = N_{m_1-m_2}/N_{tot}$). However, if there is any systematic dependence of $f_{m_1-m_2}$ on the total cluster mass, then we should find that $N_{m_1-m_2}$ does *not* scale linearly with $N_{tot}$. In particular, the power-law index for a given mass bin should be sub-linear if the fraction of stars belonging to that mass bin systematically decreases with increasing cluster mass. Conversely, the power-law index for a given

mass bin should be super-linear if the fraction of stars belonging to that mass bin systematically increases with increasing cluster mass. The slopes and y-intercepts corresponding to the weighted lines of best-fit for each mass bin provide a means of directly quantifying the number of stars belonging to each mass bin as a function of the total cluster mass. In other words, our method provides a means of quantifying cluster-to-cluster differences in the stellar mass function as a function of the total cluster mass.

We have chosen to count the number of stars belonging to each mass bin directly from the observations in order to quantify the dependence of the fraction of stars belonging to each mass bin on the total cluster mass (or, more specifically, the total number of stars spanning all mass bins). We note that an alternative, albeit considerably less precise, way to go about this would be to characterize the stellar mass functions using a log-normal function of the form given by Equation 6.2. Let this function be represented by $\Psi(\mathrm{m}) = \mathrm{dN/dlnm}$. We can normalize the distribution of stellar masses over the entire mass range of interest (0.25-0.75 $\mathrm{M}_{\odot}$) by setting:

$$\int_{m_{min}}^{m_{max}} \Psi(m) dlnm = 1, \tag{6.4}$$

where, in our case, $\mathrm{m}_{min} = 0.25\ \mathrm{M}_{\odot}$ and $\mathrm{m}_{max} = 0.75\ \mathrm{M}_{\odot}$. The fraction of stars belonging to a given mass bin would then be given by:

$$f_{m_1-m_2} = \int_{m_1}^{m_2} \Psi(m) dlnm, \tag{6.5}$$

where $\mathrm{m}_1$ and $\mathrm{m}_2$ are the lower and upper mass limits, respectively, of the mass bin under consideration.

The reason why our technique provides a means of quantifying the universality of the IMF, in addition to the effects had by two-body relaxation in modifying it, can be understood as follows. If we assume that all things are equal, such as tidal effects from the Galaxy and the degree of primordial mass segregation, two-body relaxation operates the fastest in low-mass clusters. All of the clusters in our sample are of comparably old age, which implies that the dynamical age increases with decreasing cluster mass. With increasing dynamical age, the stellar mass function should be more severely depleted of preferentially low-mass stars due to stellar evaporation induced by two-body relaxation. Based on this, if all of the clusters in our sample were born with similar IMFs, we would expect the slopes of their lines of best-fit to systematically increase with decreasing mass bin. This is because low-mass clusters should be more depleted of their low-mass stars. Therefore, the weighted lines of best-fit and, in particular their corresponding uncertainties, provide a means of quantifying the universality of the stellar IMF in the range of cluster masses and chemical compositions characteristic of Milky Way globular clusters. Large uncertainties caused by a large degree of scatter could be interpreted as evidence against a universal IMF. This is because we would only expect a systematic dependence of the number of stars belonging to each mass bin on the total cluster mass, and therefore small uncertainties for the slopes and y-intercepts corresponding to their lines of best-fit, if all clusters began with very similar IMFs in the first place. We note that although our method constrains the *universality* of the stellar IMF, it does not constrain its precise *functional form*. The reason for this is that we do not know how much dynamical evolution has actually occurred in the clusters in our sample. Therefore, we do not know how much the stellar mass function has been mod-

ified by two-body relaxation. However, as we will describe in Section 6.4, our observational analysis is ideally suited for comparison to theoretical models for globular cluster evolution, and this will allow us to constrain the exact shape of the IMF, in addition to the degree of primordial mass segregation.

Finally, we note that mass segregation should also contribute to the systematic dependence on cluster mass we have described in the previous paragraph for the slopes and y-intercepts corresponding to the lines of best-fit for each mass bin. This effect should be the most severe for small circles (centred on the cluster centre), and should become less important as increasingly larger circles are considered. This is because as we consider progressively larger fractional areas of the cluster, the number counts for each mass bin become less sensitive to the stars' spatial distributions throughout the cluster, and therefore less sensitive to the effects of mass segregation.

## 6.3 Results

In Figure 6.1, Figure 6.2 and Figure 6.3 we plot the number of stars in each mass bin versus the total number of stars spanning all five mass bins. Slopes (a) and y-intercepts (b) for the weighted lines of best-fit performed for each of these relations are shown in Table 6.1, along with their corresponding uncertainties. These were found using a bootstrap methodology in which we generated 1,000 fake data sets by randomly sampling (with replacement) number counts from the observations. We obtained lines of best fit for each fake data set, fit a Gaussian to the subsequent distribution and extracted its standard deviation. We have found that our results are insensitive to both changes in bin width and bin centering. Specifically, our slopes and y-intercepts remain consistent to

within one standard deviation upon adjusting either the bin width or centering by up to roughly half a bin width.

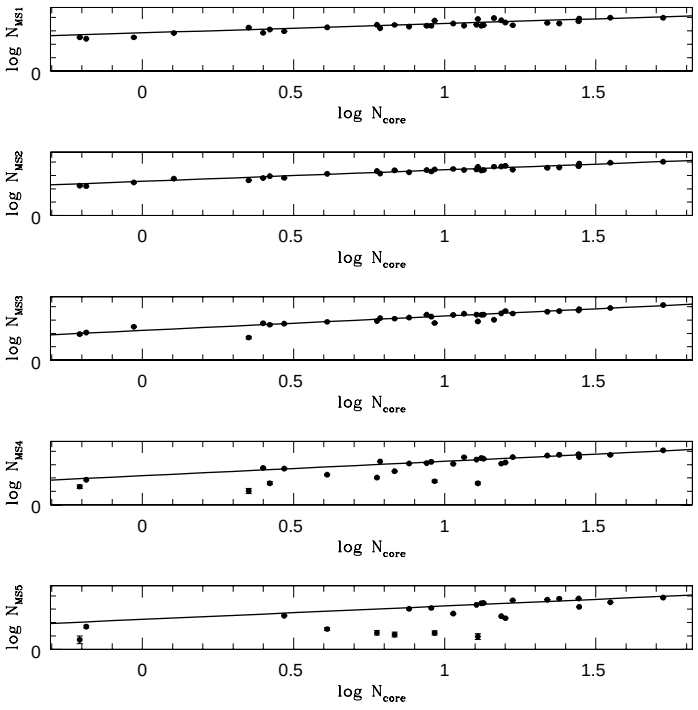



Figure 6.1 The logarithm of the number of stars belonging to each mass bin as a function of the logarithm of the total number of stars spanning all five mass bins in the core. MS1 corresponds to the mass range 0.65 - 0.75 $M_{\odot}$, MS2 to 0.55 - 0.65 $M_{\odot}$, MS3 to 0.45 - 0.55 $M_{\odot}$, MS4 to 0.35 - 0.45 $M_{\odot}$, and MS5 to 0.25 - 0.35 $M_{\odot}$. Lines of best fit are shown for each mass bin.

As shown in Table 6.1, the slopes tend to systematically increase with decreasing mass bin. For the comparison within two core radii (shown in Figure 6.2), this trend applies to all mass bins. For the comparisons within the core and within three core radii (shown in Figure 6.1 and Figure 6.3, respectively), however, only the highest three mass bins (MS1, MS2, and MS3) follow this trend of increasing slope with decreasing mass bin. After the third mass bin, the slopes for the lowest two mass bins remain about the same. Note,

Table 6.1 Lines of Best Fit for log $N_{MS}$ = (a ± Δa)log ($N_{tot}/10^3$) + (b ± Δb)

| | MS1 (0.65-0.75 $M_\odot$) | | | | MS2 (0.55-0.65 $M_\odot$) | | | | MS3 (0.45-0.55 $M_\odot$) | | | | MS4 (0.35-0.45 $M_\odot$) | | | | MS5 (0.25-0.35 $M_\odot$) | | | |
|---|---|---|---|---|---|---|---|---|---|---|---|---|---|---|---|---|---|---|---|---|
| Circle | a | Δa | b | Δb | a | Δa | b | Δb | a | Δa | b | Δb | a | Δa | b | Δb | a | Δa | b | Δb |
| $< r_c$ | 0.70 | 0.07 | 2.85 | 0.09 | 0.86 | 0.05 | 2.56 | 0.05 | 1.08 | 0.05 | 2.22 | 0.07 | 1.08 | 0.09 | 2.17 | 0.12 | 1.00 | 0.20 | 2.24 | 0.25 |
| $< 2r_c$ | 0.81 | 0.08 | 2.74 | 0.12 | 0.90 | 0.06 | 2.55 | 0.09 | 0.99 | 0.03 | 2.35 | 0.05 | 1.07 | 0.06 | 2.17 | 0.10 | 1.19 | 0.10 | 1.91 | 0.18 |
| $< 3r_c$ | 0.91 | 0.12 | 2.50 | 0.19 | 1.04 | 0.11 | 2.30 | 0.17 | 1.08 | 0.08 | 2.23 | 0.12 | 1.02 | 0.05 | 2.31 | 0.10 | 1.15 | 0.10 | 2.04 | 0.16 |

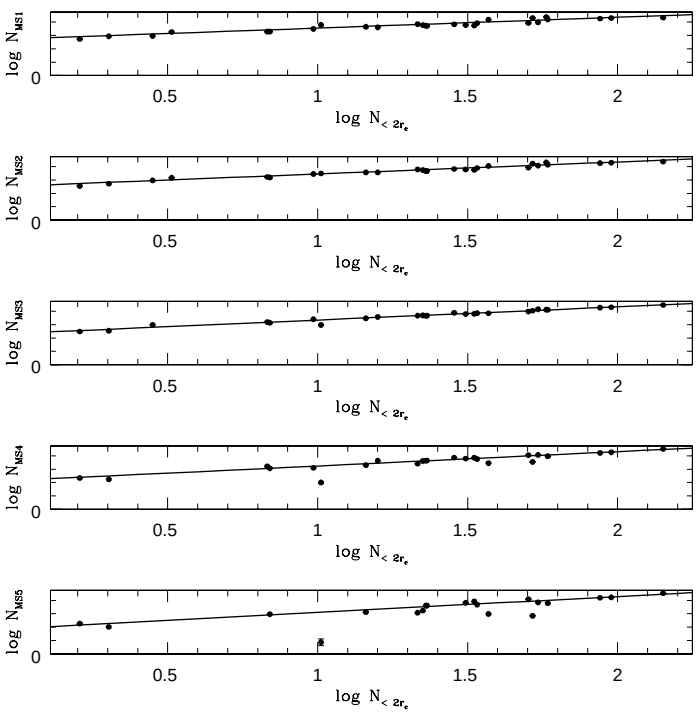



Figure 6.2 The logarithm of the number of stars belonging to each mass bin as a function of the logarithm of the total number of stars spanning all five mass bins within two core radii from the cluster centre. The mass bins are the same as in Figure 6.1.

however, that the uncertainties on the slopes and y-intercepts are also higher for the lowest mass bins (MS4 and MS5). This is likely to be due to the fact that the photometric errors are the highest at these dim magnitudes, however they remain at most $\sim 10\%$ of the width in magnitude of their corresponding mass bins. The completeness corrections are also the largest for MS4 and MS5, and this also introduces additional uncertainty. Although we have taken the appropriate measures, it is important that these effects be properly quantified in order to reliably use our technique to constrain the degree of universality of the IMF. We will return to this in Section 6.4.

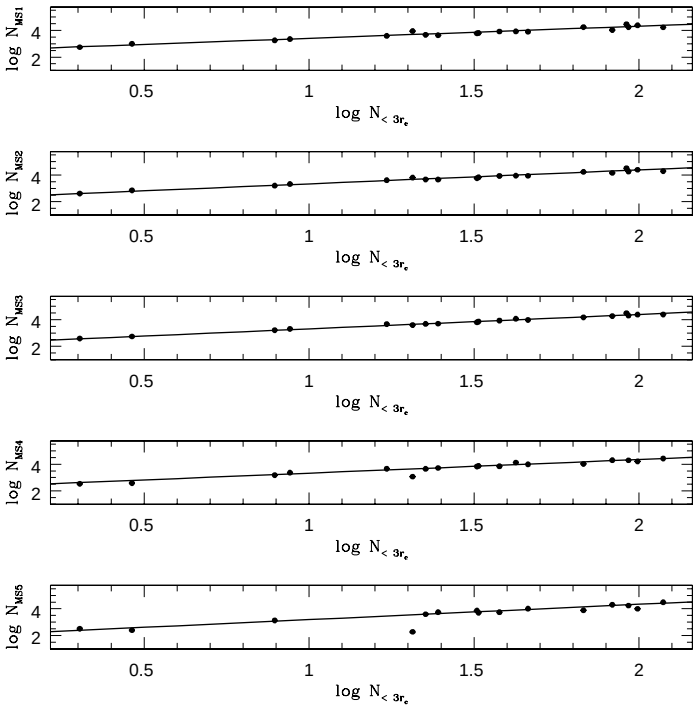



Figure 6.3 The logarithm of the number of stars belonging to each mass bin as a function of the logarithm of the total number of stars spanning all five mass bins within three core radii from the cluster centre. The mass bins are the same as in Figure 6.1.

On the other hand, when we consider only the largest three mass bins (MS1, MS2, and MS3) for which the photometric errors and level of incompleteness are the lowest, the difference in slopes and y-intercepts between adjacent mass bins can differ at better than the $2-\sigma$ confidence level. Moreover, if we compare non-adjacent mass bins, then this trend is typically significant at the $3-\sigma$ confidence level. In order to improve upon these statistics, we have also calculated reduced chi-squared values with added intrinsic dispersion for the relations for each mass bin. That is, for each mass bin we added a constant term to the uncertainty for each data point, found the value that

yielded a reduced chi-squared of one, and looked at the subsequent effects on the uncertainties for the line of best-fit. Based on this, we appear to be slightly over-estimating the uncertainties for the MS1, MS2 and MS3 mass bins using our bootstrap approach, and slightly under-estimating them for the MS4 and MS5 bins. This suggests that the slopes and y-intercepts differ at nearly the $2-\sigma$ confidence level for the MS1, MS2 and MS3 mass bins, but are consistent to within one standard deviation for the MS4 and MS5 bins. We conclude that our results are the most reliable (at nearly the $2-\sigma$ confidence level) in the mass range 0.45-0.75 $M_{\odot}$.

The change in the distribution of stellar masses as a function of the total cluster mass can be illustrated using pie charts, as shown in Figure 6.4. Using the slopes and y-intercepts provided in Table 6.1 for the comparison within two core radii, we have generated pie charts for three total numbers of stars (spanning all five mass bins), namely $N_{tot} = 10^3$, $10^4$, $10^5$. As is clear, low-mass stars are preferentially depleted, and this effect becomes increasingly severe with decreasing total cluster mass (or, equivalently, increasing dynamical age). From right to left, what the pie charts are showing are the mass functions of progressively dynamically older clusters. If this is indeed the cause of the observed depletion of low-mass stars in low-mass clusters, we are effectively looking at the evolution of the stellar mass function in time.

## 6.4 Summary & Discussion

In this chapter, we have obtained completeness-corrected stellar mass functions in the range 0.25-0.75 $M_{\odot}$ for a sample of 33 globular clusters using data taken from the ACS Survey for Globular Clusters. We have presented a



Figure 6.4 Stellar mass functions depicted in pie chart form. The total area of each circle corresponds to the total number of stars spanning all five mass bins, and each pie slice shows the fraction of this total corresponding to each mass bin. Each of these fractions was calculated using the weighted lines of best-fit provided in Table 6.1. From left to right, the total number of stars used to generate each pie chart was $10^3$, $10^4$, and $10^5$. Dark blue corresponds to MS1, red to MS2, green to MS3, purple to MS4, and light blue to MS5. From right to left, the pie charts effectively show the mass functions of progressively dynamically older clusters.

new technique to quantify cluster-to-cluster variations in the observed stellar mass functions. We have shown how our method can be used to quantify the universality of the IMF for a large sample of clusters and, when used in conjunction with theoretical models for globular cluster evolution, can be used to constrain the degree to which two-body relaxation has modified the currently observed stellar mass functions from their primordial form. To this end, we have obtained weighted lines of best-fit by comparing the number of stars in five different mass bins to the total number of stars spanning the entire mass

range within several circles centred on the cluster centre.

As shown in Table 6.1, our results suggest that the slopes for the lines of best-fit tend to systematically increase with decreasing mass bin. Assuming all of the clusters in our sample were born with similar IMFs, this is precisely what we expect from two-body relaxation. That is, we expect low-mass stars to become preferentially depleted via stellar evaporation, and we expect this effect to be the most severe in low-mass clusters. This trend is clearly seen in the observations, as demonstrated in Figure 6.4. Interestingly, the fraction of stars belonging to each mass bin is remarkably constant for all mass bins at the high-mass end of our sample. The total masses of these clusters are sufficiently high that their half-mass relaxation times are comparable to their ages (e.g. Harris, 1996, 2010 update). Therefore, we expect that the highest mass clusters in our sample should have been relatively unaffected by stellar evaporation due to two-body relaxation. It follows that their current mass functions should be relatively unchanged from their primordial values (ignoring the effects of stellar evolution). If true, our results could suggest that the slope IMF in Equation 6.1 was consistent with zero in the mass range 0.25-0.75 $M_{\odot}$ for all of the clusters in our sample. This would be inconsistent with a "standard" Kroupa IMF. This hypothesis can be tested by comparing the results of the observational analysis presented in this chapter to simulations of globular cluster evolution. These can be used to directly quantify the effects of two-body relaxation on the expected slopes and y-intercepts for each mass bin given any set of initial conditions and IMFs. By comparing the results of these simulations to the results of our observational analysis, the set of initial conditions that best reproduces the observations can be found. This will tell us about the precise functional form of the IMF for the clusters in our sample,

in addition to the degree of primordial mass segregation.

The uncertainties for the slopes and y-intercepts are sufficiently large that they are often consistent with those of their adjacent mass bins to within one standard deviation. However, when we consider only the largest three mass bins for which the photometric errors and level of incompleteness are the lowest, the difference in slopes and y-intercepts between adjacent mass bins can differ at better than the $2-\sigma$ confidence level. Moreover, the trend of increasing slope with decreasing mass is typically significant at the $3-\sigma$ confidence level if we compare non-adjacent mass bins. Based on this, we conclude that our results are consistent with a universal IMF for the clusters in our sample, and that the currently observed mass functions have primarily been modified by internal two-body relaxation. Having said that, it is important to note that a higher degree of primordial mass segregation effectively acts to increase the rate of dynamical evolution and therefore stellar evaporation (e.g. Heggie & Hut, 2003). Consequently, our results could also be consistent with a non-universal IMF that depends on the total cluster mass, provided the degree of primordial mass segregation also depends systematically on the total cluster mass. We also wish to point out here that the large uncertainties found for the slopes and y-intercepts, particularly for the two lowest mass bins, are primarily due to the relatively large photometric errors at these dim magnitudes and incompleteness resulting from crowding. Despite the high quality of the data used in this study, these issues are currently unavoidable given the nature of the observations. This will be a key challenge for future studies to resolve, however the method we have presented in this chapter offers a robust means of performing future analyses.

In terms of addressing the *degree* of universality of the IMF, our tech-

nique offers a considerable advantage over the standard power-law and log-normal forms used to characterize the stellar mass function shown in Equation 6.1 and Equation 6.2. This is the case when comparing the mass functions of a large sample of clusters. The reason for this is that our method segments the mass function into mass bins, which characterizes cluster-to-cluster differences in the stellar mass function for each mass bin individually (i.e. as a function of stellar mass). This is done using the slopes and y-intercepts of the relations found by correlating the number of stars in each mass bin with the total number of stars spanning all mass bins. Conversely, standard Kroupa or Chabrier mass functions quantify the mass function much more globally via functional fits to the data over considerably larger mass ranges. Of course, the standard forms remain as useful as ever for characterizing the mass functions of individual clusters, whereas our method is not appropriate for this purpose. That being said, it is worth stating here that our results are consistent with those of De Marchi, Paresce & Portegies Zwart (2010), who fit a tapered power-law distribution function with an exponential truncation to the stellar mass functions of a sample of 30 clusters containing both young and old members.

There are several possible sources of additional uncertainty that could have affected our analysis. For instance, we have not yet considered the role played by binaries. These tend to be unresolved in GCs, usually appearing as single objects located above the MS in the cluster CMD. Therefore, some of the objects in each mass bin are in fact binaries masquerading as single stars. Typical binary fractions in Milky Way GCs are thought to be on the order of a few to a few tens of a percent (e.g. Rubenstein & Bailyn, 1997; Cool et al., 2002; Sollima et al., 2008; Davis et al., 2008). This suggests that

a non-negligible number of binaries could often be included in our number counts for each mass bin. However, there is no reason not to expect that binaries will contribute to each mass bin in roughly equal proportions. If the fraction of binaries is the same in all mass bins, then the presence of binaries should not have significantly affected the slopes. Although they will have affected the y-intercepts, this effect should not cause them to deviate from within the uncertainties and should not have affected the interpretation of our results. On the other hand, some observational evidence suggests that the binary fraction could be inversely proportional to the total cluster mass (e.g. Sollima et al., 2008; Milone et al., 2008; Knigge, Leigh & Sills, 2009). It is not clear how this might have affected our results since we do not know how each mass bin should be affected. It is our intent to address this issue in a future study once binary fractions become available for the majority of the clusters in our sample (Ata Sarajedini; private communication).

Throughout our analysis, we have consistently compared two projected quantities. Therefore, effects related to projection should not have significantly affected our results. Moreover, these effects should become less severe upon considering progressively larger circles, and we have performed our analysis for circles with three different sizes. We note that this could perhaps help to explain why the scatter in the lowest mass bins appears to become reduced for the comparisons within two and three core radii (compared to the comparison within one core radius), although it is not clear why the agreement appears slightly better for the former comparison.

Tidal effects from the Galaxy effectively act to reduce the time-scale for two-body relaxation (e.g. Heggie & Hut, 2003). The same effect can also be had by increasing the degree of primordial mass segregation (e.g. Spitzer,

1987; Portegies Zwart et al., 2001). Therefore, on average, we would expect clusters with smaller Galactocentric radii and higher initial concentrations to have experienced a higher degree of stellar evaporation. In an effort to quantify tidal effects from the Galaxy, we performed several cuts in perigalacticon distance (Dinescu, Girard & van Altena, 1999; Casetti-Dinescu et al., 2007) and re-performed our weighted lines of best-fit. Despite removing clusters from our sample with small perigalacticon distances for which it is typically argued that tidal effects should be the most severe (e.g. Heggie & Hut, 2003), our slopes and y-intercepts, in addition to their uncertainties, remain more or less unchanged. This can be interpreted as rough evidence that tidal effects from the Galaxy have not significantly affected our results. It is much less clear which clusters in our sample, if any, were born with high central concentrations. Based on current observations, there is no known reason not to expect a universal degree of primordial mass segregation (e.g. Portegies Zwart, McMillan & Gieles, 2010). If this was the case, then our results could be interpreted as indicative of a universal IMF for Milky Way globular clusters. Unfortunately, observational constraints for primordial binary populations are also lacking (e.g. McKee & Ostriker, 2007). Binaries play an important role in star cluster evolution by, for instance, providing an energy source that serves to resist a cluster's tendency toward increasing its central density (Hut, 1983). They are therefore an important consideration in deciding the dynamical evolution of the stellar mass function, and their role will need to be addressed in future studies.

It is interesting and even surprising that, despite all of the aforementioned factors expected to affect the dynamical evolution of globular clusters, we observe relatively little scatter in the relations within two and three core

radii (Figure 6.2 and Figure 6.3). Moreover, the slopes systematically increase with decreasing mass bin. Based on this, our results are consistent with a single universal IMF for all of the clusters in our sample that has been modified via internal two-body relaxation by an amount determined by the total cluster mass. This is a new result given the old ages and therefore low metallicities ([Fe/H] $\sim$ -2.28 - (-0.37)) of the clusters that comprise our sample. However, the exact form of the IMF required to reproduce the current observations is still not clear, nor is the role of primordial mass segregation. To what degree have low-mass clusters been depleted of their low-mass stars? What combination of IMFs, Galactocentric radii, initial concentrations and primordial binary fractions should evolve dynamically to best reproduce the currently observed mass functions? These questions can only be answered using simulations of globular cluster evolution that explore a range of initial conditions and IMFs. Our observational analysis of the ACS data is ideally suited for comparison to these types of models. This would allow us to constrain the precise shape of the IMF in the mass and metallicity range of interest, as well as to learn about primordial mass segregation. This will be the focus of a forthcoming study.

## Acknowledgments

We would like to thank Ata Sarajedini, Aaron Dotter and Roger Cohen for providing the data on which this study is based and for their extensive support in its analysis. We would also like to thank Evert Glebbeek for useful discussions. This research has been supported by NSERC and OGS.

# Bibliography

Anderson J., Sarajedini A., Bedin L. R., King I. R., Piotto G., Reid I. N., Siegel M., Majewski S. R., Paust N. E. Q., Aparicio A., Milone A. P., Chaboyer B., Rosenberg A. 2008, AJ, 135, 2055

Bonnell I. A., Larson R. B., Zinnecker H. 2007, Protostars and Planets V, 149 Elmegreen B. G. 1999, ApJ, 527, 266

Chabrier G. 2005, ASSL Vol. 327: The Initial Mass Function 50 Years Later, 41

Cool A. M., Bolton A. S. 2002, in ASP Conference Series 263, Stellar Collisions, Mergers and their Consequences, ed. M. M. Shara (San Francisco: ASP), 163

Da Costa G. S. 1982, AJ, 87, 990

Davis D. S., Richer H. B., Anderson J., Brewer J., Hurley J., Kalirai J. S., Rich R. M., Stetson P. B. 2008, AJ, 135, 2155

Dinescu D. I., Girard T. M., van Altena W. F. 1999, AJ, 117, 1792

Casetti-Dinescu D. I., Girard T. M., Herrera D., van Altena W. F., Lopez C. E., Castillo D. J. 2007, AJ, 134, 195

De Angeli F., Piotto G., Cassisi S., Busso G., Recio-Blanco A., Salaris M., Aparicio A., Rosenberg A. 2005, AJ, 130, 116

De Marchi G., Paresce F., Portegies Zwart S. 2010, ApJ, 718, 105

Dotter A., Chaboyer B., Jevremovic D., Baron E., Ferguson J. W., Sarajedini A., Anderson J. 2007, AJ, 134, 376

Dotter, A., Sarajedini A., Anderson J., Aparicio A., Bedin L. R., Chaboyer B., Majewski S., Marin-Franch A., Milone A., Paust N., Piotto G., Reid N., Rosenberg A., Siegel M. 2010, ApJ, 708, 698

Elmegreen B. G. 1999, ApJ, 527, 266

Elmegreen B. G. 2001, ASP Conference Series 243: From Darkness to Light: Origin and Evolution of Young Stellar Clusters, 243, 255

Gieles M., Baumgardt H., Heggie D., Lamers H. 2010, MNRAS, 408, L16

Gieles M., Heggie D., Zhao H. 2011, MNRAS, accepted

Goldsbury R., Richer H. B., Anderson J., Dotter A., Sarajedini A., Woodley K. 2010, AJ, 140, 1830

Grenier I. A., Casandjian J. M., Terrier R. 2005, Science, 307, 1292

Harris, W. E. 1996, AJ, 112, 1487 (2010 update)

Heggie D. C., Hut P. 2003, The Gravitational Million-Body Problem: A Multidisciplinary Approach to Star Cluster Dynamics (Cambridge: Cambridge University Press)

Henon M. 1960, Annales d'Astrophysique, 23, 668

Henon M. 1973, Dynamical Structure and Evolution of Dense Stellar Systems, ed. L. Martinet & M. Mayor (Geneva Obs.)

Hurley, J. R., Pols, O. R., Aarseth, S. J. & Tout, C. A. 2005, MNRAS, 363, 293

Hut P. 1983, ApJ, 272, 29

Knigge C., Leigh N., Sills A. 2009, Nature, 457, 288

Kroupa P. 2001, MNRAS, 322, 231

Lada C. J. 1985, ARA&A, 23, 267

Lada E. A., Lada C. J. 1995, AJ, 109, 1682

Lada C. J., Lada E. A. 2003, ARA&A, 41, 57

Lada C. J., Alves J. F., Lombardi M. 2007, Protostars and Planets V, 3

McKee C. F., Ostriker E. C. 2007, ARA&A, 45, 565

Miller G. E., Scalo J. M. 1979, ApJS, 41, 513

Milone A. P., Piotto G., Bedin L. R., Sarajedini A. 2008, MmSAI, 79, 623

Murray N. 2009, ApJ, 691, 946

Portegies Zwart S. F., McMillan S. L. W., Hut P., Makino J. 2001, MNRAS, 321, 199

Portegies Zwart S. F., McMillan S. L. W., Gieles M. 2010, ARA&A, 48, 431

Rubenstein E. P., Bailyn C. D. 1997, ApJ, 474, 701

Sarajedini A., Bedin L. R., Chaboyer B., Dotter A., Siegel M., Anderson J., Aparicio A., King I., Majewski S., Marin-Franch A., Piotto G., Reid I. N., Rosenberg A., Steven M. 2007, AJ, 133, 1658

Scalo J. 1998, ASP Conference Series 142: The Stellar Initial Mass Function (38th Herstmonceux Conference), 142, 201

Sollima A., Beccari G., Ferraro F. R., Fusi Pecci F., Sarajedini A. 2008, MNRAS, 380, 781

Sollima A., Beccari G., Ferraro F. R., Fusi Pecci F., Sarajedini A. 2007, A&A, 481, 701

Spitzer L. 1987, Dynamical Evolution of Globular Clusters (Princeton: Princeton University Press)

von Hippel T., Sarajedini A. 1998, AJ, 116, 1789

Chapter 7

# Summary & Future Work

Within the last few decades, theoretical work has painted a comprehensive picture for the various forms of gravitational interactions operating within star clusters. And yet, direct observational confirmation that many of these processes are actually occurring is still lacking. The results presented in this thesis have connected several of these processes to real observations of star clusters, in many cases for the first time. This has allowed us to directly link the observed properties of several peculiar stellar populations to the physical processes responsible for their origins. Given the importance of star clusters for star formation, this also represents a key step toward re-constructing the history of our Galaxy.

In Chapter 2, we have presented a new adaptation of the mean free path approximation. Our technique provides analytic time-scales for the rate of close gravitational encounters between single, binary and triple stars in dense star systems. With it, we showed that encounters involving triple stars occur more commonly than any other type of dynamical interaction in at least some star clusters, and that these could be the dominant dynamical pro-

duction mechanism for stellar mergers. This is a new result with important implications for both star cluster evolution and the formation of several types of stellar exotica. Our method can be generalized for application to systems composed of several different types of particles that evolve under the influence of any force-mediated interactions. For example, our technique is well suited for application to collisions between atoms and dust grains in the interstellar medium (ISM) (e.g. Spitzer, 1941a,b, 1942). In this case, the relevant forces governing the dynamics are electromagnetic instead of gravitational, however the general form adopted for the mean free path approximation remains the same. Specifically, we must only replace the gravitationally-focused collisional cross-sections with their charge-focused analogues. Recent observations have provided estimates for the concentrations of the different constituents of the ISM, in addition to their temperatures (e.g. del Burgo et al., 2003; Kiss et al., 2008). These data provide the required ingredients to obtain analytic estimates for the rates of collisions between atoms, molecules, as well as both small and large dust grains in the ISM, and would allow us to make predictions for the evolution of their relative concentrations. This is an important step in the development of our understanding of dust grain coagulation and, by extension, the initial phases of star formation in dense molecular clouds (e.g. McKee & Ostriker, 2007), the interaction of winds from evolved stars with the surrounding ISM (e.g. Glassgold, 1996), and planet formation in protoplanetary disks (e.g. Absil & Mawet, 2010).

In Chapter 3, we introduced a statistical technique to compare the relative sizes of different populations of stars in a large sample of star clusters. We refined this technique in Chapter 4, and applied it to a large sample of clusters collected using state-of-the-art observations. Our results suggest that

dynamical effects do not significantly affect the relative sizes of the different stellar populations. This is the case for all stellar populations above the main-sequence turn-off in the cluster CMD. Blue stragglers alone present a possible exception to this, since we have identified a general trend in which more massive clusters are home to proportionately smaller blue straggler populations. This provides compelling evidence in favour of a binary origin for blue stragglers in even the dense cores of massive star clusters where direct collisions between stars are expected to occur frequently (Knigge, Leigh & Sills, 2009). Although we have applied these techniques to observations of dense star clusters throughout this thesis, they can be generalized for application to a number of other studies related to population statistics. For example, massive elliptical galaxies have been identified in Galaxy Clusters and Groups, and these could have formed from the mergers of smaller galaxies. Observational studies have now been performed that are allowing for the compilation of catalogues providing population statistics for several different galaxy types in a large number of Galaxy Clusters and Groups (e.g. Abell, 1958; Abell, Corwin & Olowin, 1989). Our technique is well suited for application to these data, and would allow for a systematic comparison between the relative population sizes of the different galaxy types. Among other things, this would help to constrain the origins of massive elliptical galaxies in Galaxy Clusters in much the same way we have constrained the origins of BSs in globular clusters.

In Chapter 5, we present an analytic model for blue straggler formation in globular clusters. Our model considers the production of blue stragglers throughout the entire cluster, and tracks their accumulation in the core due to dynamical friction (or, equivalently, two-body relaxation). Our results support the conclusion that blue stragglers are descended from binary stars, as

first reported in Knigge, Leigh & Sills (2009) using the technique presented in Chapter 3 and Chapter 4. Our model is applicable to studying the radial distributions of other stellar and binary populations in globular clusters. This is a sorely needed theoretical tool that can be used to address a number of recent observational studies that reported peculiarities among the radial distributions of several different stellar and binary populations (e.g. Rood, 1973; Fusi Pecci et al., 1993; Ferraro et al., 2004; Lanzoni et al., 2007).

Finally, in Chapter 6, we extend the statistical technique introduced in Chapter 3 and Chapter 4 to include the entire main-sequence. By applying our method to the ACS data, we have obtained the first quantitative constraints for the degree of universality of the stellar initial mass function for a large sample of star clusters spanning a wider range of masses and chemical compositions than ever before considered. Given the very old ages of the clusters in our sample, our results have important implications for our understanding of star formation in the early Universe. Our results are consistent with a remarkably universal IMF in old massive star clusters, and are well suited for comparison to theoretical simulations of globular cluster evolution. This would provide a simple means of directly quantifying the extent to which the stellar mass function has been modified from its primordial form by two-body relaxation. In future studies, this will allow us to obtain the very first constraints for the precise functional form of the IMF and the degree of primordial mass segregation in a large sample of old star clusters.

The results presented in this thesis have significantly advanced our understanding of stellar dynamics, stellar evolution and, in particular, the interplay that occurs between the two in dense star clusters. But we are not yet done. Our results have raised several important questions related to these

topics and, by extension, the history of our Galaxy. Once again, we are left asking: Where do we go from here? For example, how else might we use observations of blue straggler populations to learn about the dynamical histories of their host clusters? How can we use this information to constrain the interactions that occur in clusters between stellar dynamics and binary star evolution? How do these interactions affect the observed properties of their binary populations and the various types of stellar exotica they are home to? There is also the issue of the universality of the stellar initial mass function. What combination of initial concentrations and mass functions should have evolved dynamically over the lifetimes of star clusters to reproduce the currently observed mass functions? What can this tell us about primordial mass segregation in massive star clusters, and the exact form of the stellar IMF? All of these issues relate to the over-arching questions: How do stars form?; and: How did the history of our Galaxy unfold? The next few years promise to hold exciting advances in the search for answers to these questions.

# Bibliography


Abell G. O. 1958, ApJS, 3, 211

Abell G. O., Corwin Jr. H. G., Olowin R. P. 1989, ApJS, 70, 1

Absil O., Mawet D. 2010, A&ARv, 18, 317

del Burgo C., Laureijs R. J., Abraham P., Kiss Cs., 2003, MNRAS, 346, 403

Ferraro F. R., Beccari G., Rood, R. T., Bellazzini M., Sills A., Sabbi E. 2004, ApJ, 603, 127

Fusi Pecci F., Ferraro F. R., Bellazzini M., et al. 1993, AJ, 105, 1145

Glassgold A. E. 1996, ARA&A, 34, 241

Kiss Cs., Abraham P., Laureijs R. J., Moor A., Birkmann S. M. 2006, MNRAS, 373, 1213

Knigge C., Leigh N., Sills A. 2009, Nature, 457, 288

Lanzoni B., Dalessandro E., Perina S., Ferraro F. R., Rood R. T., Sollima A. 2007, ApJ, 670, 1065

McKee C. F., Ostriker E. C. 2007, ARA&A, 45, 565

Rood R. T. 1973, ApJ, 184, 815

Spitzer L. Jr. 1941, ApJ, 93, 369

Spitzer L. Jr. 1941, ApJ, 94, 232

Spitzer L. Jr. 1942, ApJ, 95, 329

Appendix A

# Appendix A

In this appendix, we present the collisional cross sections and time-scales used in Chapter 2. The gravitationally-focused cross sections for 1+1, 1+2, 2+2, 1+3, 2+3 and 3+3 collisions can be found using Equation 6 from Leonard (1989). Neglecting the first term and assuming that binary and triple stars are on average twice and three times as massive as single stars, respectively, this gives for the various collisional cross sections:

$$\sigma_{1+1} \sim \frac{8\pi GmR}{v_{rel}^2}, \tag{A.1}$$

$$\sigma_{1+2} \sim \frac{3\pi Gma_b}{v_{rel}^2}, \tag{A.2}$$

$$\sigma_{2+2} \sim \frac{8\pi Gma_b}{v_{rel}^2}, \tag{A.3}$$

$$\sigma_{1+3} \sim \frac{4\pi Gma_t}{v_{rel}^2}, \tag{A.4}$$

$$\sigma_{2+3} \sim \frac{5\pi Gm(a_b + a_t)}{v_{rel}^2}, \tag{A.5}$$

$$\sigma_{3+3} \sim \frac{12\pi Gma_t}{v_{rel}^2}. \tag{A.6}$$

Table A.1 Pericenters Assumed for Each Encounter Type

| Encounter Type | Pericenter |
|---|---|
| 1+1 | $2R$ |
| 1+2 | $a_b/2$ |
| 1+3 | $a_t/2$ |
| 2+2 | $a_b$ |
| 2+3 | $(a_b + a_t)/2$ |
| 3+3 | $a_t$ |

Values for the pericenters assumed for the various types of encounters are shown in Table A.1, where $R$ is the average stellar radius, $a_b$ is the average binary semi-major axis and $a_t$ is the average semi-major axis of the outer orbits of triples.

In general, the time between each of the different encounter types can be found using Equation 2.10 and the gravitationally-focused cross sections for collision given above. Following the derivation of Leonard (1989), we can write the encounter rate in the general form:

$$\Gamma_{x+y} = N_x n_y \sigma_{x+y} v_{x+y}, \tag{A.7}$$

where $N_x$ and $n_y$ are the number and number density, respectively, of single, binary or triple stars and $v_{x+y}$ is the relative velocity at infinity between objects $x$ and $y$. For instance, the time between binary-binary encounters in the core of a cluster is given by:

$$\begin{aligned}\tau_{2+2} = 1.3 \times 10^7 f_b^{-2} \Big(\frac{1pc}{r_c}\Big)^3 \Big(\frac{10^3 pc^{-3}}{n_0}\Big)^2 \\ \Big(\frac{v_{rms}}{5km/s}\Big)\Big(\frac{0.5M_\odot}{< m >}\Big)\Big(\frac{1AU}{a_b}\Big) \text{ years.}\end{aligned} \tag{A.8}$$

Similarly, the times between 1+1, 1+2, 1+3, 2+3 and 3+3 encounters are

given by:

$$\tau_{1+1} = 1.1 \times 10^{10}(1 - f_b - f_t)^{-2}\Big(\frac{1pc}{r_c}\Big)^3\Big(\frac{10^3 pc^{-3}}{n_0}\Big)^2 \Big(\frac{v_{rms}}{5km/s}\Big)\Big(\frac{0.5M_\odot}{< m >}\Big)\Big(\frac{0.5R_\odot}{< R >}\Big) \text{ years}, \tag{A.9}$$

$$\tau_{1+2} = 3.4 \times 10^{7}(1 - f_b - f_t)^{-1} f_b^{-1}\Big(\frac{1pc}{r_c}\Big)^3\Big(\frac{10^3 pc^{-3}}{n_0}\Big)^2 \Big(\frac{v_{rms}}{5km/s}\Big)\Big(\frac{0.5M_\odot}{< m >}\Big)\Big(\frac{1AU}{a_b}\Big) \text{ years}, \tag{A.10}$$

$$\tau_{1+3} = 2.6 \times 10^{7}(1 - f_b - f_t)^{-1} f_t^{-1}\Big(\frac{1pc}{r_c}\Big)^3\Big(\frac{10^3 pc^{-3}}{n_0}\Big)^2 \Big(\frac{v_{rms}}{5km/s}\Big)\Big(\frac{0.5M_\odot}{< m >}\Big)\Big(\frac{1AU}{a_t}\Big) \text{ years}, \tag{A.11}$$

$$\tau_{2+3} = 2.0 \times 10^{7} f_b^{-1} f_t^{-1}\Big(\frac{1pc}{r_c}\Big)^3\Big(\frac{10^3 pc^{-3}}{n_0}\Big)^2 \Big(\frac{v_{rms}}{5km/s}\Big)\Big(\frac{0.5M_\odot}{< m >}\Big)\Big(\frac{1AU}{a_b + a_t}\Big) \text{ years}, \tag{A.12}$$

and

$$\tau_{3+3} = 8.3 \times 10^{6} f_t^{-2}\Big(\frac{1pc}{r_c}\Big)^3\Big(\frac{10^3 pc^{-3}}{n_0}\Big)^2 \Big(\frac{v_{rms}}{5km/s}\Big)\Big(\frac{0.5M_\odot}{< m >}\Big)\Big(\frac{1AU}{a_t}\Big) \text{ years}. \tag{A.13}$$

Appendix B

# Appendix B

In this appendix, we present our selection criteria for BS, RGB, HB and MSTO stars used in Chapter 4. Our method is similar to that described in Leigh, Sills & Knigge (2007), and we have used this as a basis for the selection criteria presented in this chapter. First, we define a location for the MSTO in the (F606W-F814W)-F814W plane using our isochrone fits. The MSTO is chosen to be the bluest point along the MS of each isochrone, which we denote by ((V-I)$_{MSTO}$,I$_{MSTO}$). In order to distinguish BSs from MSTO stars, we impose the conditions:

$$F814W \leq m_1(F606W - F814W) + b_{11}, \tag{B.1}$$

where the slope of this line is $m_1 = -9$ and its y-intercept is given by:

$$b_{11} = (I_{MSTO} - 0.10) - m_1((V - I)_{MSTO} - 0.10) \tag{B.2}$$

Similarly, we distinguish BSs from HB stars by defining the following additional boundaries:

$$F814W \quad \geq \quad m_1(F606W - F814W) + b_{12} \tag{B.3}$$

$$F814W \geq m_2(F606W - F814W) + b_{21} \quad \text{(B.4)}$$

$$F814W \leq m_2(F606W - F814W) + b_{22} \quad \text{(B.5)}$$

$$F814W \geq m_{HB}(F606W - F814W) + b_{HB} \quad \text{(B.6)}$$

$$(F606W - F814W) \geq (V - I)_{HB} \quad \text{(B.7)}$$

$$F814W \leq I_{MSTO}, \quad \text{(B.8)}$$

where $m_2 = 6$, $m_{HB} = -1.5$ and $(V - I)_{HB} = (V - I)_{MSTO} - 0.4$. We also define:

$$b_{12} = (I_{MSTO} - 0.55) - m_1((V - I)_{MSTO} - 0.55) \quad \text{(B.9)}$$

$$b_{21} = (I_{MSTO} - 0.80) - m_2((V - I)_{MSTO} + 0.10) \quad \text{(B.10)}$$

$$b_{22} = (I_{MSTO} + 0.30) - m_2((V - I)_{MSTO} - 0.20), \quad \text{(B.11)}$$

and $b_{HB} = I_{HB} + 1.2$, where $I_{HB}$ roughly corresponds to the mid-point of points that populate the HB and is chosen by eye for each cluster so that our selection criteria best fits the HB in all of the CMDs in our sample.

We apply a similar set of conditions to the RGB in order to select stars belonging to this stellar population. These boundary conditions are:

$$F814W \geq m_{HB}(F606W - F814W) + b_{HB} \quad \text{(B.12)}$$

$$F814W \geq m_{RGB}(F606W - F814W) + b_{31} \quad \text{(B.13)}$$

$$F814W \leq m_{RGB}(F606W - F814W) + b_{32} \quad \text{(B.14)}$$

$$F814W \leq I_{RGB}, \quad \text{(B.15)}$$

where $m_{RGB} = -23$, $I_{RGB}$ is defined as the F814W magnitude corresponding to a core helium mass of 0.08 $M_\odot$ and:

$$b_{31} = (I_{MSTO} - 0.60) - m_{RGB}((V - I)_{MSTO} + 0.05) \quad \text{(B.16)}$$

$$b_{32} = (I_{MSTO} - 0.60) - m_{RGB}((V-I)_{MSTO} + 0.25) \quad \text{(B.17)}$$

Core helium-burning stars, which we refer to as HB stars, are selected if they satisfy one of the following sets of criteria:

$$F814W \geq m_{HB}(F606W - F814W) + (b_{HB} - 1.0) \quad \text{(B.18)}$$

$$F814W \leq m_{HB}(F606W - F814W) + b_{HB} \quad \text{(B.19)}$$

$$(F606W - F814W) \leq (V-I)_{MSTO} + (V-I)_{HB}, \quad \text{(B.20)}$$

$$F814W > m_{HB}(F606W - F814W) + b_{HB} \quad \text{(B.21)}$$

$$F814W \leq I_{MSTO} + 2.5 \quad \text{(B.22)}$$

$$(F606W - F814W) < (V-I)_{MSTO} - 0.4, \quad \text{(B.23)}$$

or

$$F814W < m_1(F606W - F814W) + b_{12} \quad \text{(B.24)}$$

$$F814W > m_{HB}(F606W - F814W) + b_{HB} \quad \text{(B.25)}$$

$$(F606W - F814W) \geq (V-I)_{MSTO} - 0.4 \quad \text{(B.26)}$$

We define $(V-I)_{HB}$ on a cluster-by-cluster basis in order to ensure that we do not over- or under-count the number of HB stars. This is because the precise value of (F606W-F814W) at which the HB becomes the RGB varies from cluster-to-cluster. In addition, the precise location of the transition in the cluster CMD between HB and EHB stars remains poorly understood. To avoid this ambiguity, we consider HB and EHB stars together throughout our analysis, and collectively refer to all core helium-burning stars as HB stars throughout this chapter.

Finally, MSTO stars are selected according to the following criteria:

$$F814W > I_{RGB} \tag{B.27}$$

$$F814W > m_1(F606W - F814W) + b_{11} \tag{B.28}$$

$$F814W \leq (V - I)_{MSTO} \tag{B.29}$$